Electromagnetic separators

Ulli Köster

Institut Laue-Langevin
Grenoble, France

Institut Laue-Langevin

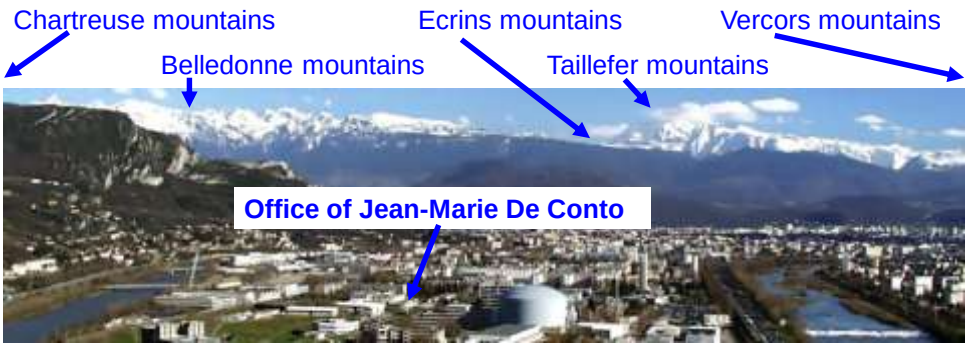

- **founded 1967**
- **today 13 member states**
- **operates most powerful neutron source of the world:**
  58 MW high flux reactor, $1.5 \cdot 10^{15}$ n./cm^2/s maximum neutron flux
- **over 40 instruments, mainly for neutron scattering**
- **user facility: 2000 scientific visitors from 45 countries per year**
- **Nuclear physics instruments: LOHENGRIN, GAMS, (PF1B)**

LOHENGRIN: an electromagnetic separator

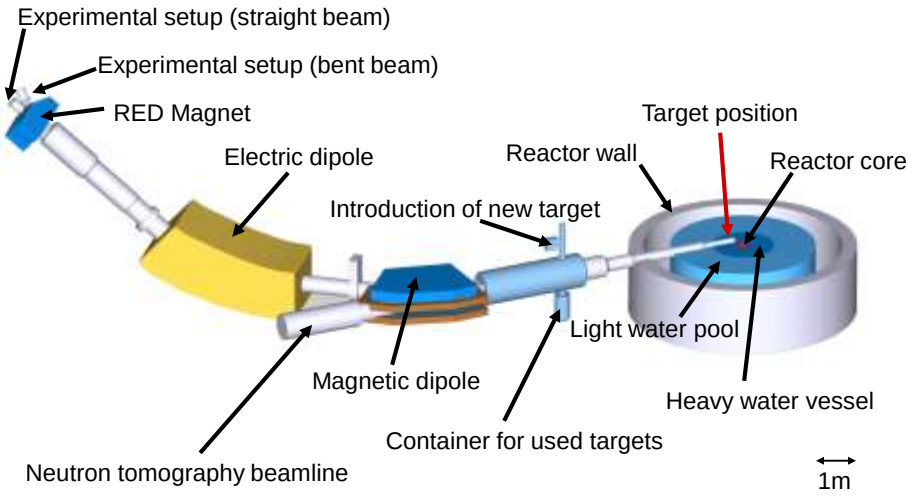

Electromagnetic separators at GANIL

BigRIPS at RIBF Facility, RIKEN, Japan

Super-FRS at FAIR, Germany

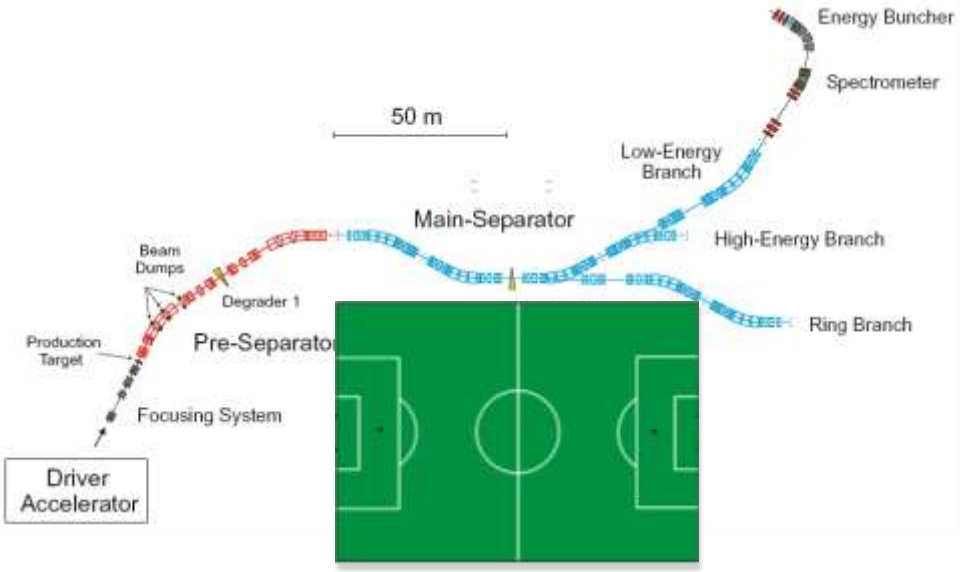

Importance of electromagnetic spectrometers

Outline

1. **Definitions and history**
2. **Basics of ion optics and dispersive elements**
3. **Static fields**
   a) deflection spectrometer
   b) retardation spectrometer
4. **Dynamic fields/separation**
   a) Time-of-Flight spectrometer
   b) Radiofrequency spectrometer
   c) Traps
5. **Technical realization (ion sources, etc.)**
6. **“Real examples” for nuclear physics applications**
   a) ISOL
   b) Recoil separators
   c) Fragment separators
   d) Spectrometer

Definitions

- **spectrometer: electrical detection**
- **spectrograph: photographic or other non-electrical detection**
- **also used: spectroscope**

- **mass / energy / isotope separator: assures a physical separation of different masses / energies / isotopes**

Thomson 1897: cathode rays

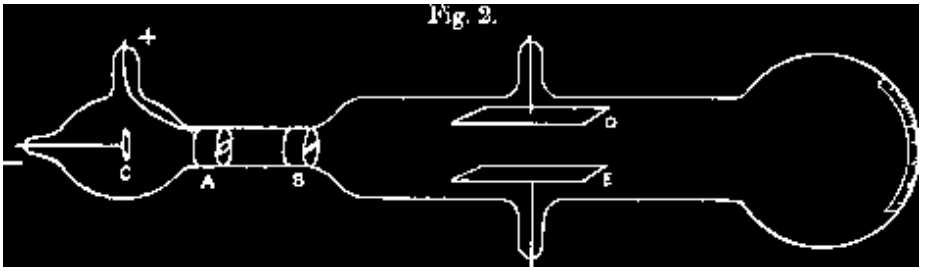

"Cathode rays", J.J. Thompson, Phil. Mag. 44 (1897) 293.

Noble prize in physics 1906 for discovery of the electron and the determination of its m/q ratio.

Goldstein 1886: *Kanalstrahlen*

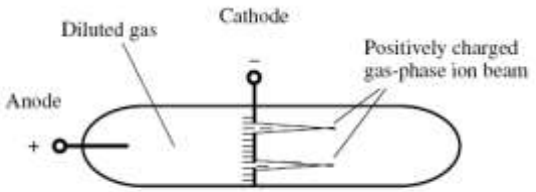

Figure 1.3 Goldstein's glow discharge tube (1886) for generation of positively charged ions. (C. Brunnée, Int. J. Mass. Spectrom. Ion Proc. 76, 125 (1987). Reproduced by permission of Elsevier.)

First fluorescent lamp and ion source.

Wien 1902: Wien filter

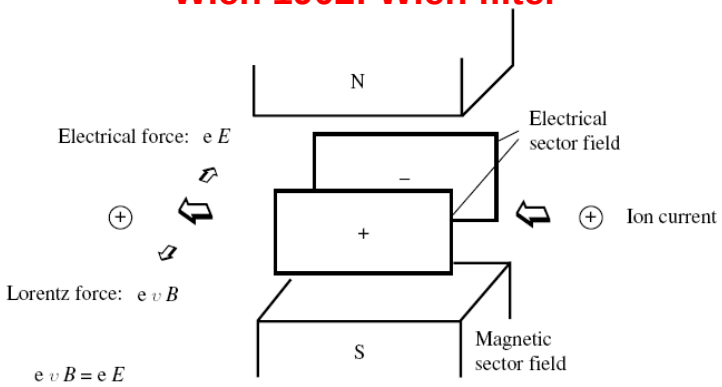

$e\,v\,B = e\,E$

$v = \frac{E}{B}$

Electric field perpendicular to magnetic field

Figure 1.4 Schematic of a Wien velocity filter with EB configuration: combination of electric (E) and magnetic (B) field (Wien,1898). (C. Brunnée, Int. J. Mass. Spectrom. Ion Proc. 76, 125 (1987). Reproduced by permission of Elsevier.)

Wien: Nobel price in physics 1911 for discovery that "Kanalstrahlen" carry positive charge

Thomson 1910: parabola mass spectrograph

Electric field parallel to magnetic field

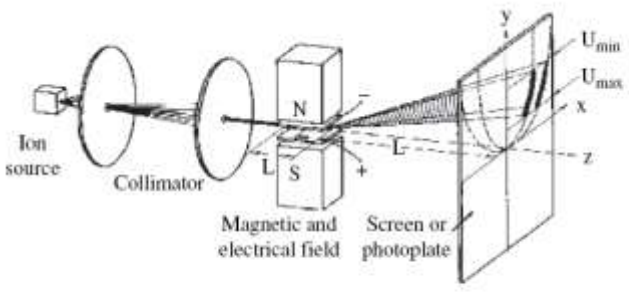

Figure 1.5 Parabola mass spectrograph constructed by J.J. Thomson (1910) with a discharge tube as ion source, a superimposed electrical field and a magnetic field oriented parallel to it for ion separation, and a photoplate for ion detection. (H. Kienitz (ed.), Massenspektrometrie (1968), Verlag Chemie, Weinheim. Reproduced by permission of Wiley-VCH.)

Neon consists of two isotopes with mass 20 and 22

Thomson 1913: mass spectrum of neon

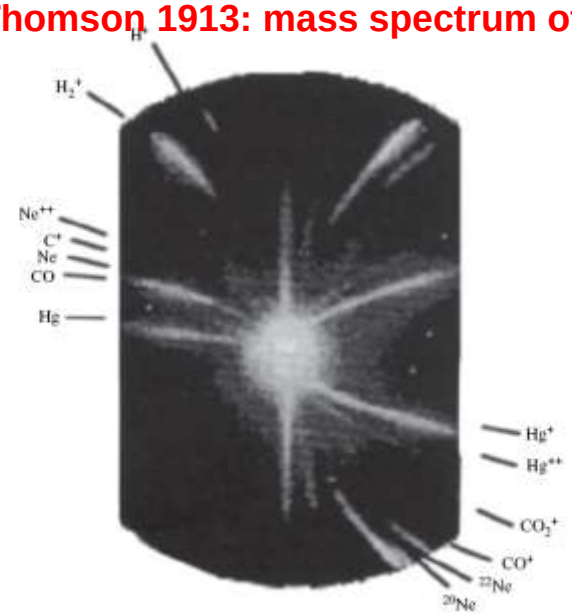

Figure 1.6. Mass spectrum of neon with masses 20 and 22 u measured by J.J. Thomson (1913) using his parabola mass spectrograph is shown in Figure 1.5. (H. Kienitz (ed.), Massenspektrometrie (1968), Verlag Chemie, Weinheim. Reproduced by permission of Wiley-VCH.)

Parabola spectrograph

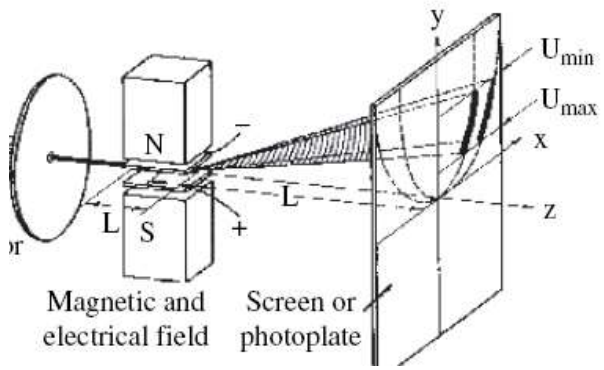

transit time through field: $t = L/v$

vertical displacement: $y = ½\ U/d\ q/m\ (L/v)^2$

horizontal displacement: $x = ½\ B\ q/m\ L^2/v$

$y = k\ m/q\ x^2$; $k = 2\ U/(d\ B^2\ L^2)$

The LOHENGRIN fission fragment separator

Angular focusing in x and y direction.

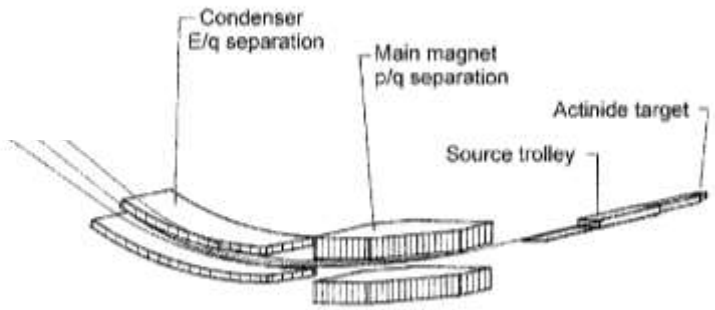

$m\,v^2 / r_{el} = q\,E$ $\qquad$ $m\,v^2 / r_{magn} = q\,v\,B$

$E_{kin} / q = E / 2\,r_{el}$ $\qquad$ $m\,v / q = B\,r_{magn}$

Aston 1919: velocity focusing spectrograph

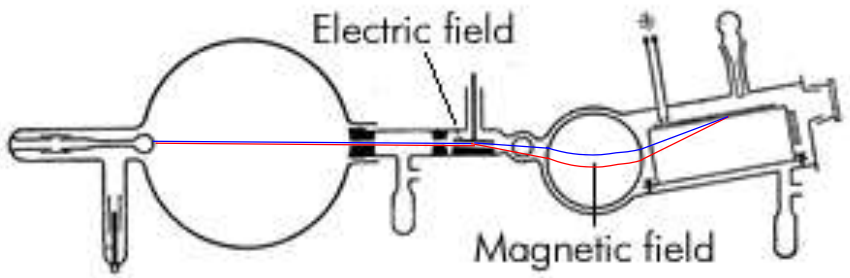

Aston's design for the mass spectrograph.

Aston: velocity focusing gives factor 10 improvement in mass resolution ($\Delta m/m = 1/130$)

Noble prize in chemistry 1922 for the discovery that elements may have isotopes of different mass (^{20}Ne, ^{21}Ne and ^{22}Ne).

Dempster 1918: 180 degree spectrometer

- electron bombardment ion source for monoenergetic ions
- 180 degree magnetic field provides angular focusing
- scan of magnetic field to measure mass spectra

1920: discovery of isotopes in Mg, Li, K, Ca, Zn

$$q/m = 2\,U / (B^2\, r^2)$$

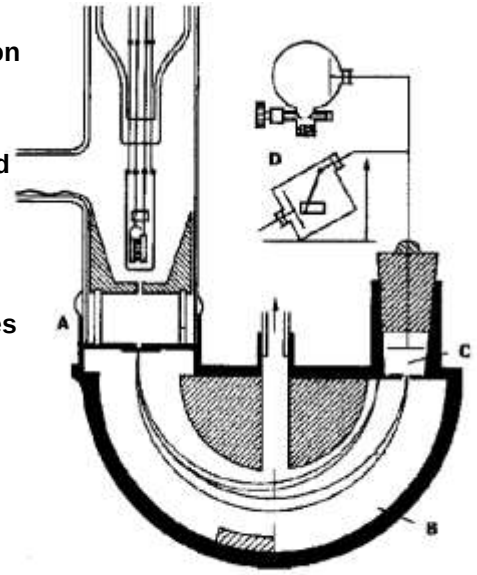

Figure 1.7 Mass spectrometer from A.J. Dempster (1918). A – ion source; B – electromagnet; C – Faraday cup; D – electrometer. (H. Klenitz (ed.), Massenspektrometrie (1968), Verlag Chemie, Weinheim. Reproduced by permission of Wiley-VCH.)

Calutron 1942: electromagnetic isotope separation

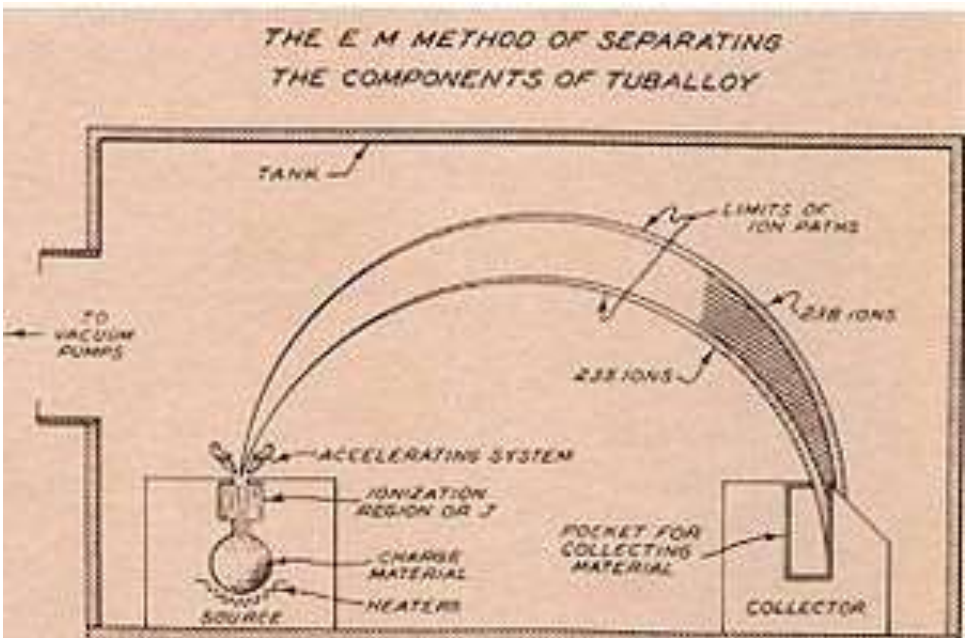

Large scale electromagnetic isotope separation

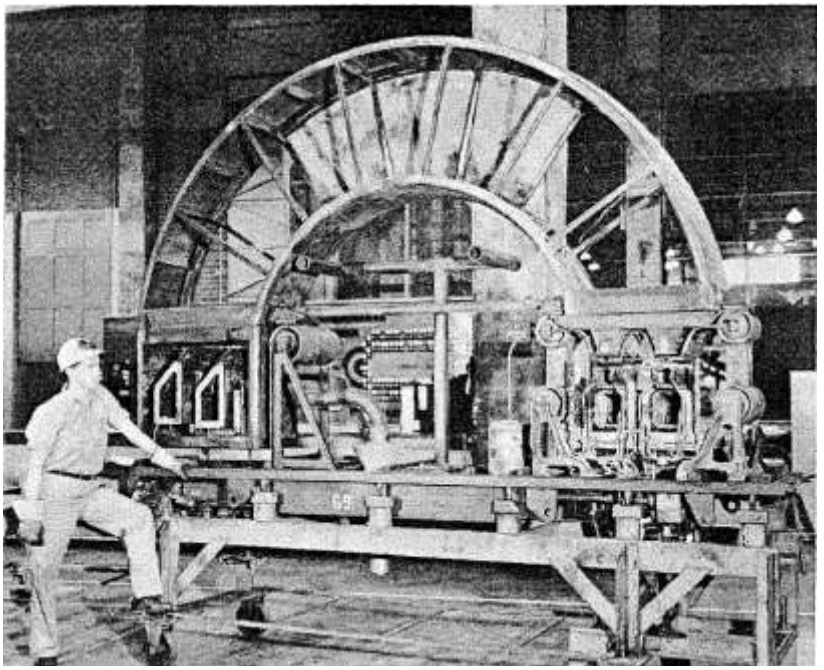

Collector plates of a Calutron

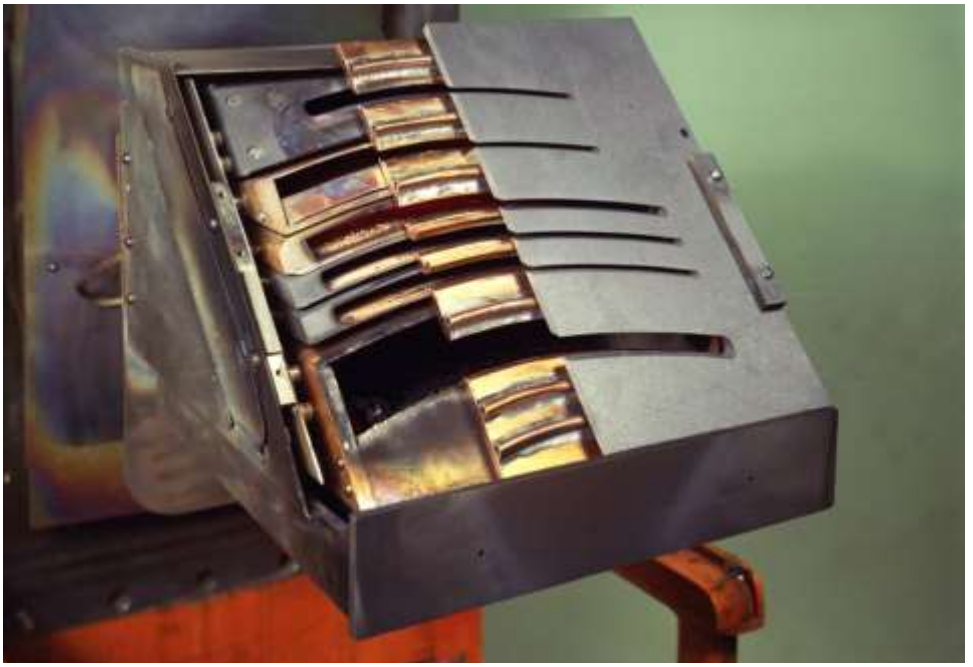

1945: large scale electromagnetic isotope separation

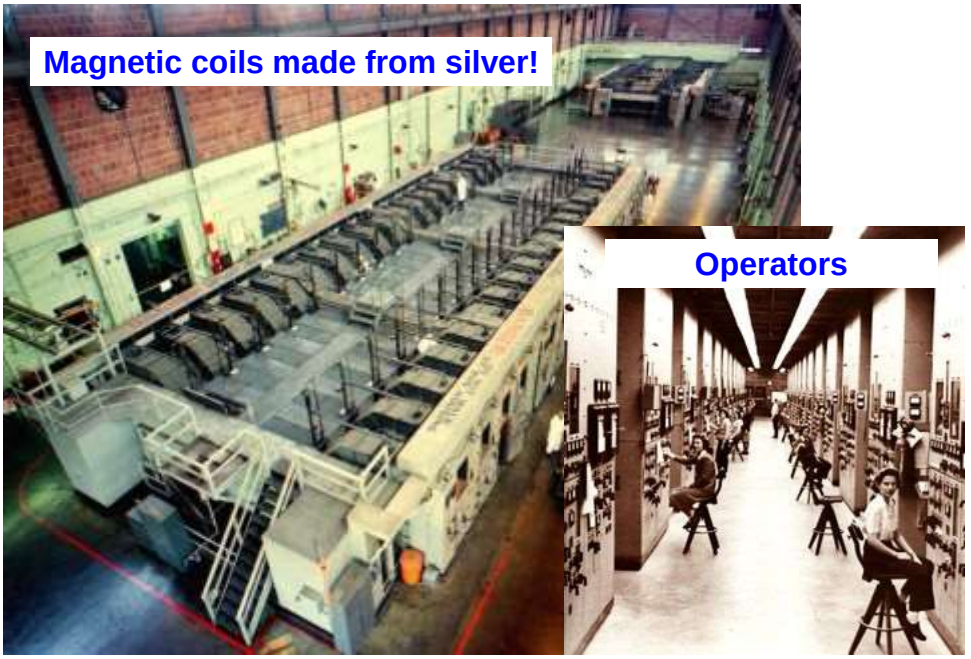

1945: “Impact” of electromagnetic isotope separation

Hiroshima: 60 kg of isotopically enriched ^{235}U

Present enrichment technology for ^{235}U

boiling point: UF_6 56 °C

⇒ centrifuges

Today: very high enrichment of stable isotopes

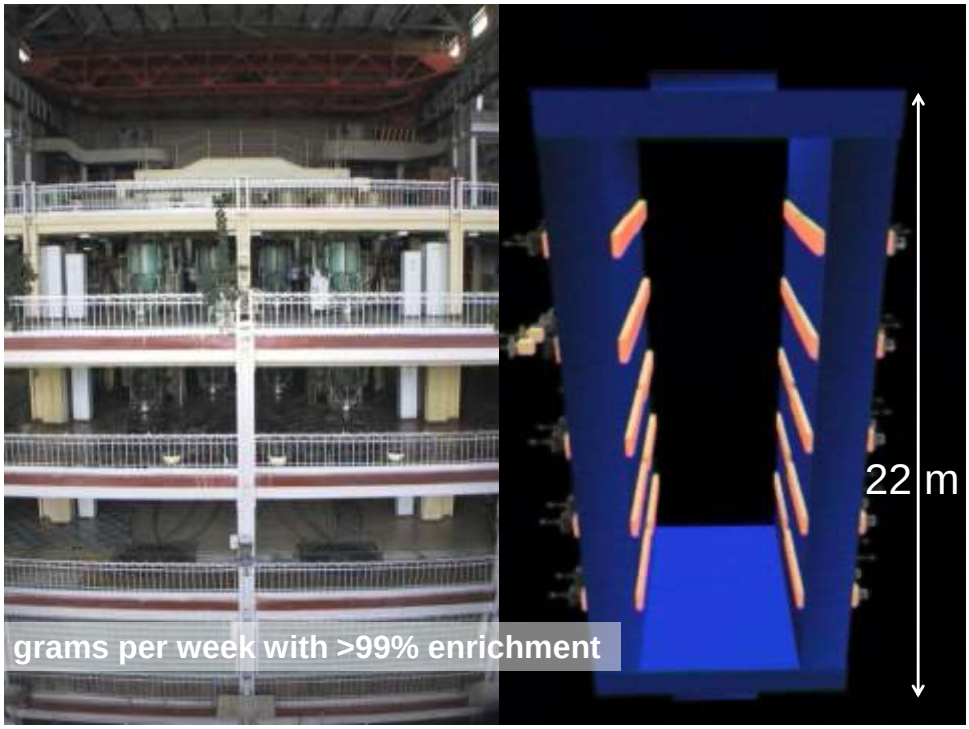

Cancer and efficiency of treatments

At time of diagnosis	Primary tumor	With metastases	Total
Diagnosed	**58%**	**42%**	**100%**
Cured by:			
Surgery	**22%**		
Radiation therapy	**12%**		
Surgery+radiation therapy	**6%**		
All other treatments and combinations incl. chemotherapy		**5%**	
Total cured	**40%**	**5%**	**45%**
Fraction cured	**69%**	**12%**	**45%**

Per year over one million cancer deaths in the EU.

⇒ improve early diagnosis

⇒ improve systemic treatments

Mammary Carcinoma
Survival time since diagnosis of metastases

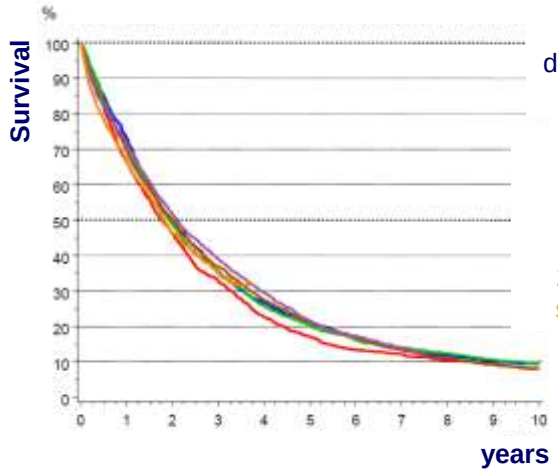

Results for 6 time periods
data from tumor centre Munich
n = 9228

1980-1984
1985-1989
1990-1994
1995-1999
2000-2003
since 2004

Comparison of Therapies

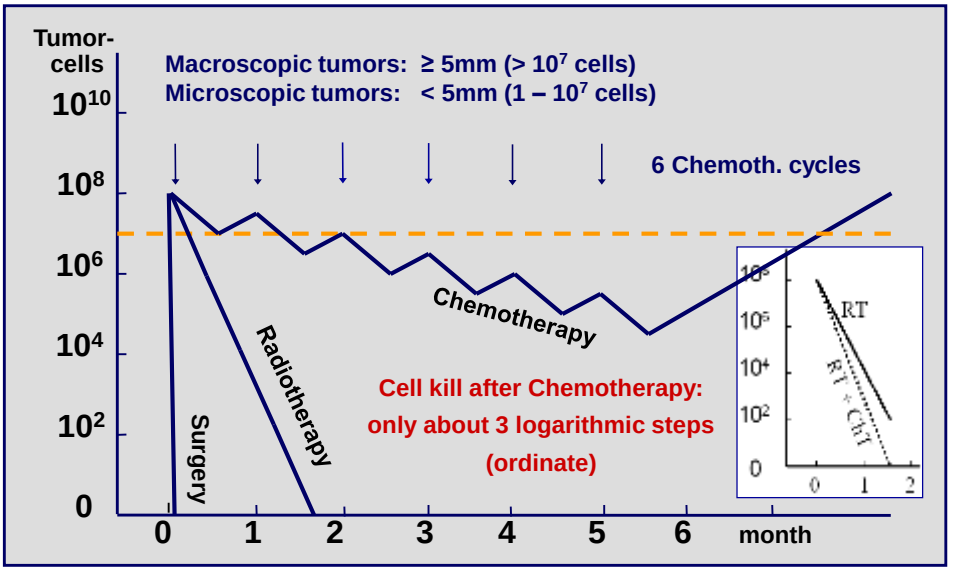

(Molls, TU München; according to Tannock: Lancet 1998, Nature 2006)

The principle of targeted therapies

- “attractive” vector > high uptake by the target
- transportable
- good in-vivo stability
- warriors “not visible”
- delayed uptake > suitable half-life
- limited space > high specific activity
- optimum arms
- specific

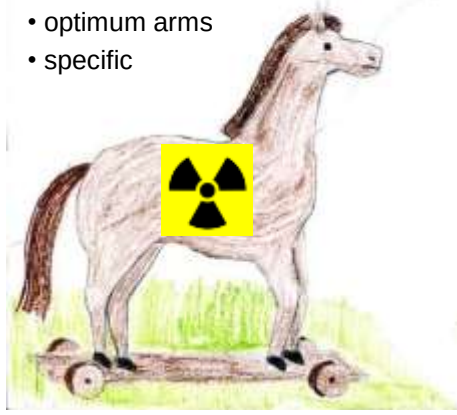

Multidisciplinary collaboration to fight cancer

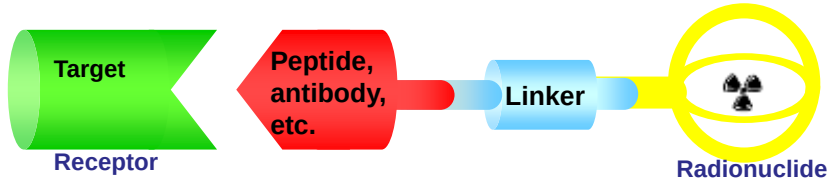

Immunology Structural biology	Coordination chemistry	Nuclear physics and radiochemistry

Nuclear medicine and medical physics

Structural Formula of DOTA-TOC/TATE

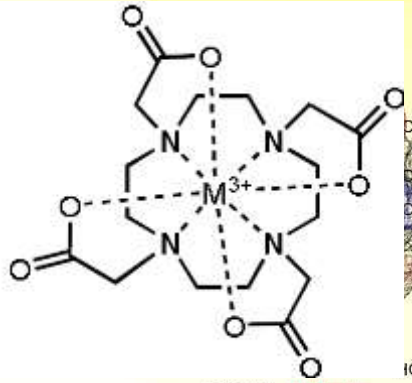

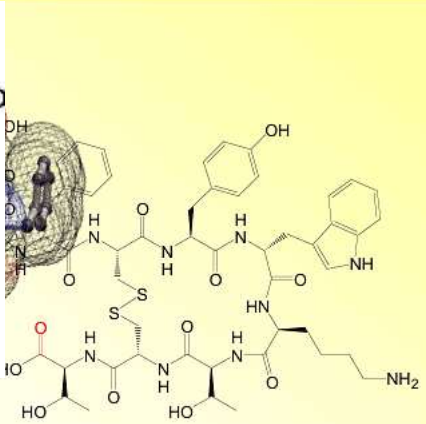

DOTA-TATE

1,4,7,10-tetraazacyclododecantetraacetate

^{111}In ^{90}Y
^{67}Ga ^{177}Lu
^{68}Ga ^{213}Bi

IC_{50} (Y^{III}) = 1.6 ± 0.4 nM

Helmut Maecke, EANM-2007.

Universitätsspital Basel

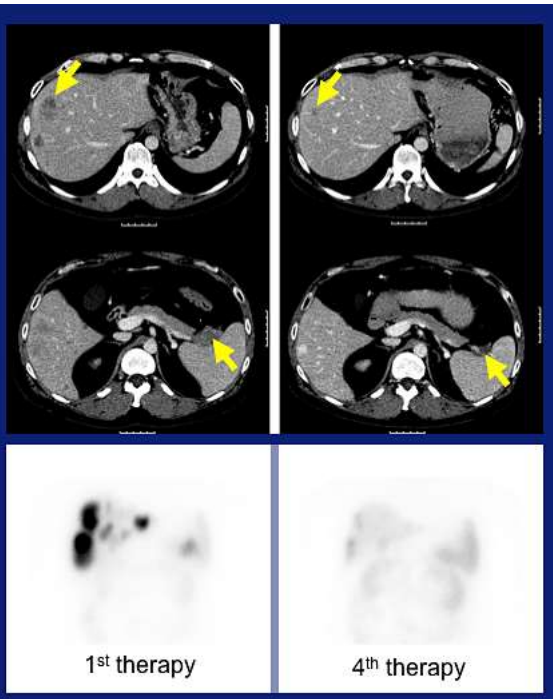

Male
36 years of age

Small cell pancreatic neuroendocrine tumour
Liver metastases
Ki-67 index 10-15% (liver biopsy)

4 cycles with ^{177}Lu-octreotate and capecitabine

Partial remission

Roelf Valkema, EANM-2008.

What success does PRRT offer?

- ✓ CR+ PR + MR in about 50% of patients: YES
- ✓ Reduce symptoms and improve quality of life: YES
- ✓ Increase survival time: YES
- ✓ Safety and tolerability: YES

Roelf Valkema, EANM-2008.

Erasmus MC

Lymphoma therapy: RITUXIMAB+^{177}Lu

E.B., 1941 (m): UPN 6

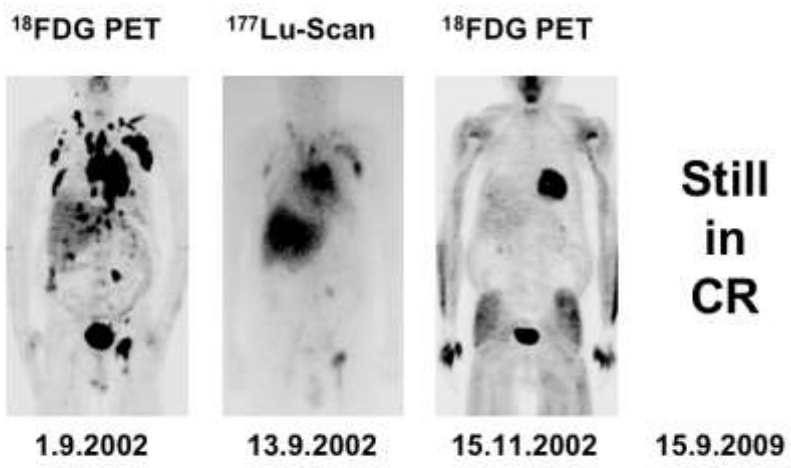

F. Forrer et al., J Nucl Med 2013;54:1045.

University Hospital Basel, CH

Production of non-carrier-added ^{177}Lu

1. Enrichment of stable isotope (^{176}Yb or ^{176}Lu)
2. Irradiation in high flux reactor

The rising star for targeted therapy

ESI-TOF-MS for DOTA-peptides analysis

Electrospray ionization/TOF-MS positive ion mode

Identification of radiometallated species

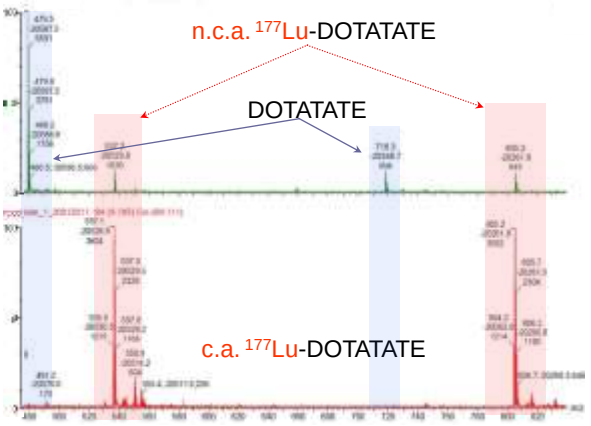

1:4 ^{177}Lu to ligand
10 MBq ^{177}Lu-DOTATATE
0.014 nmol

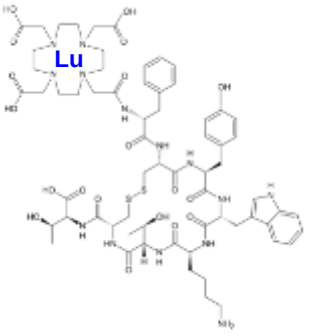

K. Zhernosekov et al., ICTR-PHE 2012.

back to electromagnetic separators…

Aston 1925: improved mass spectrograph

Improved version gives mass resolution: $\Delta m/m = 1/600$

Accuracy of mass determination: 10^{-4}

Used to study deviations of atomic masses m from A.

Introduced: "packing fraction" = m/A – 1

Systematic investigation of nuclear binding energies

Carbon isotopes

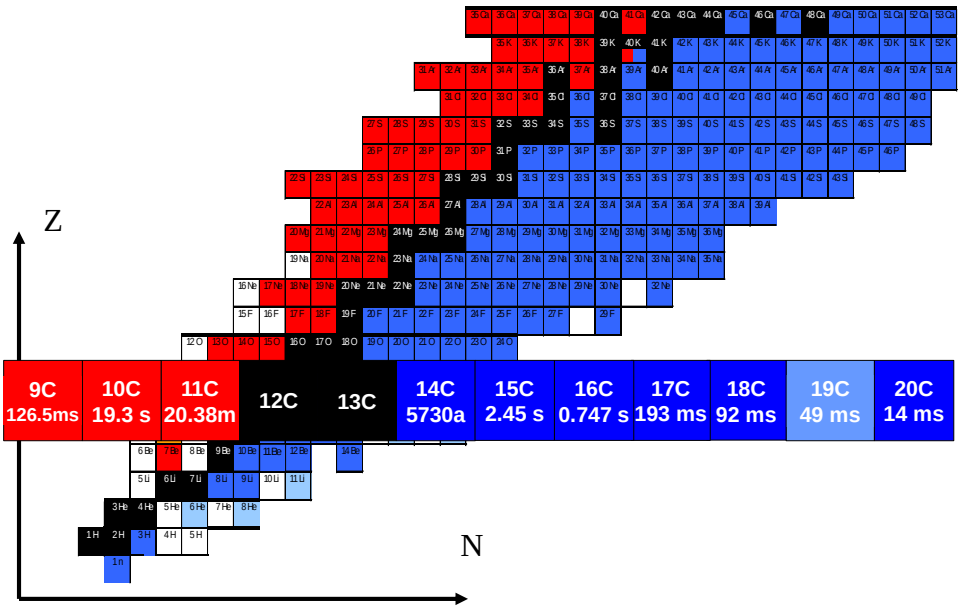

Chart of the nuclides

>3000 isotopes known, thereof less than 10% are stable

>3000 additional isotopes are expected to exist!

Production of radioisotopes via nuclear reactions!

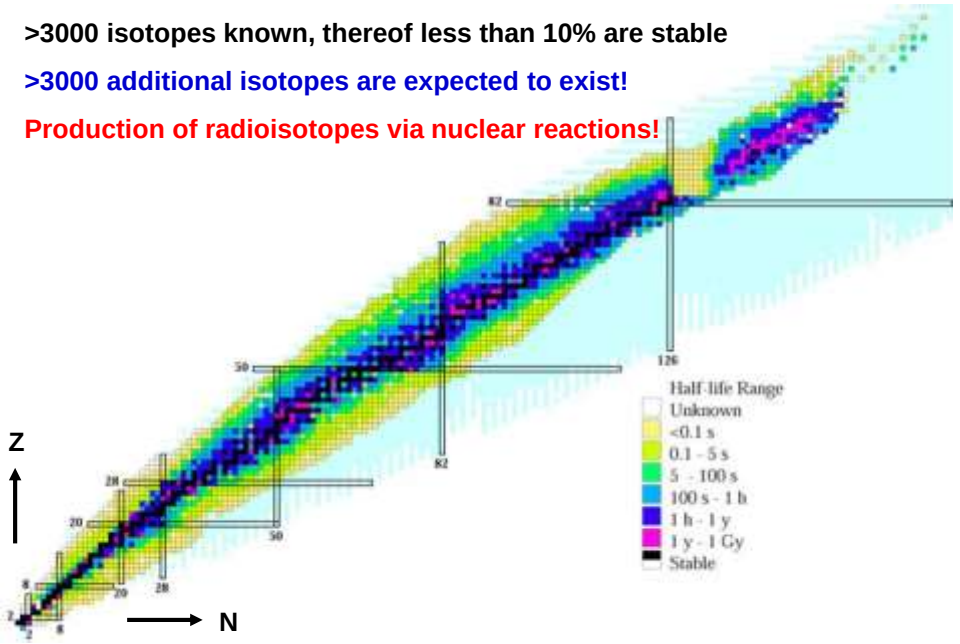

Why "ion beams"?

Production:

high radiation environment

Detection:

low radiation background

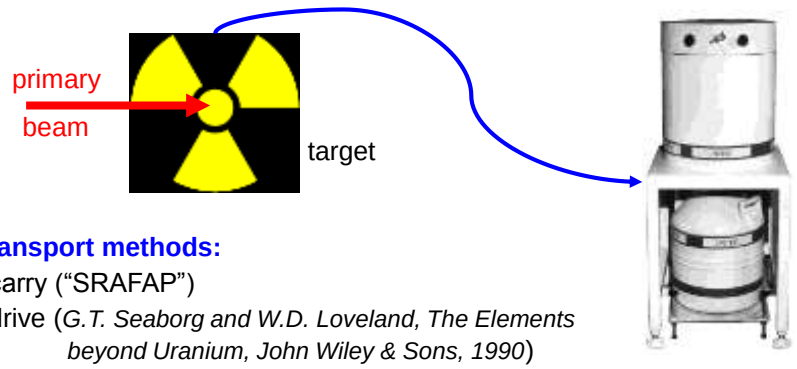

Transport methods:

- carry ("SRAFAP")
- drive (*G.T. Seaborg and W.D. Loveland, The Elements beyond Uranium, John Wiley & Sons, 1990*)
- transport shuttle with pressurized air
- transport in gas-jet
- pump through vacuum system
- send as ion beam

Irradiations of targets

Off-line mass separator

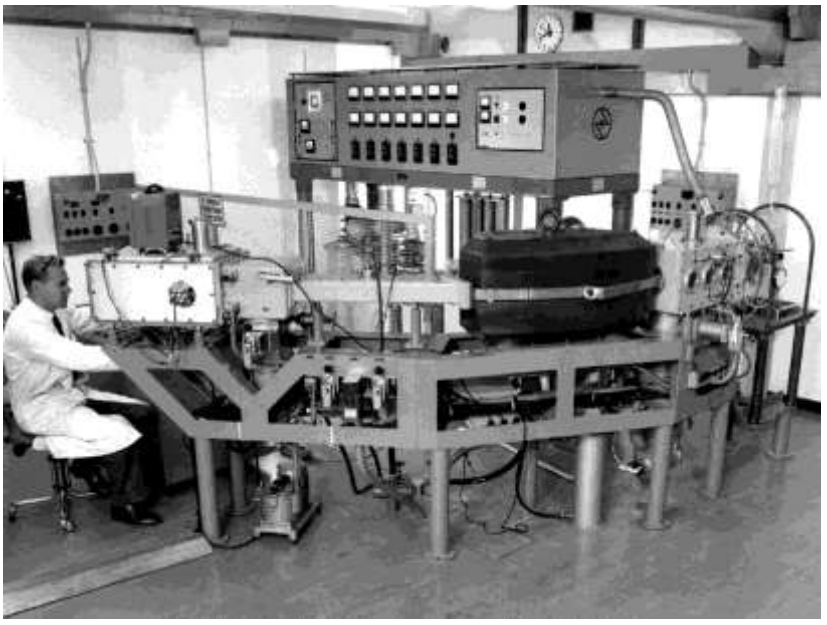

1951: first ISOL experiment at Niels Bohr Institute

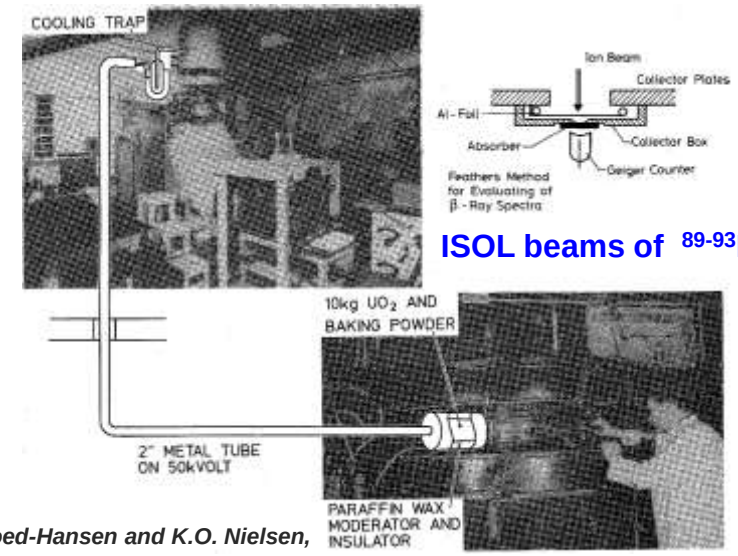

ISOL beams of $^{89\text{-}93}$Kr

O. Kofoed-Hansen and K.O. Nielsen, Mat. Fys. Medd. Dan. Vid. Selsk. 26, Nr. 7 (1951).

*I*sotope *S*eparation *O*n-*L*ine

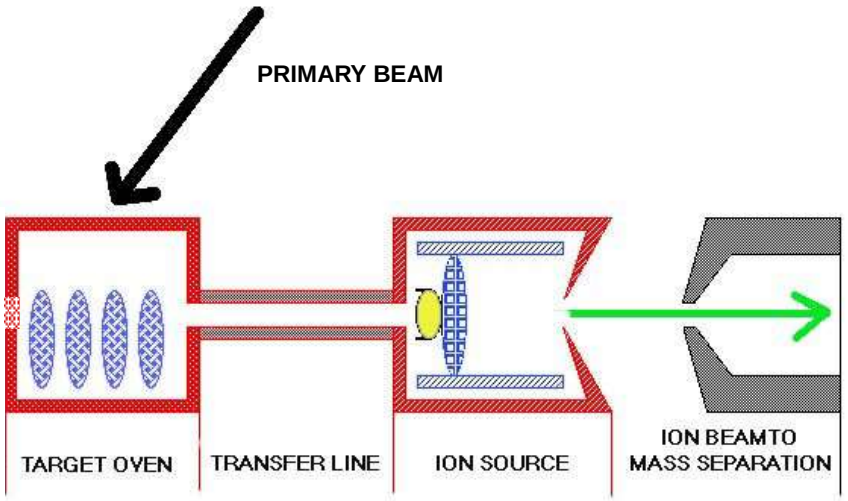

Isotope selection

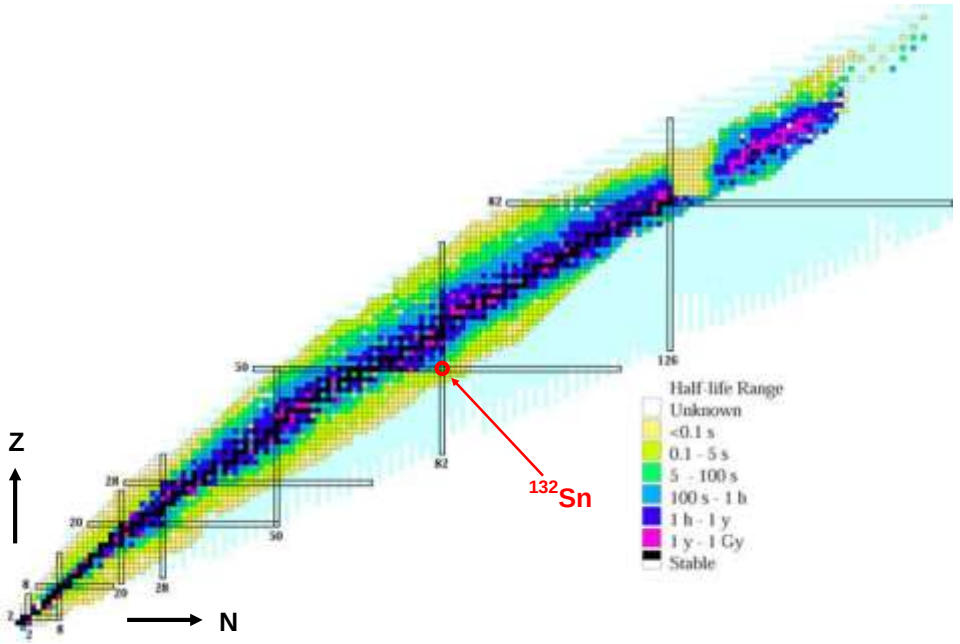

Isotope selection with ISOL method

- Ionization to q = 1+
- Acceleration to 60 keV
- Mass selection by magnetic deflection
- $B\rho = p/q \propto \sqrt{A}$

Z selection by chemically selective step

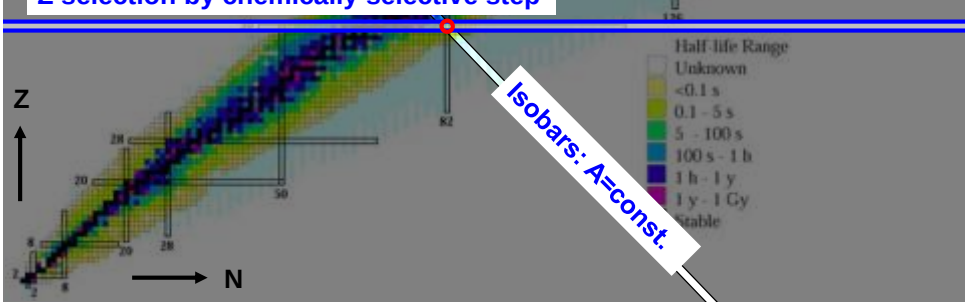

The challenge of the extremes!

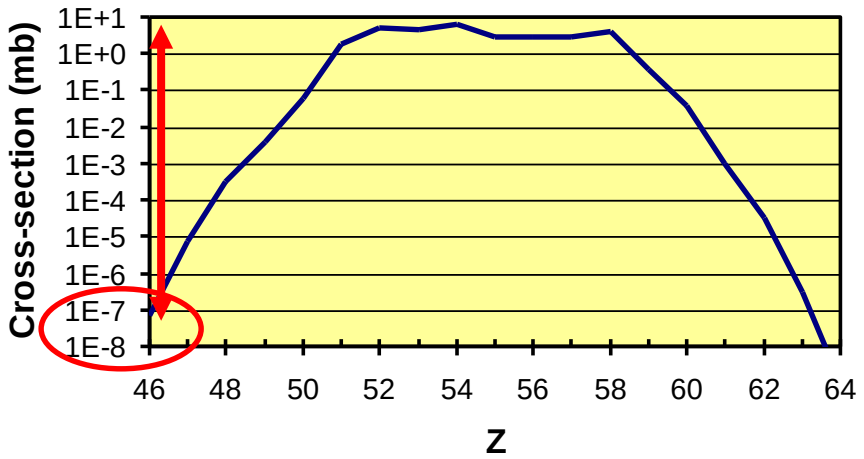

1. low cross-sections ⇒ optimize efficiency
2. enormous production of isobars ⇒ optimize selectivity
3. short half-lives ⇒ optimize rapidity

Optimize event rate

All steps of the separation chain need to be optimized!

$$r = \underbrace{\Phi \cdot \sigma \cdot N}_{\text{In-target production}} \cdot \underbrace{\varepsilon_{target} \cdot \varepsilon_{source} \cdot \varepsilon_{transp} \cdot \varepsilon_{det}}_{\text{Efficiency}}$$

Optimize RIB intensity

All steps of the separation chain need to be optimized!

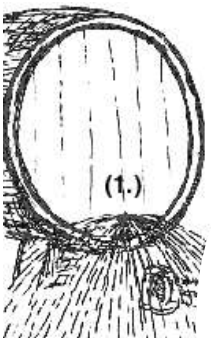

$$r = \Phi \cdot \sigma \cdot N \cdot \varepsilon_{target} \cdot \varepsilon_{source} \cdot \varepsilon_{transp} \cdot \varepsilon_{det}$$

powerful accelerator

$\Rightarrow$ **accelerator technology**

Optimize RIB intensity

All steps of the separation chain need to be optimized!

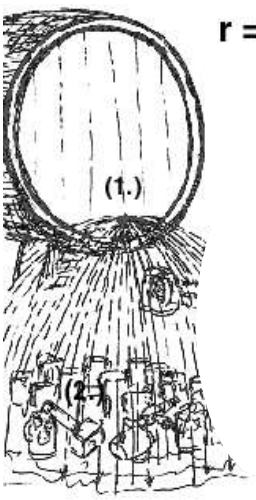

$$r = \Phi \cdot \sigma \cdot N \cdot \varepsilon_{target} \cdot \varepsilon_{source} \cdot \varepsilon_{transp} \cdot \varepsilon_{det}$$

high production cross-sections

$\Rightarrow$ **nuclear physics**

Optimize RIB intensity

All steps of the separation chain need to be optimized!

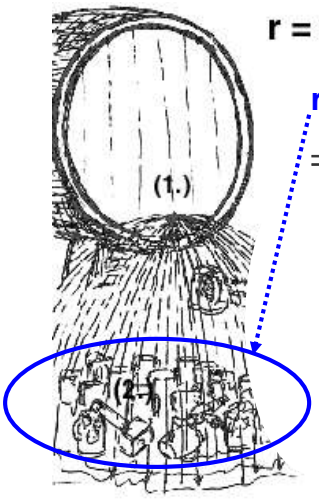

$$r = \Phi \cdot \sigma \cdot N \cdot \varepsilon_{target} \cdot \varepsilon_{source} \cdot \varepsilon_{transp} \cdot \varepsilon_{det}$$

reliable "thick" targets

⇒ materials science

Optimize RIB intensity

All steps of the separation chain need to be optimized!

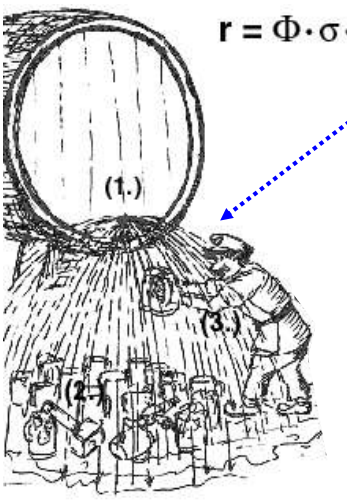

$$r = \Phi \cdot \sigma \cdot N \cdot \varepsilon_{target} \cdot \varepsilon_{source} \cdot \varepsilon_{transp} \cdot \varepsilon_{det}$$

Extraction efficiency from target determined by:

- bulk diffusion
  ⇒ **solid state physics**
- surface desorption
  ⇒ **surface chemistry**
- effusion
  ⇒ **gas phase chemistry**

strongly element dependent!

Optimize RIB intensity

All steps of the separation chain need to be optimized!

$$r = \Phi \cdot \sigma \cdot N \cdot \varepsilon_{target} \cdot \varepsilon_{source} \cdot \varepsilon_{transp} \cdot \varepsilon_{det}$$

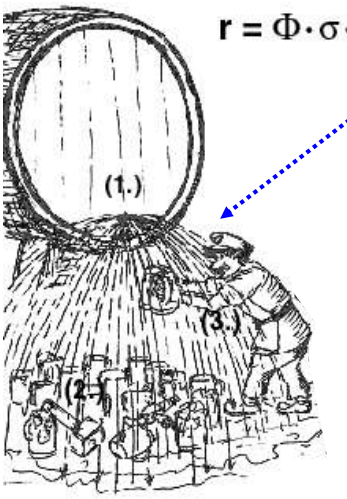

high ionization and extraction efficiency

⇒ ion source technology

Optimize RIB intensity

All steps of the separation chain need to be optimized!

$$r = \Phi \cdot \sigma \cdot N \cdot \varepsilon_{target} \cdot \varepsilon_{source} \cdot \varepsilon_{transp} \cdot \varepsilon_{det}$$

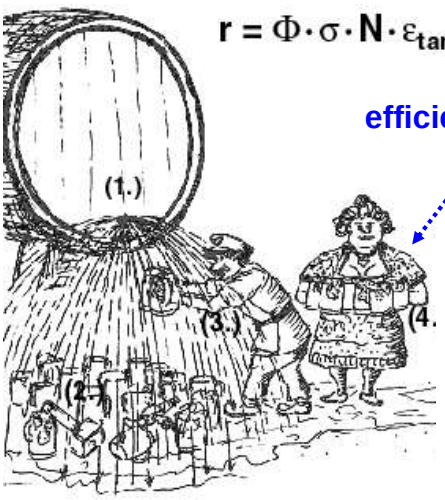

efficient transport of RIB

⇒ ion optics

Optimize RIB intensity

All steps of the separation chain need to be optimized!

$$r = \Phi \cdot \sigma \cdot N \cdot \underbrace{\varepsilon_{target} \cdot \varepsilon_{source} \cdot \varepsilon_{transp}} \cdot \varepsilon_{det}$$

Mind the decay losses during delays

⇒ efficiency strongly half-life dependent

⇒ rapid extraction required!

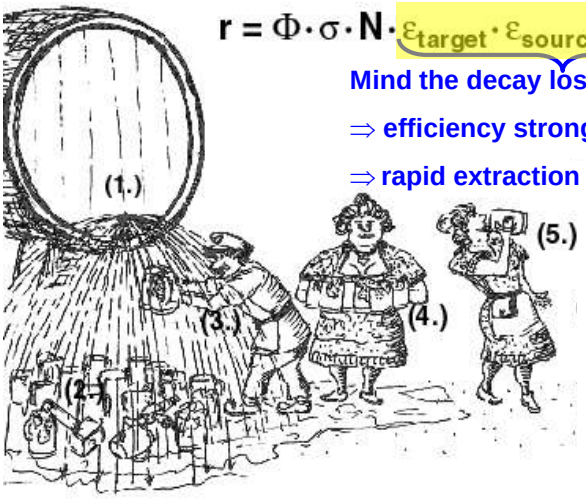

Optimize RIB intensity

All steps of the separation chain need to be optimized!

$$r = \Phi \cdot \sigma \cdot N \cdot \varepsilon_{target} \cdot \varepsilon_{source} \cdot \varepsilon_{transp} \cdot \varepsilon_{det}$$

Detection efficiency

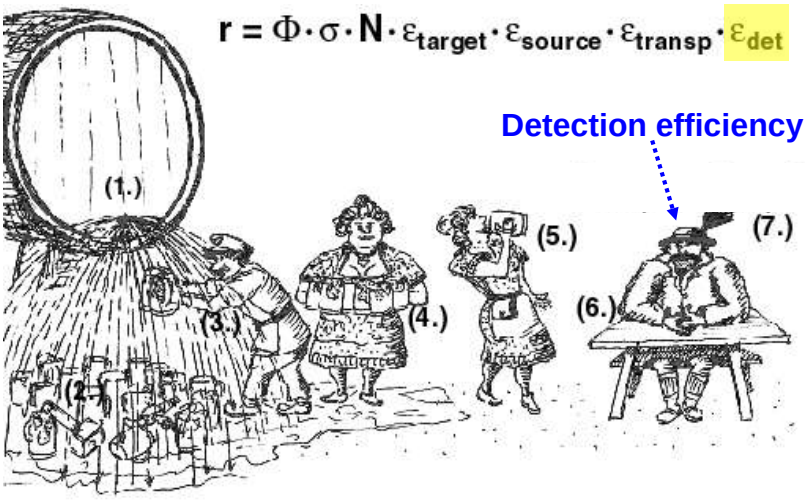

Optimize RIB intensity and purity

All steps of the separation chain need to be optimized!

$$r = \Phi \cdot \sigma \cdot N \cdot \varepsilon_{target} \cdot \varepsilon_{source} \cdot \varepsilon_{transp} \cdot \varepsilon_{det}$$

Selective separation required for exotic isotopes!

⇒ chemistry

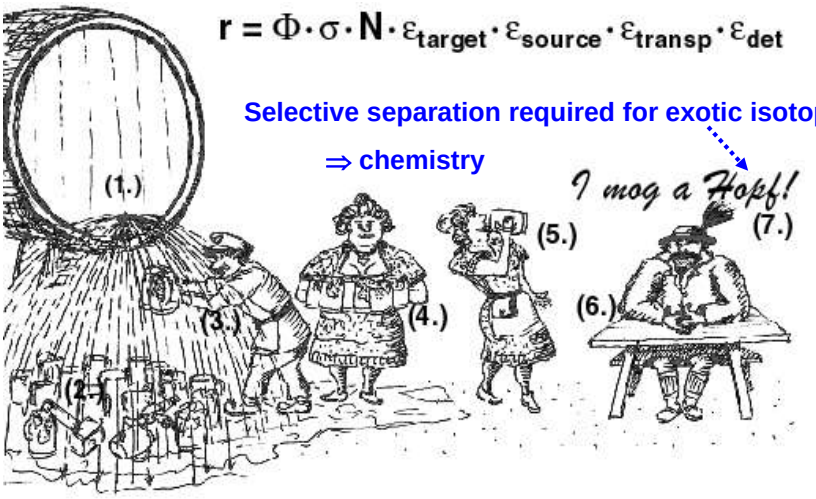

Optimize RIB intensity

Factors are highly correlated and isotope dependent!

$$r = \Phi \cdot \sigma \cdot N \cdot \varepsilon_{target} \cdot \varepsilon_{source} \cdot \varepsilon_{transp} \cdot \varepsilon_{det}$$

Individual optimisation!

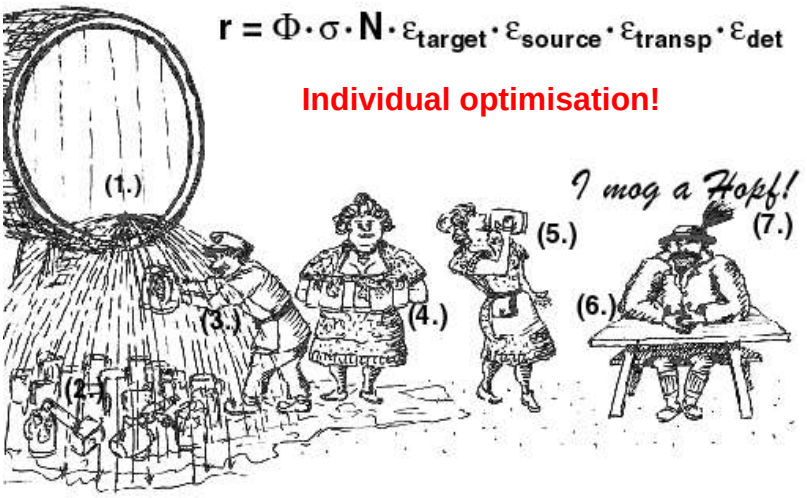

Prog. Part. Nucl. Phys. 46 (2001) 411.

Particle accelerators

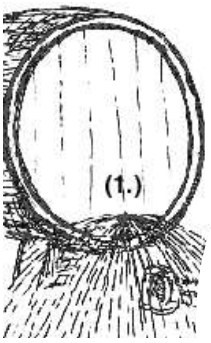

$$r = \Phi \cdot \sigma \cdot N \cdot \varepsilon_{target} \cdot \varepsilon_{source} \cdot \varepsilon_{transp} \cdot \varepsilon_{det}$$

CERN synchrocyclotron 1957-1990

600 MeV p

up to 4 μA

910 MeV ^{3}He

1 GeV ^{12}C

CERN accelerator structure

CERN-PS Booster Synchrotrons

E_p = 1.4 GeV

$3 \cdot 10^{13}$ protons/pulse = 5 μC

$I_{average}$ = 4 μA

$p_{average}$ = 6 kW

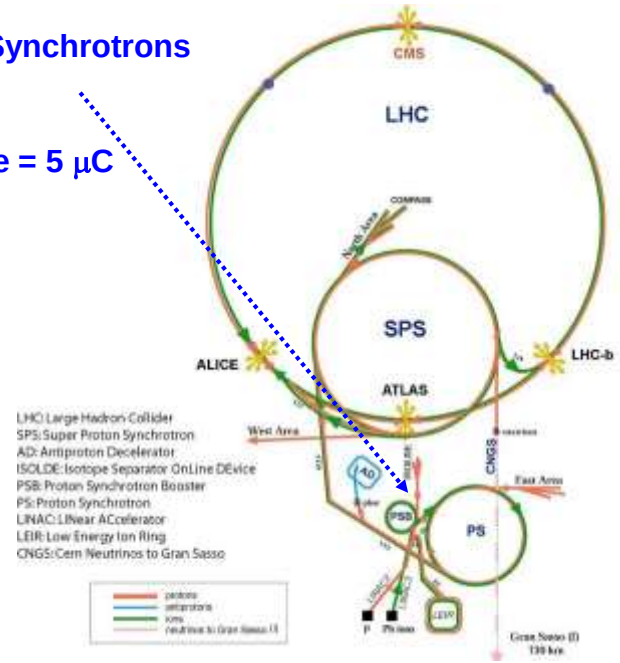

Nuclear reactions

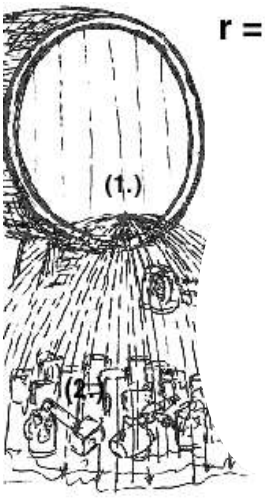

$$r = \Phi \cdot \sigma \cdot N \cdot \varepsilon_{target} \cdot \varepsilon_{source} \cdot \varepsilon_{transp} \cdot \varepsilon_{det}$$

Direct reactions

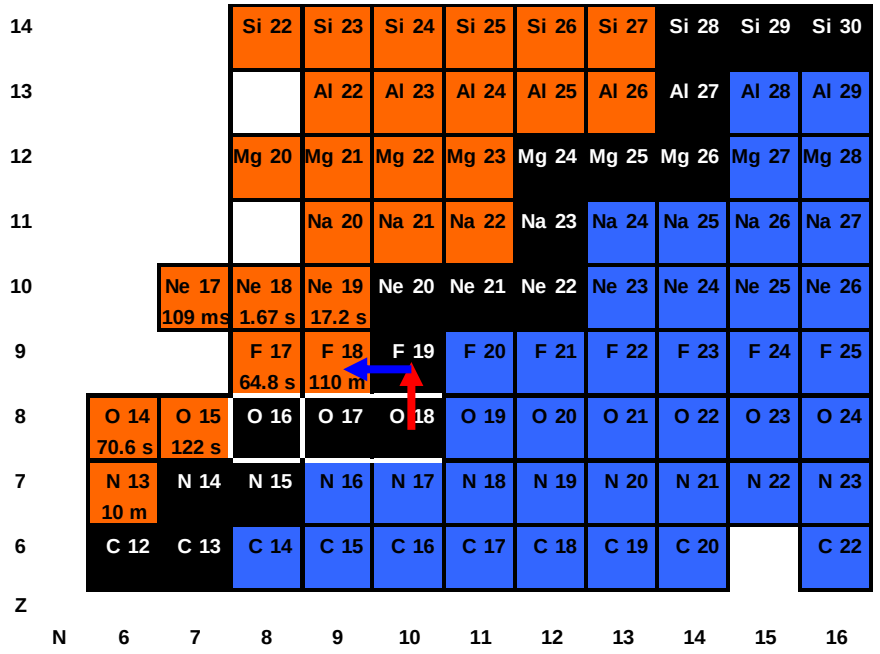

$^{18}O(p,n)^{18}F$ cross-sections

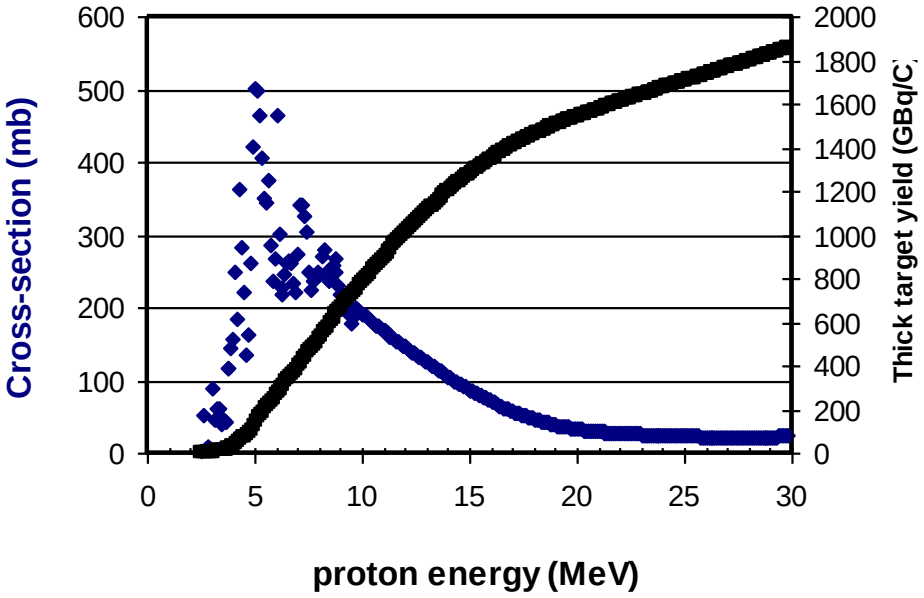

Nuclear reactions

1. Direct reactions and light ion fusion-evaporation

- (p,n), (^{3}He,n), (α,n), (n,α),...
- high cross-sections, products relatively close to stability
- driver beams from (low-cost) cyclotrons

Fusion-evaporation

^{58}Ni(^{58}Ni,2n)^{114}Ba

^{58}Ni(^{58}Ni,α2n)^{110}Xe

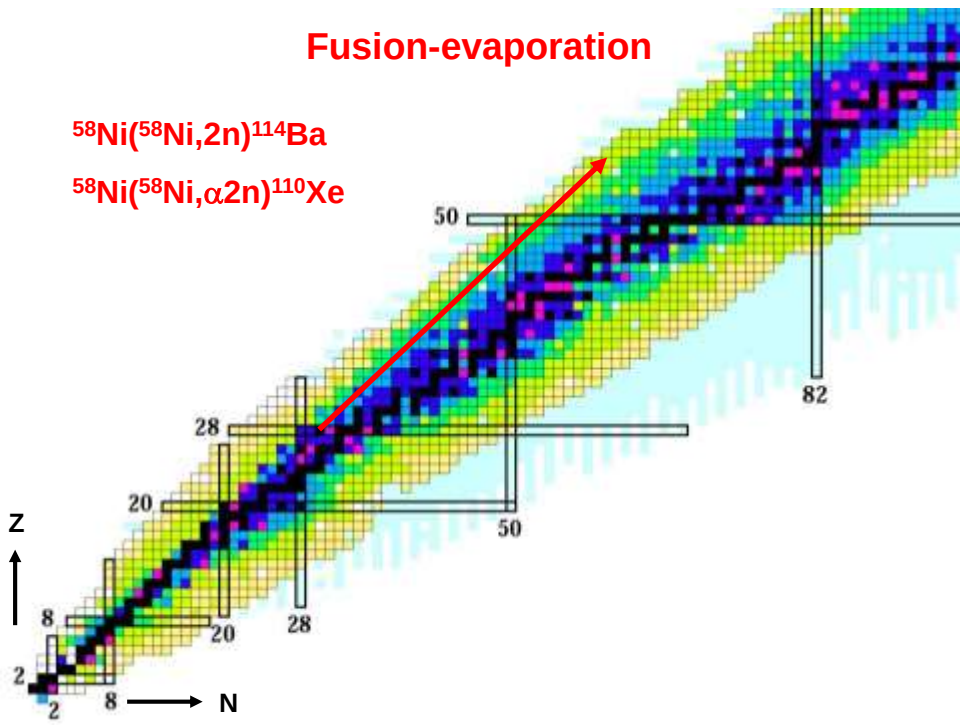

Nuclear reactions

1. Direct reactions and light ion fusion-evaporation

- (p,n), (^{3}He,n), (α,n), (n,α),...
- high cross-sections, products relatively close to stability
- driver beams from (low-cost) cyclotrons

2. Heavy-ion fusion-evaporation

- produces neutron-deficient heavier isotopes
- small energy window in vicinity of Coulomb barrier (some MeV/nucl.)
- requires heavy ion beams $\Rightarrow$ bigger cyclotrons or LINACs

Multinucleon transfer reactions

^{186}W(^{64}Ni,X)^{184}Lu

K. Krumbholz et al., Z. Phys. A352 (1995) 1.

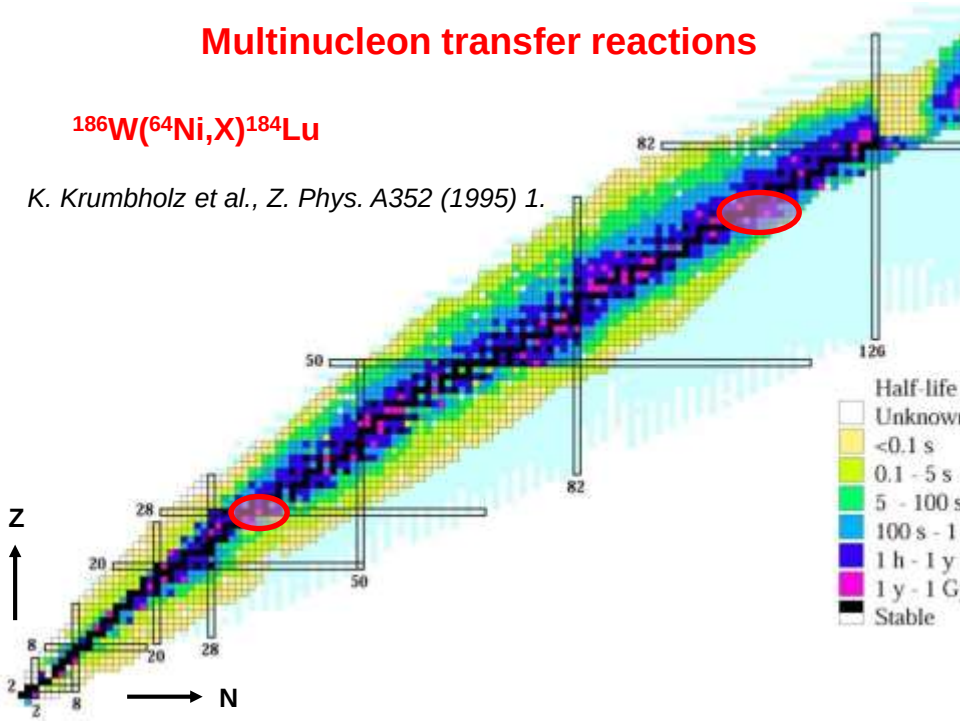

Nuclear reactions

1. Direct reactions
- high cross-sections, products relatively close to stability
- driver beams from (low-cost) cyclotrons

2. Heavy-ion fusion-evaporation
- produces neutron-deficient heavier isotopes
- small energy window in vicinity of Coulomb barrier (some MeV/nucleon)
- requires heavy ion beams ⇒ bigger cyclotrons or LINACs

3. Deep inelastic collisions (multi-nucleon transfer)
- products close to target, mass-flow towards stability
- light to heavy ion beams (tens of MeV/nucleon)
- only method to reach neutron-rich isotopes with $N_{product} > N_{target} + 1$

4. Spallation
- intranuclear cascade heats nucleus
- evaporation of preferentially neutrons ⇒ neutron-deficient products
- high cross-sections for products close to target
- requires protons of >100 MeV ⇒ big p cyclotron, synchrotron or LINAC

Spallation + Fragmentation + Fission

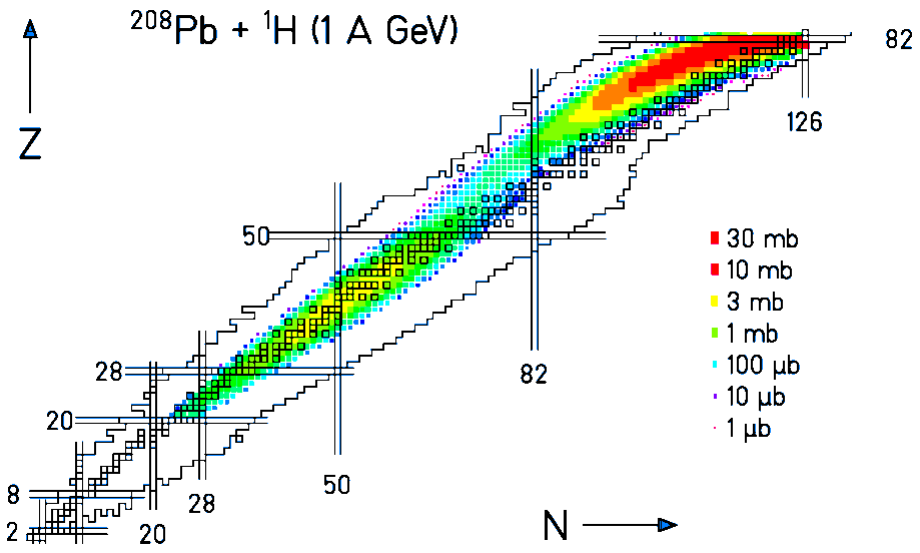

T. Enqvist et al., Nucl. Phys. A686 (2001) 481.

Low-energy fission

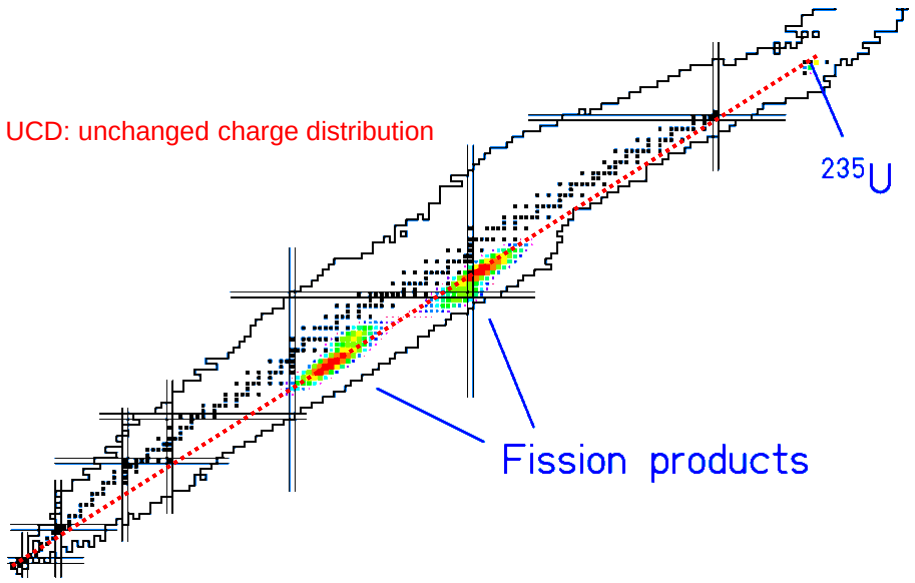

"Low-energy" fission ($^{238}U(\gamma,f)$ from 50 MeV e^-)

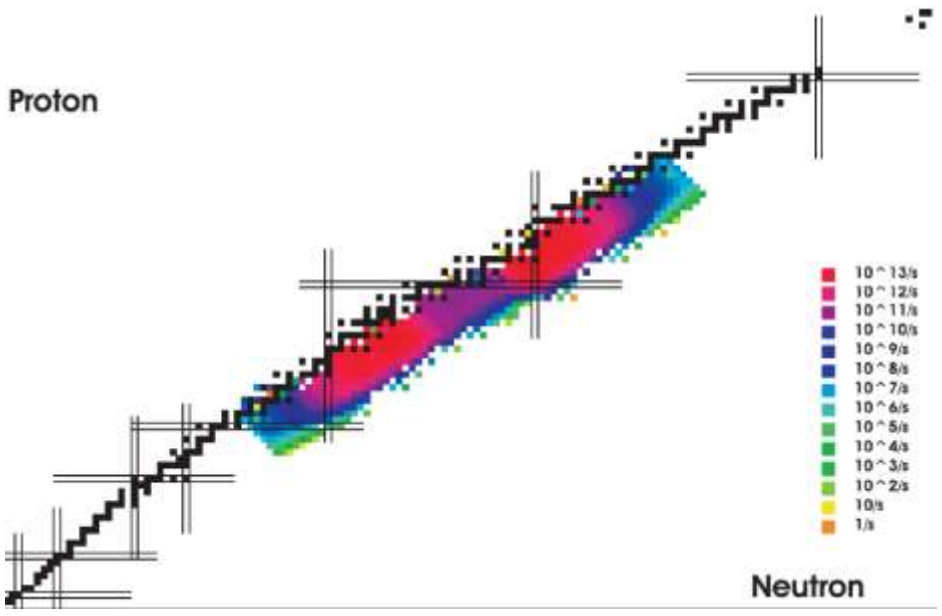

High-energy fission (500 MeV p on ^{238}U)

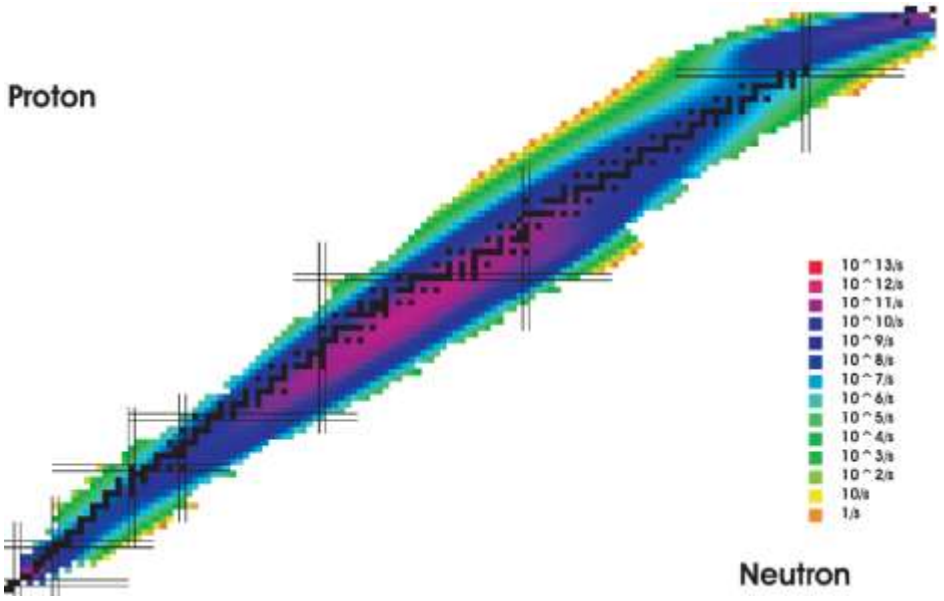

Nuclear reactions

5. Fragmentation

- many cross-sections show little energy dependence in the region 40-2000 MeV/nucleon
- target fragmentation needs high energy protons (see spallation)
- projectile fragmentation needs high energy heavy ions
  ⇒ huge cyclotron, synchrotron or LINAC

6. Fission

- induced by: “time” (**spontaneous**), **neutrons**, **photons**, **protons**, **heavy ions**, antiprotons, pions, post fusion-evaporation, beta-decay/EC
- highest cross-sections for thermal neutrons
- with increasing excitation energy symmetric and far asymmetric fission is favored, but the products get in average less neutron-rich!
- driver accelerators: reactors, medium-energy (some MeV to tens MeV) deuterons from cyclotron or LINAC, microtron or LINAC for electron beams,…

Radioactive ion beam facilities for fission products

Previous, presently operating and future RIB facilities using fission:

^{252}Cf(sf)	CARIBU
^{235}U(n_{th},f)	OSTIS, OSIRIS, LOHENGRIN, TRIGA-SPEC, CARR-ISOL, PIAFE, MAFF, PIK-ISOL
^{238}U(p,f)	ISOLDE, IRIS, LISOL, JYFL, HRIBF, TRIAC, ISAC-II, SPES, ISOL@MYRRHA, EURISOL
W(p,xn..) > ^{238}U(n,f)	ISOLDE, IRIS, ISAC-II, EURISOL
^{12}C(d,n) > ^{238}U(n,f)	PARRNe, SPIRAL-II
^{2}H(d,n) > ^{238}U(n,f)	SPIRAL-II
^{9}Be(d,n) > ^{238}U(n,f)	PARRNe
^{7}Li(d,n) > ^{238}U(n,f)	FRIB
W(e^-,γ) > ^{238}U(γ,f)	ALTO, DRIBS, ARIEL
^{1}H, ^{9}Be..^{208}Pb(^{238}U,f)	GSI-FRS, RIKEN, FRIB, FAIR

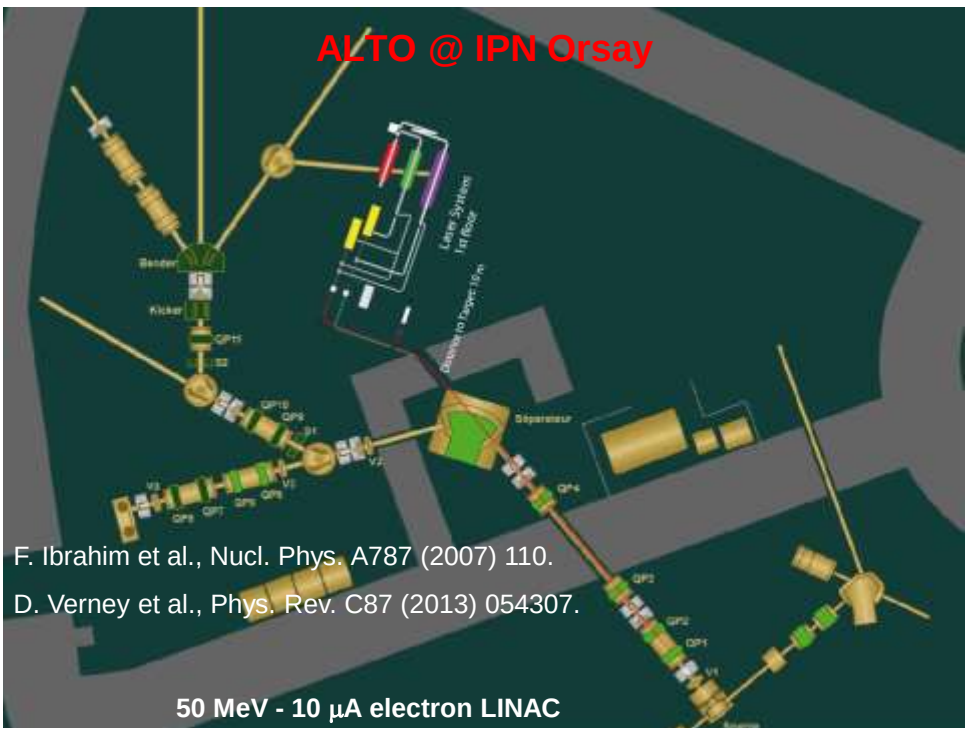

ISAC @ TRIUMF: ARIEL photo-fission upgrade

- **50 MeV, 10 mA electron LINAC**
- **<100 kW till 2015, 500 kW till 2020**
- **aim 4.6E13 fissions/s with liquid Hg converter**
- **but also 500 MeV protons with maximum 10 μA on UC_x**

SPIRAL2 facility at GANIL

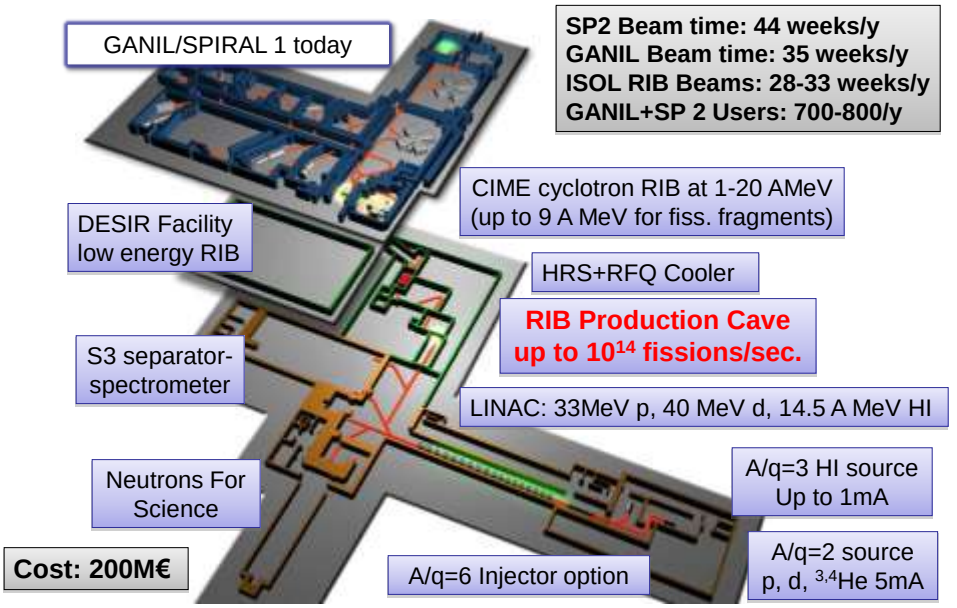

SPIRAL2 RIB production module

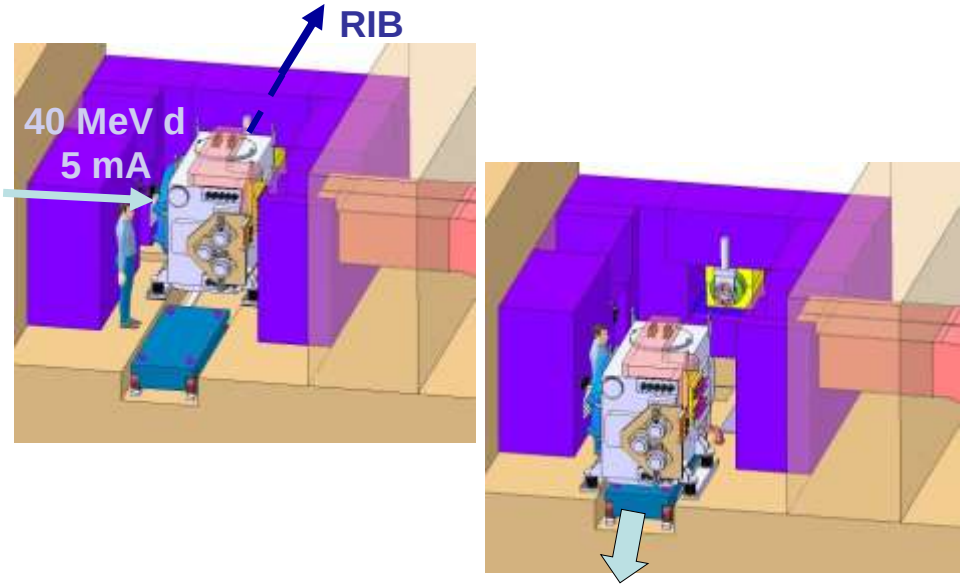

EURISOL

1-2.2 GeV, multi-MW proton driver

Several direct target stations (ca. 100 kW)

One Hg spallation + fission target station (>1 MW, i.e. 1E15 fissions/s)

Multiple user operation in parallel

Low-energy beam area

Post-acceleration with LINAC up to ca. 10 A.MeV

Post-acceleration to ca. 100 A.MeV with LINAC or cyclotron

Fragmentation of post-accelerated RIBs

Commissioning: >> 2020?

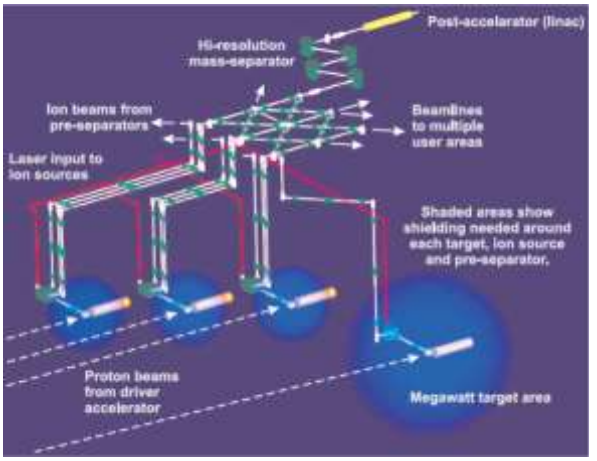

IGISOL method

$X^{n+} + He^0 \rightarrow X^{(n-1)+} + He^+$ or

$X^{n+} + Ar^0 \rightarrow X^{(n-1)+} + Ar^+$

rapid reduction of ionic charge state to 2+ or 1+ by charge exchange reactions with buffer gas

IP(He)=24.6 eV, IP(Ar)=15.8 eV

~~$X^+ + He^0 \rightarrow X^0 + He^+$~~ or

~~$X^+ + Ar^0 \rightarrow X^0 + Ar^+$~~

remains in 1+ or 2+ charge state until charge exchange reaction with impurity molecule (O_2, N_2,...) occurs

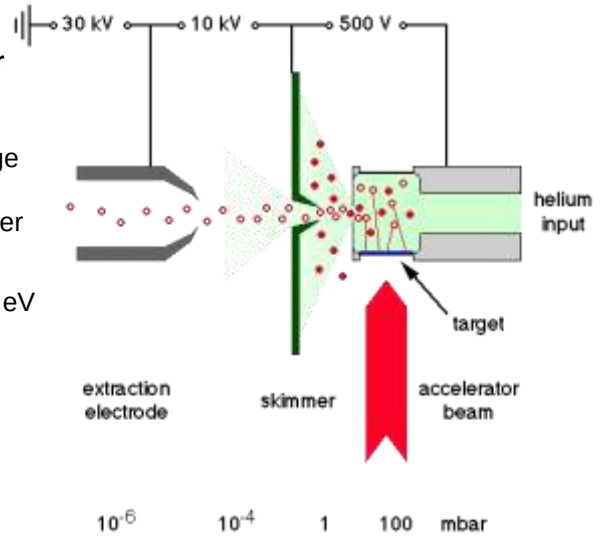

Volatility of the elements

T (p vapor > 0.01 mbar) < 100 °C
T (p vapor > 0.01 mbar) < 400 °C
T (p vapor > 0.01 mbar) < 1000 °C
T (p vapor > 0.01 mbar) < 2000 °C
T (p vapor > 0.01 mbar) > 2000 °C

1 H																	2 He
3 Li	4 Be											5 B	6 C	7 N	8 O	9 F	10 Ne
11 Na	12 Mg											13 Al	14 Si	15 P	16 S	17 Cl	18 Ar
19 K	20 Ca	21 Sc	22 Ti	23 V	24 Cr	25 Mn	26 Fe	27 Co	28 Ni	29 Cu	30 Zn	31 Ga	32 Ge	33 As	34 Se	35 Br	36 Kr
37 Rb	38 Sr	39 Y	40 Zr	41 Nb	42 Mo	43 Tc	44 Ru	45 Rh	46 Pd	47 Ag	48 Cd	49 In	50 Sn	51 Sb	52 Te	53 I	54 Xe
55 Cs	56 Ba	57 La	72 Hf	73 Ta	74 W	75 Re	76 Os	77 Ir	78 Pt	79 Au	80 Hg	81 Tl	82 Pb	83 Bi	84 Po	85 At	86 Rn
87 Fr	88 Ra	89 Ac	104 Rf	105 Db	106 Sg	107 Bh	108 Hs	109 Mt	110 Ds	111 Rg	112 Cn	113	114 Fl	115	116 Lv	117	118

58 Ce	59 Pr	60 Nd	61 Pm	62 Sm	63 Eu	64 Gd	65 Tb	66 Dy	67 Ho	68 Er	69 Tm	70 Yb	71 Lu
90 Th	91 Pa	92 U	93 Np	94 Pu	95 Am	96 Cm	97 Bk	98 Cf	99 Es	100 Fm	101 Md	102 No	103 Lr

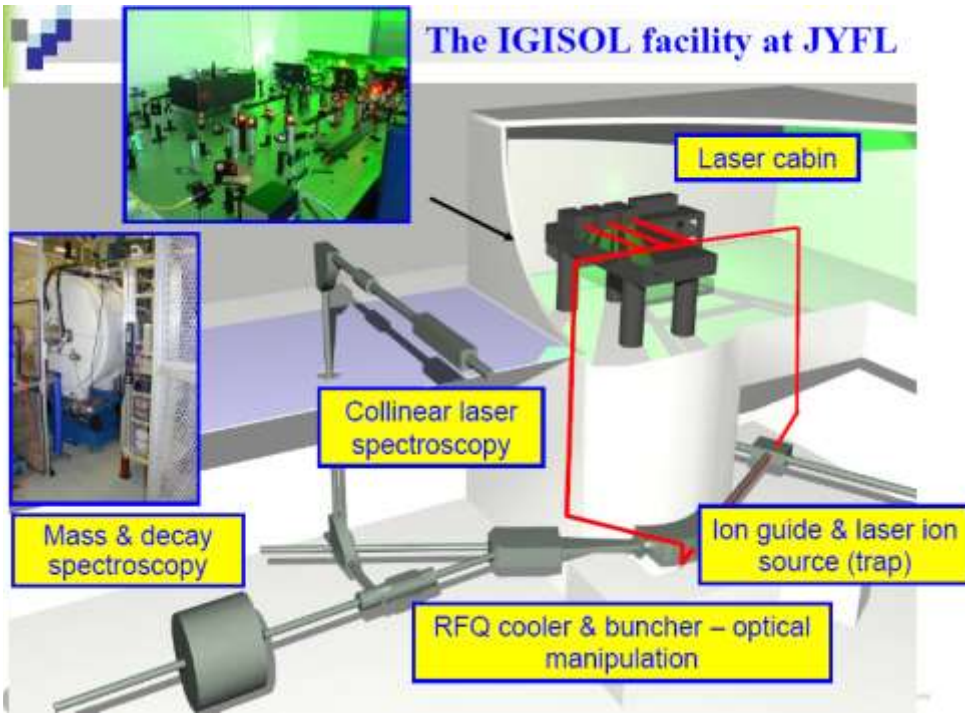

CARIBU: Radioactive Beams from ^{252}Cf(sf)

R. M. Yee et al., Phys. Rev. Lett. 110 (2013) 092501.

J. Van Schelt et al., Phys. Rev. C 85 (2012) 045805.

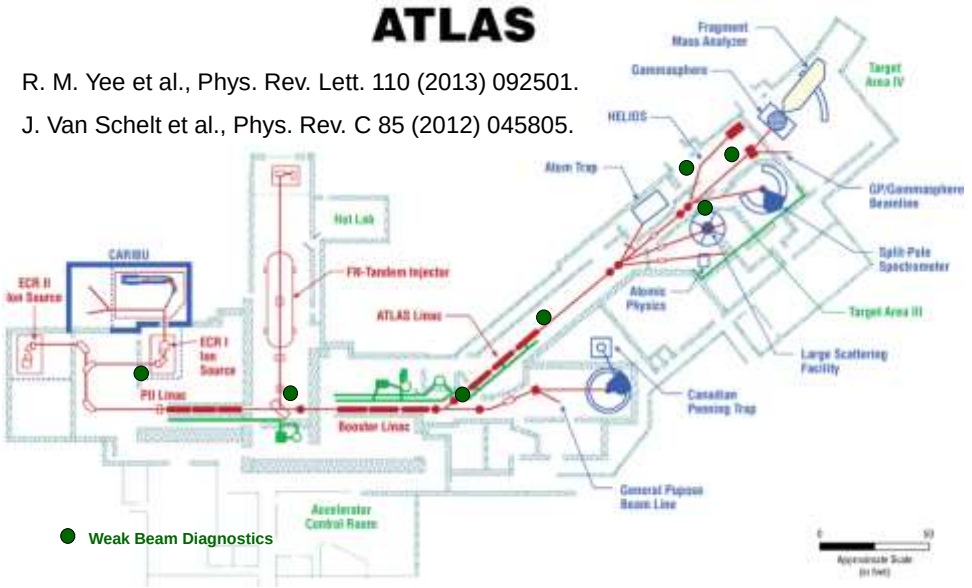

1 Ci ^{252}Cf source: 1E9 fissions/s

TRIGA-SPEC at Mainz reactor

- **0.5 mg ^{235}U or 0.5 mg ^{239}Pu or 0.3 mg ^{249}Cf**
- **1.8E11 n./cm^2/s**
- **2E8 fissions/s**

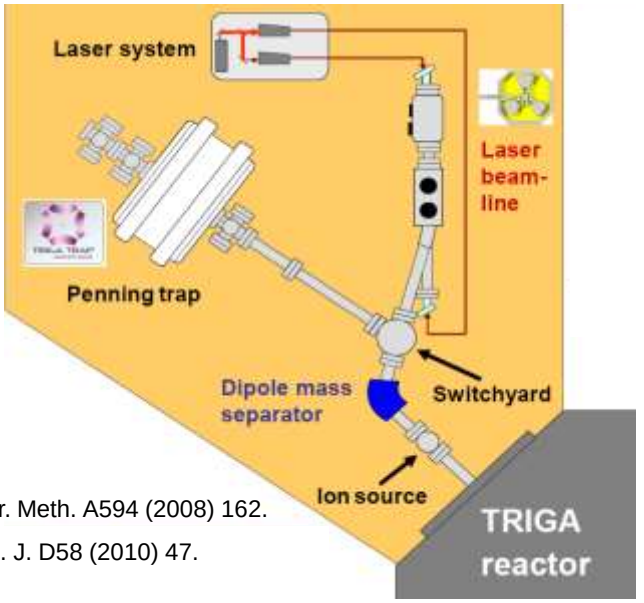

J. Ketelaer et al., Nucl. Instr. Meth. A594 (2008) 162.

J. Ketelaer et al., Eur. Phys. J. D58 (2010) 47.

Optimize RIB intensity

All steps of the separation chain need to be optimized!

$$r = \Phi \cdot \sigma \cdot N \cdot \varepsilon_{target} \cdot \varepsilon_{source} \cdot \varepsilon_{transp} \cdot \varepsilon_{det}$$

ISOLDE Target (1967)

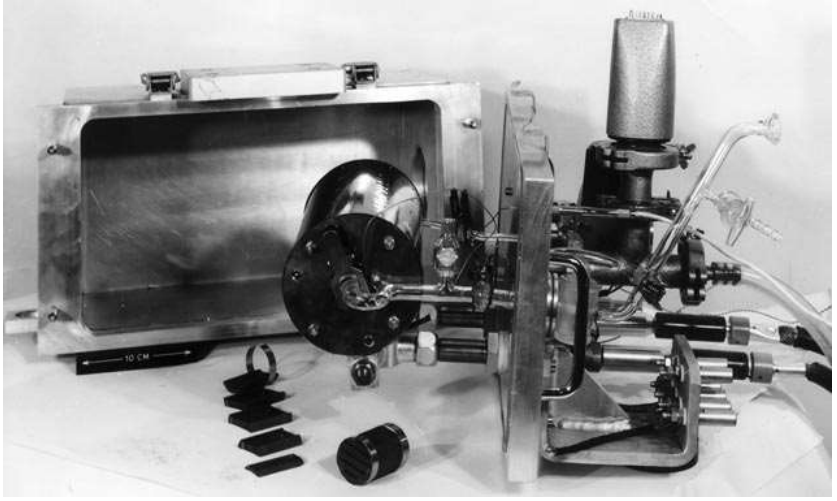

ISOLDE Target and ion source (1968)

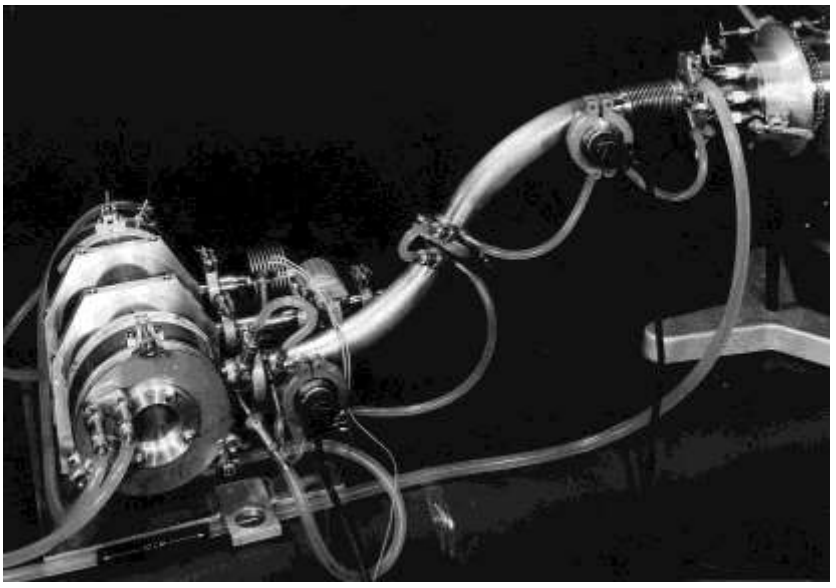

ISOLDE Compact target and ion source (1974)

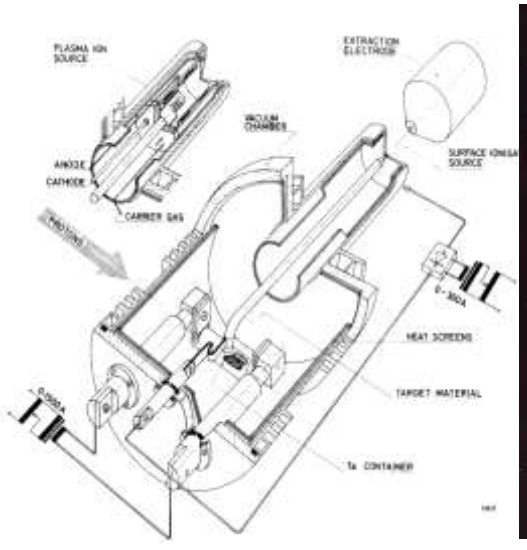

Robot handling

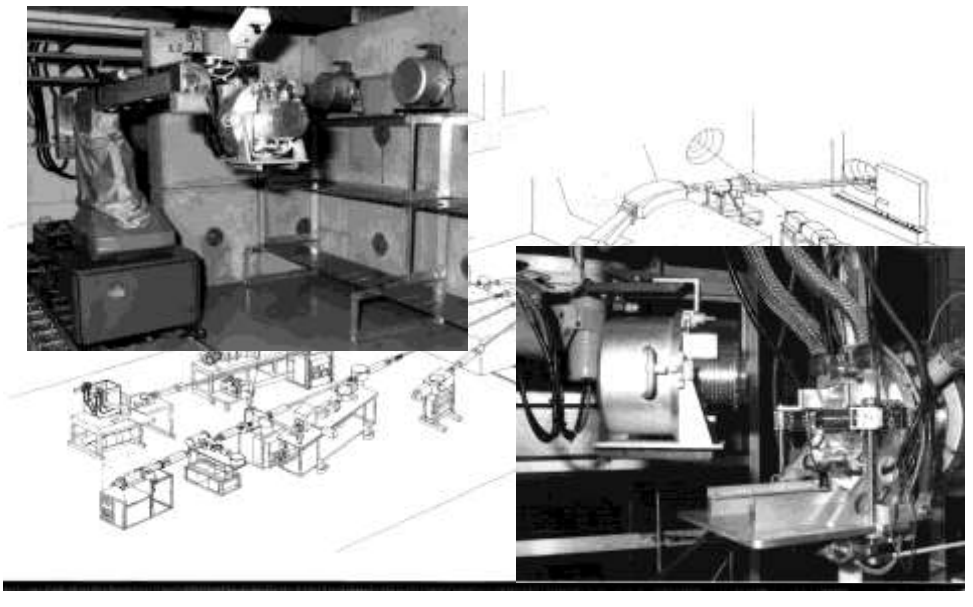

ISOLDE target and ion source unit

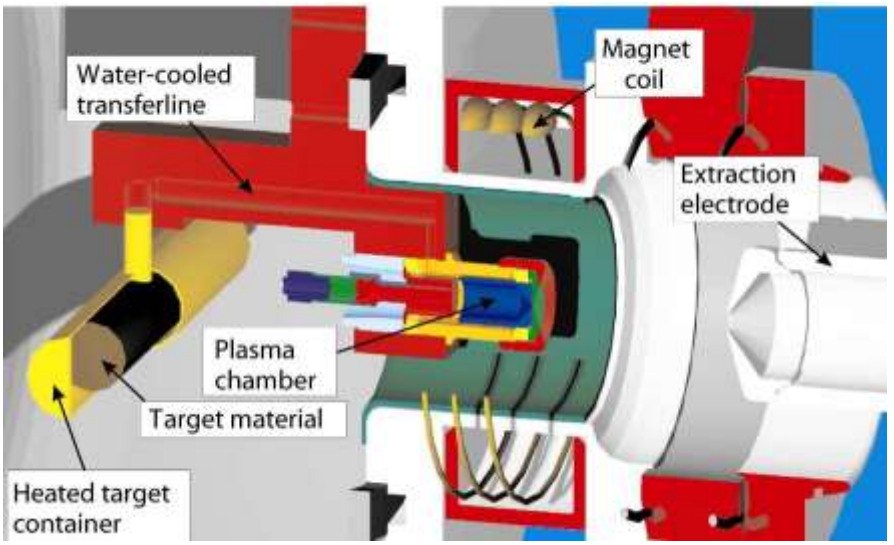

Historical development

Miniaturisation ⇒ **faster release**

Standardisation ⇒ **easier mass-production**

Remote handling ⇒ **higher activities**

SPIRAL target and ion source unit

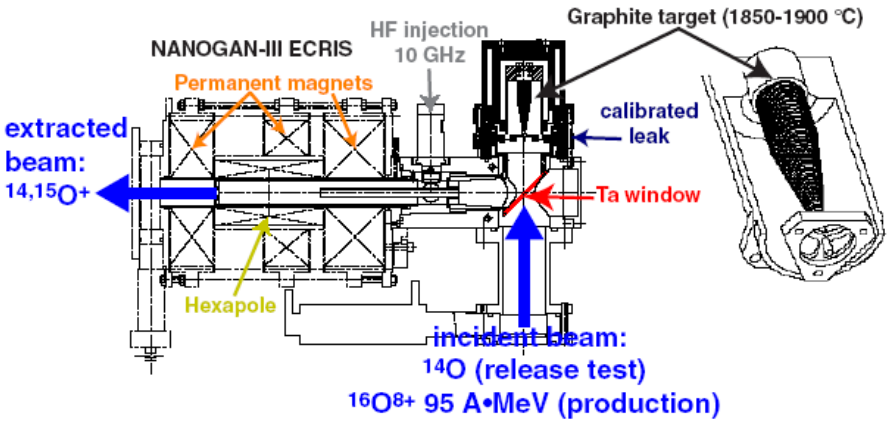

GSI-ISOL target and ion source unit

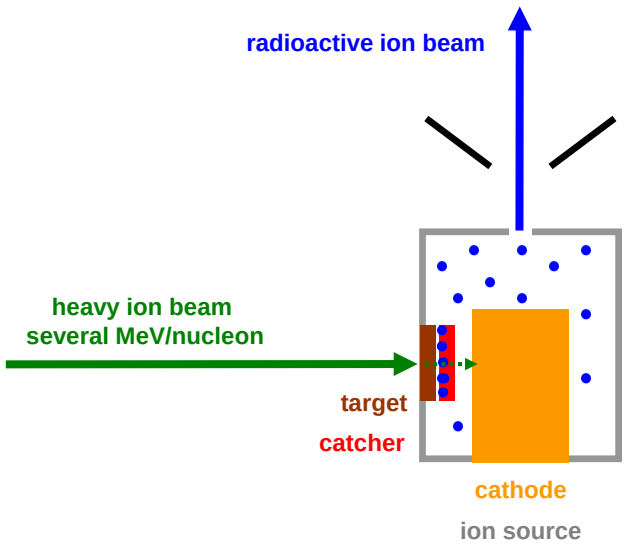

Variants of ISOL facilities

1a protons on thick (heavy) target: fragmentation, spallation, fission
ISOLDE-CERN (1.4 GeV), IRIS-PNPI (1 GeV), ISAC-TRIUMF (0.5 GeV)

1b direct reactions in thick target
CRC Louvain-la-Neuve, HRIBF Oak Ridge, TRIAC Tokai

1c fission in thick target
OSIRIS (Studsvik), HRIBF Oak Ridge, TRIAC Tokai, SPIRAL2 (GANIL)

2 projectile fragmentation in thick (carbon) target
SPIRAL (GANIL), DRIBS (Dubna), EXCYT (LNS Catania)

3 fusion-evap. or multinucleon transfer in thin target plus solid catcher
GSI-ISOL, UNIRIB (ORNL), DOLIS (Daresbury), LISOL (Leuven), IMP Lanzhou, TRIμP KVI Groningen, MASHA (Dubna), SPIRAL2 (GANIL)

4 fusion-evap., direct reaction or fission in thin target plus gas catcher (Ion Guide ISOL = IGISOL)
IGISOL (Jyväskylä), LISOL (Leuven), JAEA Tandem ISOL (Tokai),…

5 liquid helium catcher
JYFL Jyväskylä, KVI Groningen

ISOL targets

Target materials:

1. **molten metals:** Ge, Sn, La, Pb, Bi, U,...
2. **solid metals:** Ti, Zr, Nb, Mo, Ta, W, Th,...
3. **carbides:** Al_4C_3, SiC, VC, ZrC, LaC_x, ThC_x, UC_x,...
4. **oxides:** MgO, Al_2O_3, CaO, TiO_x, ZrO_2, CeO_x, ThO_2,...
5. **others:** graphite, borides, silicides, sulfides, zeolithes,...

Target dimensions:

target container: 20 cm long, 2 cm diameter

target thickness 2—200 g/cm^2, 10—100% of bulk density

micro-dimensions of foils, fibers or pressed powder: 1—30 μm

Radiochimica Acta 89 (2001) 749.

Diffusion characteristics

Bad diffusion hosts (narrow and/or stiff crystal lattice):

Re, diamond, SiC,...

Good diffusion hosts (wide crystal lattice):

Ti, Zr, Hf (fcc metals), Nb, Ta, graphite,
polycrystalline oxides (in particular fibers!)

Characteristic diffusion length:

$d = (2\ n\ D\ t)^{1/2}$ n=1 (foil), n=2 (fiber), n=3 (sphere)

Maximize D and minimize diffusion path:

⇒ thin metal foils (2 μm ... 30 μm)
⇒ fine powders (μm)
⇒ thin fibers (some μm)

Effusion: random walk release

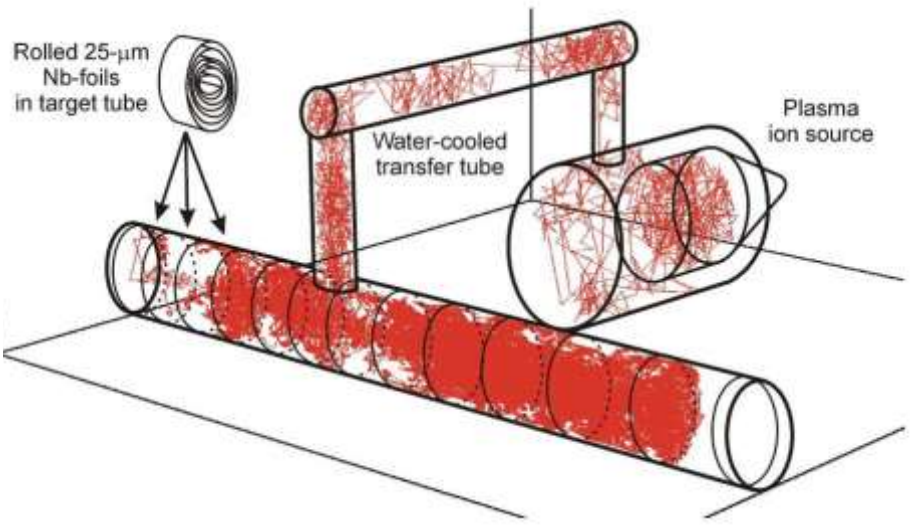

Optimize RIB intensity

All steps of the separation chain need to be optimized!

$$r = \Phi \cdot \sigma \cdot N \cdot \varepsilon_{target} \cdot \varepsilon_{source} \cdot \varepsilon_{transp} \cdot \varepsilon_{det}$$

*I*sotope *S*eparation *O*n-*L*ine

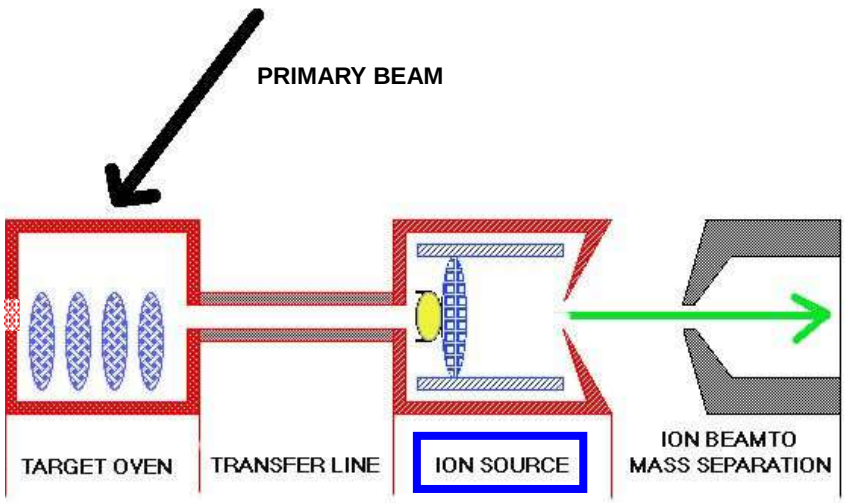

The first ionization energy of the elements

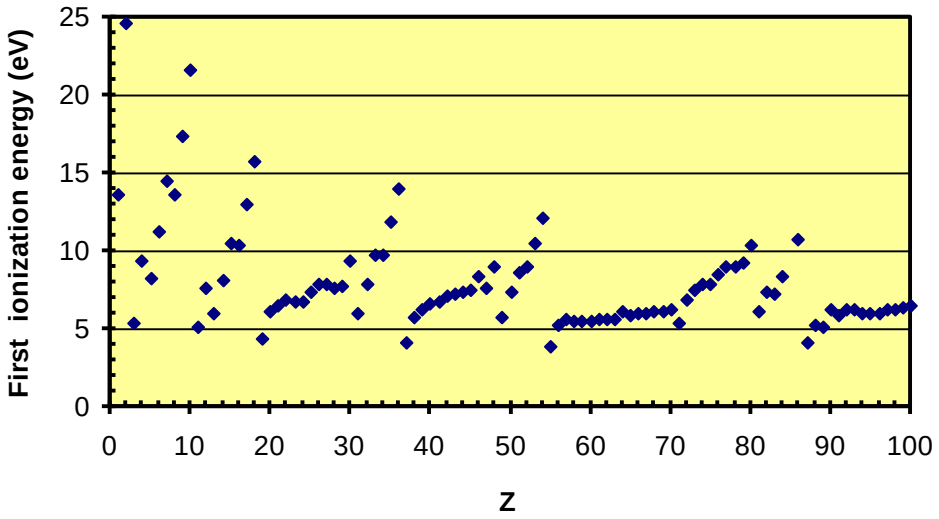

Positive surface ionization source

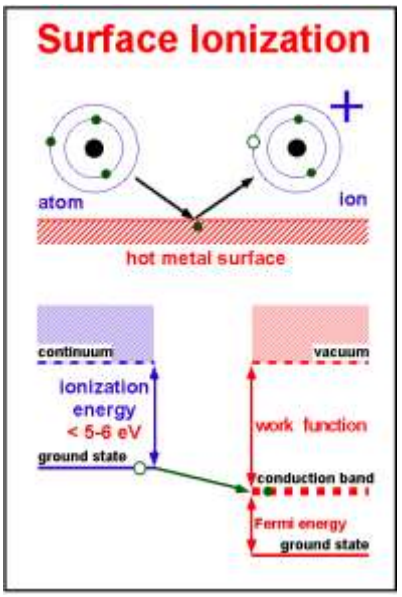

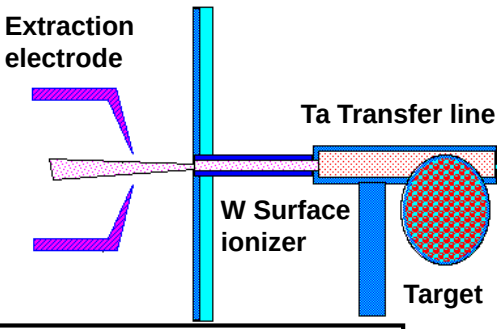

$$\alpha_s = g_+/g_0 \exp(-(IP - \Phi)/kT))$$

$$\varepsilon_s = \alpha_s / (1 + \alpha_s)$$

Saha-Langmuir equation

ε_s	surface ionization efficiency
Φ	work function of surface
IP	ionization potential of atom
g=2J+1	stat. factor (g_0=2, g_+=1 for alkalis)

Surface ionization versus thermal ionization

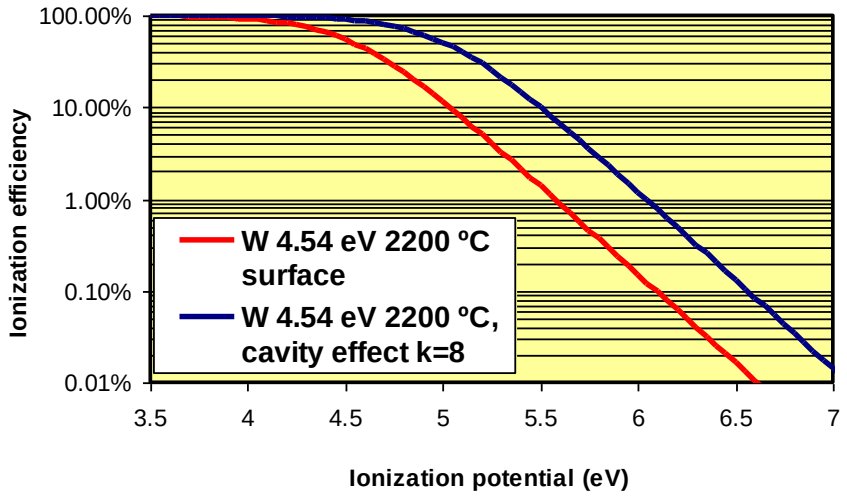

$$\varepsilon_{th} = 1/(1 + g_0/g_+/k \exp((IP - \Phi)/kT))$$

Thermal ionization efficiency in realistic ionizer cavity

R. Kirchner, Nucl. Instr. Meth. A292 (1987) 204.

Ionization potentials of the elements

Ionization potential: < 5 eV

Ionization potential: 5.0 - 5.8 eV

Ionization potential: 5.8 - 6.5 eV

1 H																	2 He
3 Li	4 Be											5 B	6 C	7 N	8 O	9 F	10 Ne
11 Na	12 Mg											13 Al	14 Si	15 P	16 S	17 Cl	18 Ar
19 K	20 Ca	21 Sc	22 Ti	23 V	24 Cr	25 Mn	26 Fe	27 Co	28 Ni	29 Cu	30 Zn	31 Ga	32 Ge	33 As	34 Se	35 Br	36 Kr
37 Rb	38 Sr	39 Y	40 Zr	41 Nb	42 Mo	43 Tc	44 Ru	45 Rh	46 Pd	47 Ag	48 Cd	49 In	50 Sn	51 Sb	52 Te	53 I	54 Xe
55 Cs	56 Ba	57 La	72 Hf	73 Ta	74 W	75 Re	76 Os	77 Ir	78 Pt	79 Au	80 Hg	81 Tl	82 Pb	83 Bi	84 Po	85 At	86 Rn
87 Fr	88 Ra	89 Ac	104 Rf	105 Db	106 Sg	107 Bh	108 Hs	109 Mt	110	111	112						

58 Ce	59 Pr	60 Nd	61 Pm	62 Sm	63 Eu	64 Gd	65 Tb	66 Dy	67 Ho	68 Er	69 Tm	70 Yb	71 Lu
90 Th	91 Pa	92 U	93 Np	94 Pu	95 Am	96 Cm	97 Bk	98 Cf	99 Es	100 Fm	101 Md	102 No	103 Lr

Ingredients of a plasma ion source

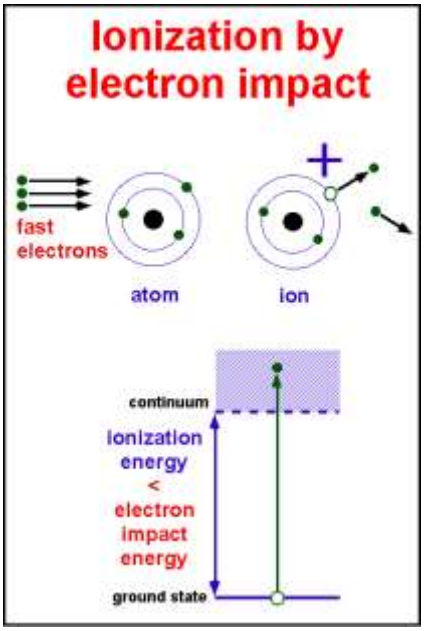

- Fast electrons:
  - A) Thermionic emission + accelerating field
  - B) RF heating
- Atom confinement: plasma chamber
- Electron "recycling": magnetic field
- Ion extraction system

$I[A] = A^* T[K]^2 \exp(-\Phi[eV]/kT[K])$

$A^* = 120\ A\ cm^{-2}\ K^{-2}$

$\nu_{cyc}[GHz] = 28\ B[T]$

$r[mm] = 0.35\ E_e[eV]^{1/2}/B[T]$

Ionization and neutralization

$X^0 + e^- \rightarrow X^+ + 2\ e^-,\ \ Q = -\ IP_1$

$X^0 + e^- \rightarrow X^{2+} + 3\ e^-,\ Q = -\ (IP_1 + IP_2)$

$X^0 + e^- \rightarrow X^{3+} + 4\ e^-,\ Q = -\ (IP_1 + IP_2 + IP_3)$

$X^+ + e^- \rightarrow X^{2+} + 2\ e^-,\ Q = -\ IP_2$

$X^+ + e^- \rightarrow X^0,\qquad Q = IP_1$ Neutralization

$X^0 + Y^+ \rightarrow X^+ + Y^0,\quad Q = IP_Y - IP_X$ Charge exchange

Electron impact ionization cross-sections

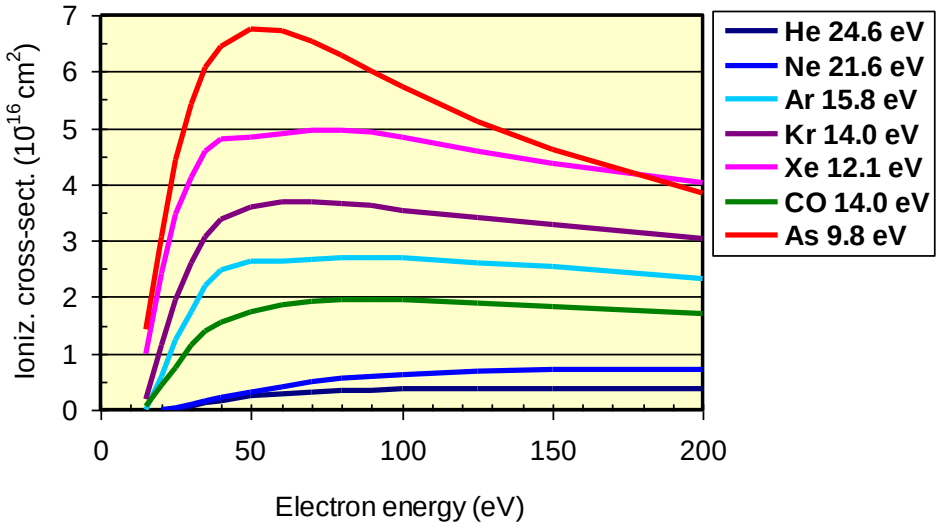

Forced Electron Beam Ion Arc Discharge (FEBIAD)

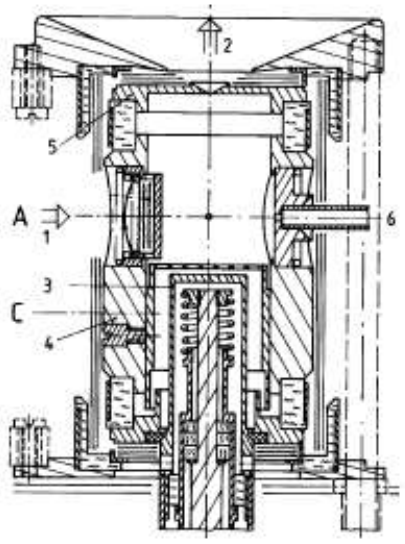

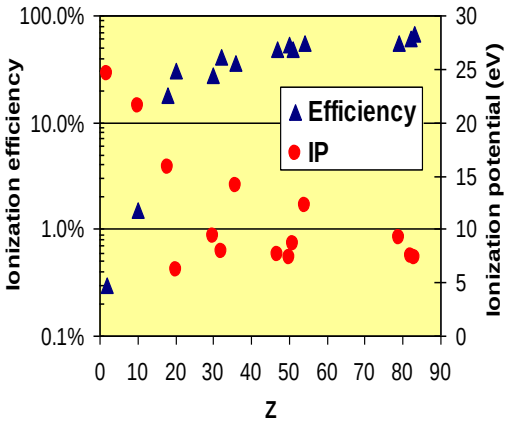

FEBIAD ion sources are excellent for heavier elements!

R. Kirchner, Rev. Sci. Instr. 67 (1996) 928.

ISOLDE "FEBIAD"

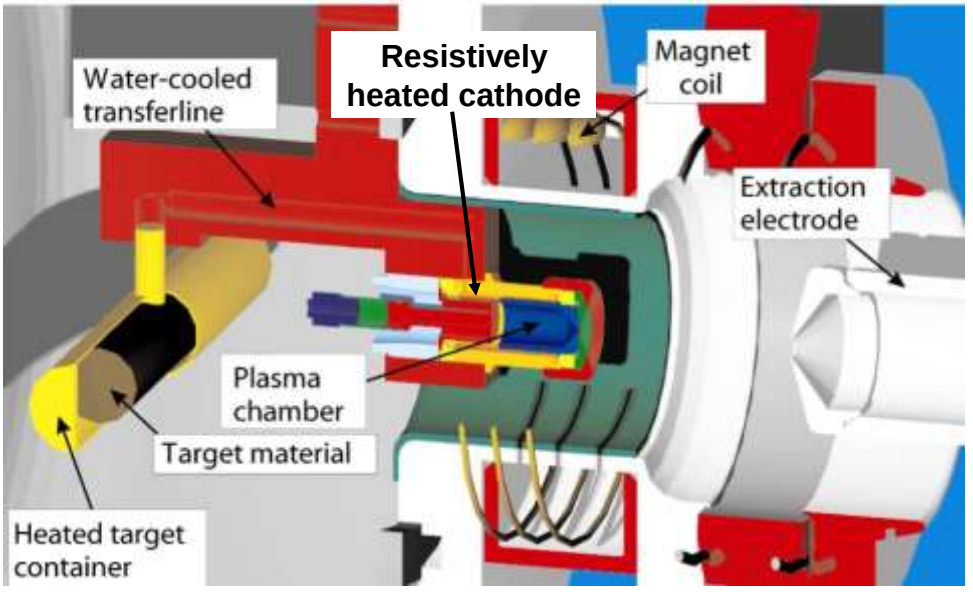

2001: $^{94\text{-}99}$Kr decay studied at ISOLDE

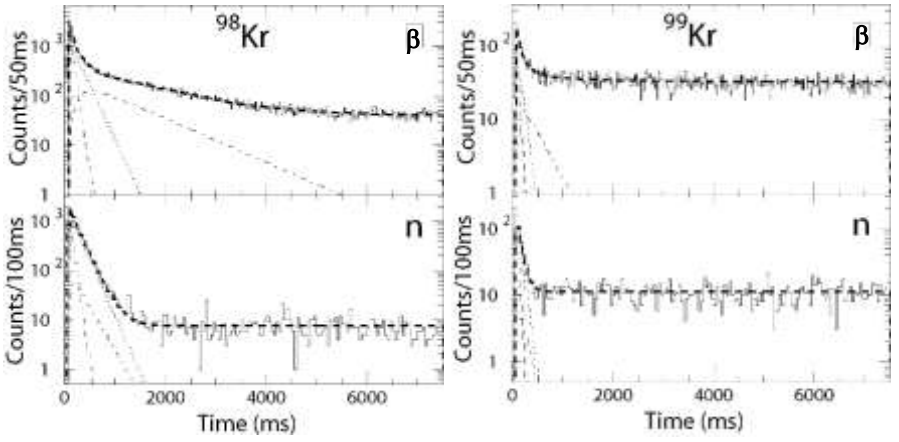

U.C. Bergmann et al., Nucl. Phys. A 714 (2003) 21.

ISOLDE VADIS

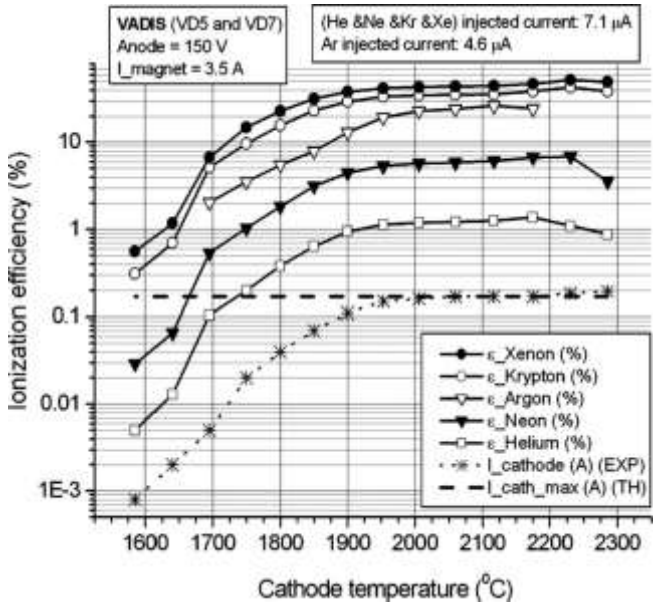

L. Penescu et al., Rev. Sci. Instr. 81 (2010) 02A906.

Electron Cyclotron Resonance Ion Source (ECRIS)

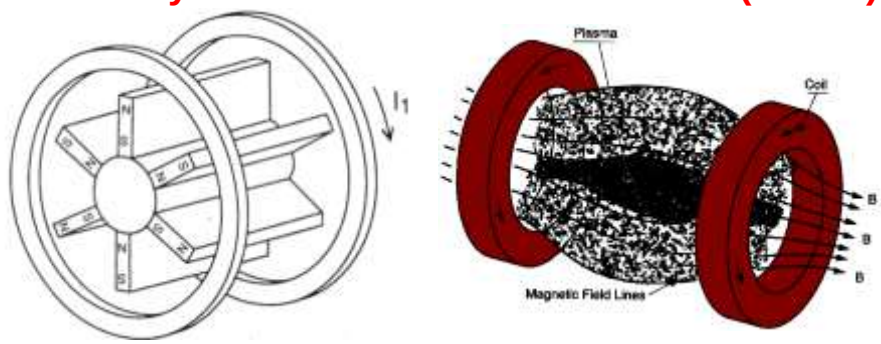

radial plasma confinement by magnetic multipole field

longitudinal plasma confinement by magnetic bottle effect (1+ ECRIS) or minimum B configuration (n+ ECRIS)

plasma heating by RF (typically 2.45 – 30 GHz)

good efficiency for light elements (20% He^+, 50% C^+, O^+, Ar^+, 90% Xe^+)

R. Geller, Electron Cyclotron Resonance Ion Sources and ECR Plasmas, IOP, Bristol, 1996.

Volatility of the elements

T (p vapor > 0.01 mbar) < 100 °C
T (p vapor > 0.01 mbar) < 400 °C
T (p vapor > 0.01 mbar) < 1000 °C
T (p vapor > 0.01 mbar) < 2000 °C
T (p vapor > 0.01 mbar) > 2000 °C

1 H																	2 He
3 Li	4 Be											5 B	6 C	7 N	8 O	9 F	10 Ne
11 Na	12 Mg											13 Al	14 Si	15 P	16 S	17 Cl	18 Ar
19 K	20 Ca	21 Sc	22 Ti	23 V	24 Cr	25 Mn	26 Fe	27 Co	28 Ni	29 Cu	30 Zn	31 Ga	32 Ge	33 As	34 Se	35 Br	36 Kr
37 Rb	38 Sr	39 Y	40 Zr	41 Nb	42 Mo	43 Tc	44 Ru	45 Rh	46 Pd	47 Ag	48 Cd	49 In	50 Sn	51 Sb	52 Te	53 I	54 Xe
55 Cs	56 Ba	57 La	72 Hf	73 Ta	74 W	75 Re	76 Os	77 Ir	78 Pt	79 Au	80 Hg	81 Tl	82 Pb	83 Bi	84 Po	85 At	86 Rn
87 Fr	88 Ra	89 Ac	104 Rf	105 Db	106 Sg	107 Bh	108 Hs	109 Mt	110 Ds	111 Rg	112 Cp	113	114 Fl	115	116 Lv	117	118

58 Ce	59 Pr	60 Nd	61 Pm	62 Sm	63 Eu	64 Gd	65 Tb	66 Dy	67 Ho	68 Er	69 Tm	70 Yb	71 Lu
90 Th	91 Pa	92 U	93 Np	94 Pu	95 Am	96 Cm	97 Bk	98 Cf	99 Es	100 Fm	101 Md	102 No	103 Lr

Laser Ionization

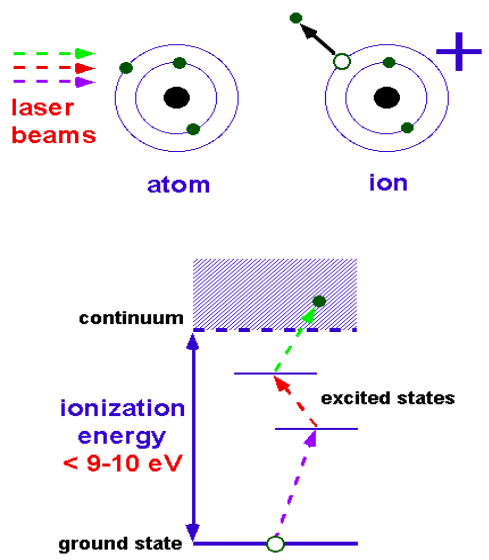

Resonance Ionization Laser Ion Source

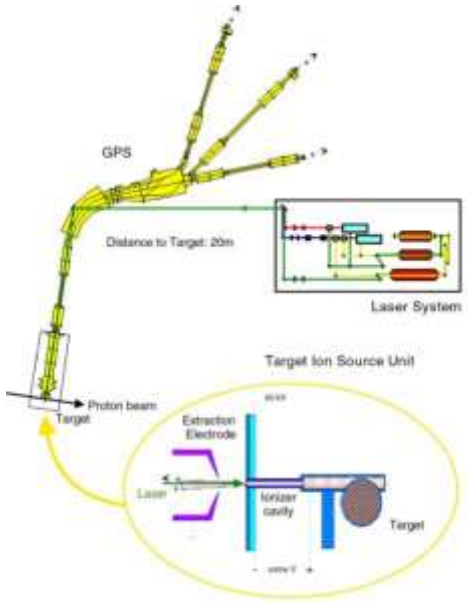

Spectrochimica Acta B58 (2003) 1047.

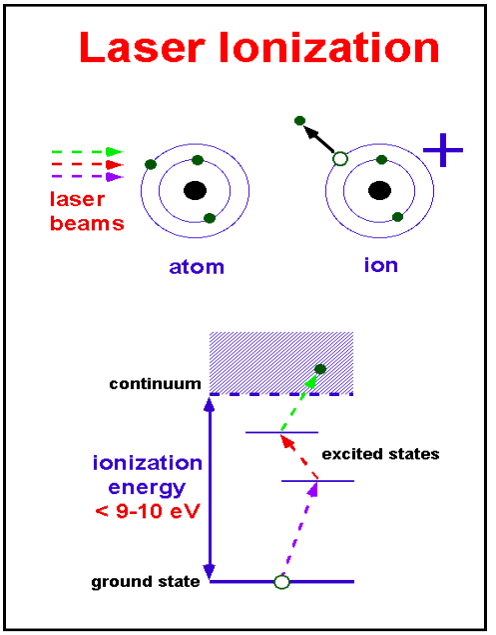

Ionization of Cu

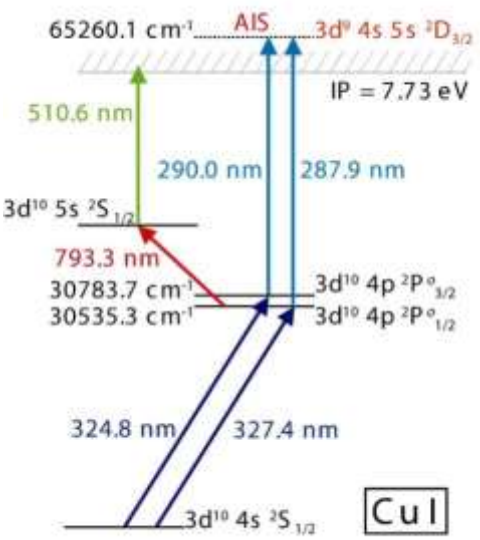

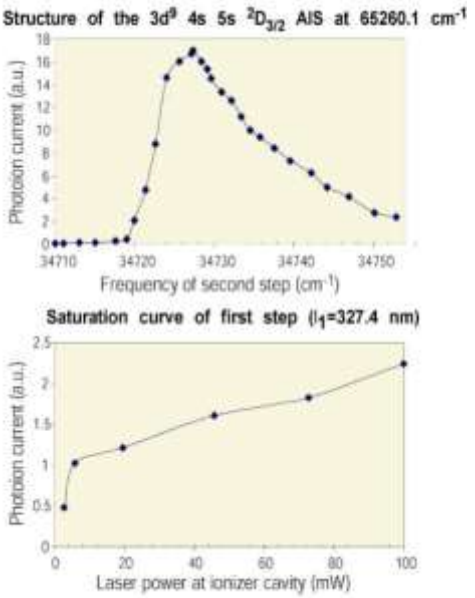

Neutron-rich Mn isotopes from UC_x/graphite target

M. Hannawald et al., Phys. Rev. Lett. 82 (1999) 1391.

Surface ionized background

Ionization potential: < 5 eV

Ionization potential: 5.0 - 5.8 eV

Ionization potential: 5.8 - 6.5 eV

1 H																	2 He
3 Li	4 Be											5 B	6 C	7 N	8 O	9 F	10 Ne
11 Na	12 Mg											13 Al	14 Si	15 P	16 S	17 Cl	18 Ar
19 K	20 Ca	21 Sc	22 Ti	23 V	24 Cr	25 Mn	26 Fe	27 Co	28 Ni	29 Cu	30 Zn	31 Ga	32 Ge	33 As	34 Se	35 Br	36 Kr
37 Rb	38 Sr	39 Y	40 Zr	41 Nb	42 Mo	43 Tc	44 Ru	45 Rh	46 Pd	47 Ag	48 Cd	49 In	50 Sn	51 Sb	52 Te	53 I	54 Xe
55 Cs	56 Ba	57 La	72 Hf	73 Ta	74 W	75 Re	76 Os	77 Ir	78 Pt	79 Au	80 Hg	81 Tl	82 Pb	83 Bi	84 Po	85 At	86 Rn
87 Fr	88 Ra	89 Ac	104 Rf	105 Db	106 Sg	107 Bh	108 Hs	109 Mt	110 Ds	111 Rg	112 Cp	113	114 Fl	115	116 Lv	117	118

58 Ce	59 Pr	60 Nd	61 Pm	62 Sm	63 Eu	64 Gd	65 Tb	66 Dy	67 Ho	68 Er	69 Tm	70 Yb	71 Lu
90 Th	91 Pa	92 U	93 Np	94 Pu	95 Am	96 Cm	97 Bk	98 Cf	99 Es	100 Fm	101 Md	102 No	103 Lr

ISOLDE beams around N=50

^{81}Rb background is 150000 times more abundant than ^{81}Zn!

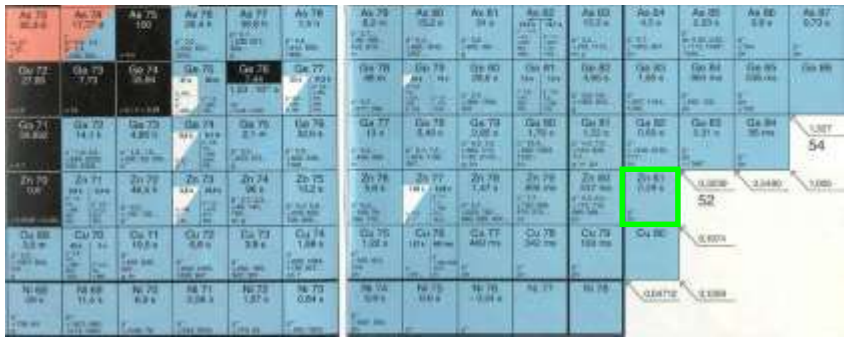

Zn/Rb discrimination on quartz surface!

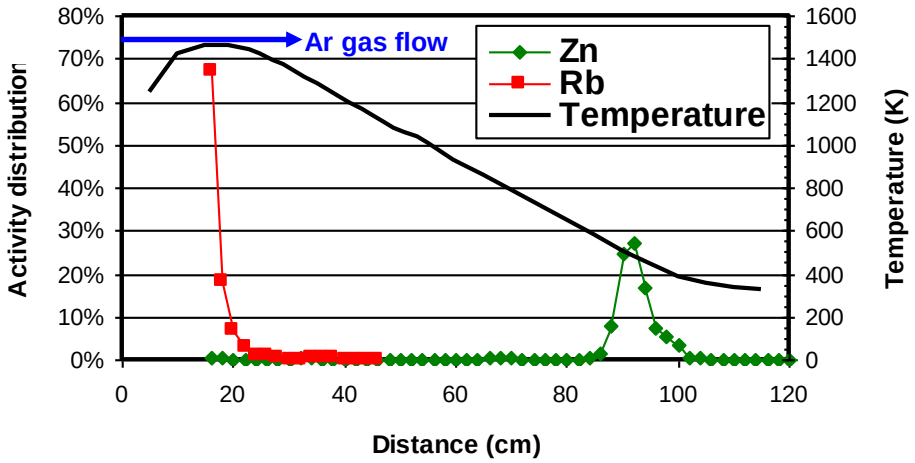

Combination of neutron converter and quartz transfer line provides ^{81}Zn/^{81}Rb selectivity gain of 100000!

Nucl. Instr. Meth. B266 (2008) 4229.

Zn/Rb discrimination on quartz surface!

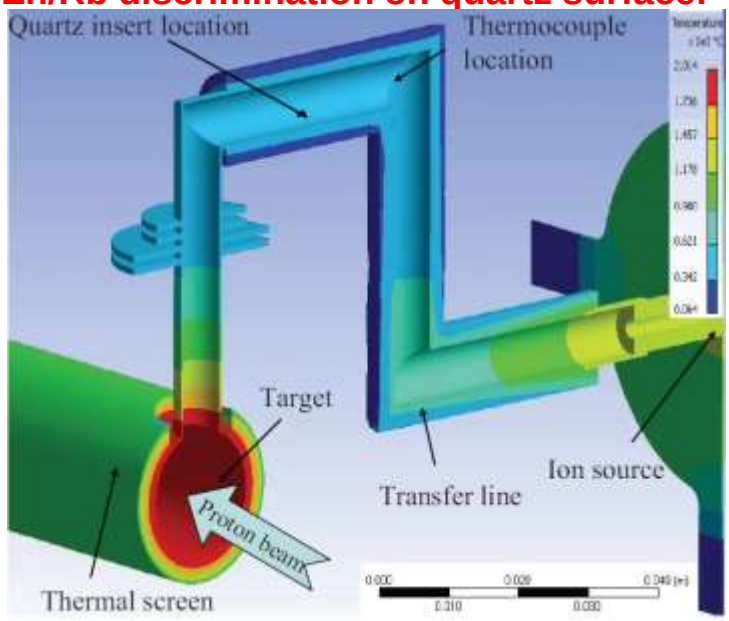

E. Boucquerel et al., Nucl. Instr. Meth. B266 (2008) 4298.

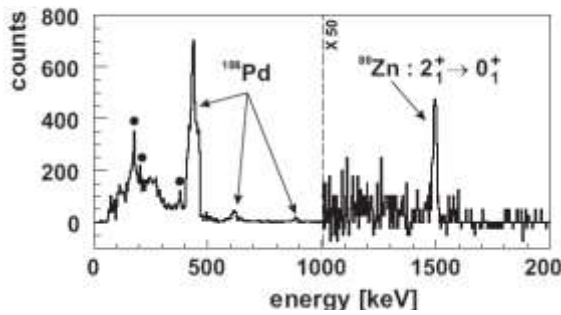

J. Van de Walle et al., Phys. Rev. Lett. 99 (2007) 142501.

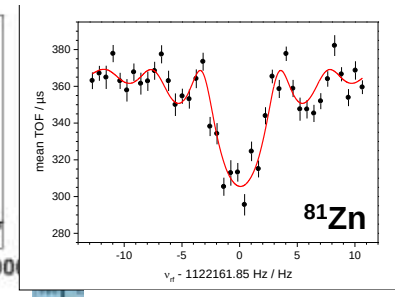

S. Baruah et al., Phys. Rev. Lett. 101 (2008) 262501.

REX performs Coulex measurement of ^{80}Zn observing its 2^+ state

ISOLTRAP performs direct mass measurement of r-process nucleus!

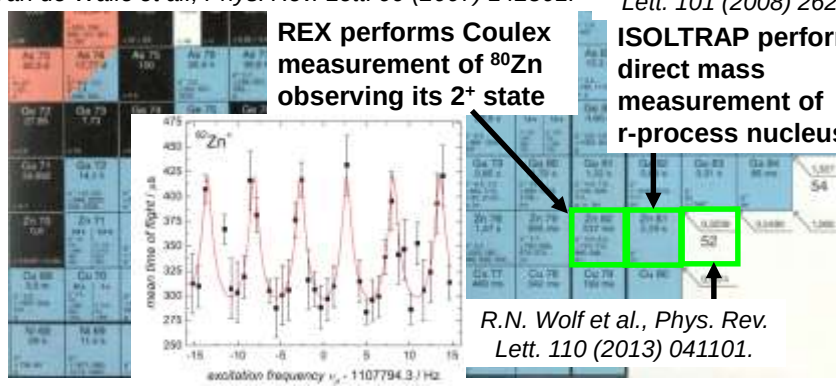

R.N. Wolf et al., Phys. Rev. Lett. 110 (2013) 041101.

RILIS laser setup

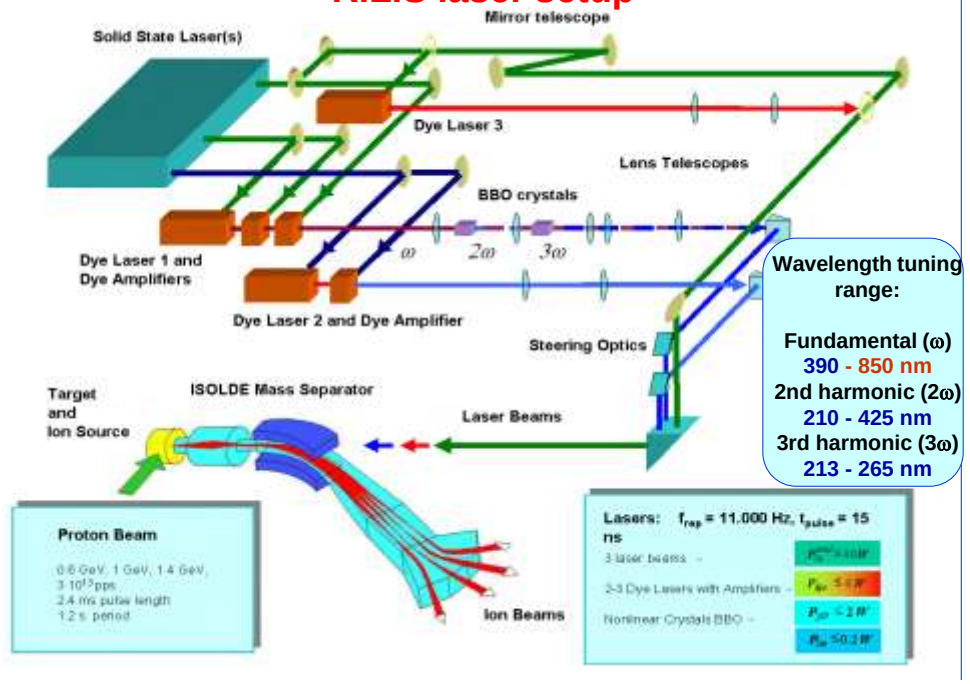

Elements ionizable with CVL or Nd-YAG pumped dye or Ti:Sa lasers

elements ionized with ISOLDE RILIS

tested ionization scheme

possible ionization scheme (untested)

1 H																	2 He
3 Li	4 Be											5 B	6 C	7 N	8 O	9 F	10 Ne
11 Na	12 Mg											13 Al	14 Si	15 P	16 S	17 Cl	18 Ar
19 K	20 Ca	21 Sc	22 Ti	23 V	24 Cr	25 Mn	26 Fe	27 Co	28 Ni	29 Cu	30 Zn	31 Ga	32 Ge	33 As	34 Se	35 Br	36 Kr
37 Rb	38 Sr	39 Y	40 Zr	41 Nb	42 Mo	43 Tc	44 Ru	45 Rh	46 Pd	47 Ag	48 Cd	49 In	50 Sn	51 Sb	52 Te	53 I	54 Xe
55 Cs	56 Ba	57 La	72 Hf	73 Ta	74 W	75 Re	76 Os	77 Ir	78 Pt	79 Au	80 Hg	81 Tl	82 Pb	83 Bi	84 Po	85 At	86 Rn
87 Fr	88 Ra	89 Ac	104 Rf	105 Db	106 Sg	107 Bh	108 Hs	109 Mt	110 Ds	111 Rg	112 Cp	113	114 Fl	115	116 Lv	117	118

58 Ce	59 Pr	60 Nd	61 Pm	62 Sm	63 Eu	64 Gd	65 Tb	66 Dy	67 Ho	68 Er	69 Tm	70 Yb	71 Lu
90 Th	91 Pa	92 U	93 Np	94 Pu	95 Am	96 Cm	97 Bk	98 Cf	99 Es	100 Fm	101 Md	102 No	103 Lr

Isomer separation

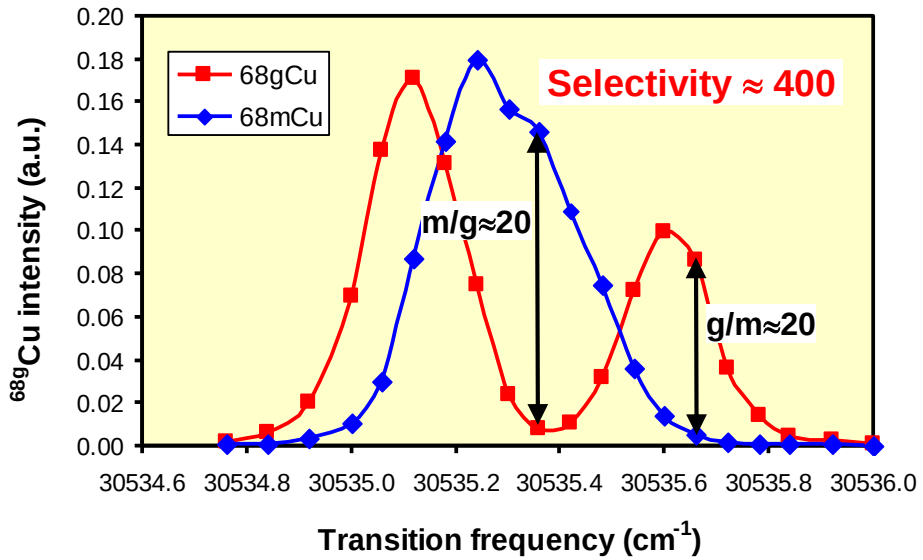

Hyperfine Interactions 127 (2000) 417.

Mass measurements with Penning traps

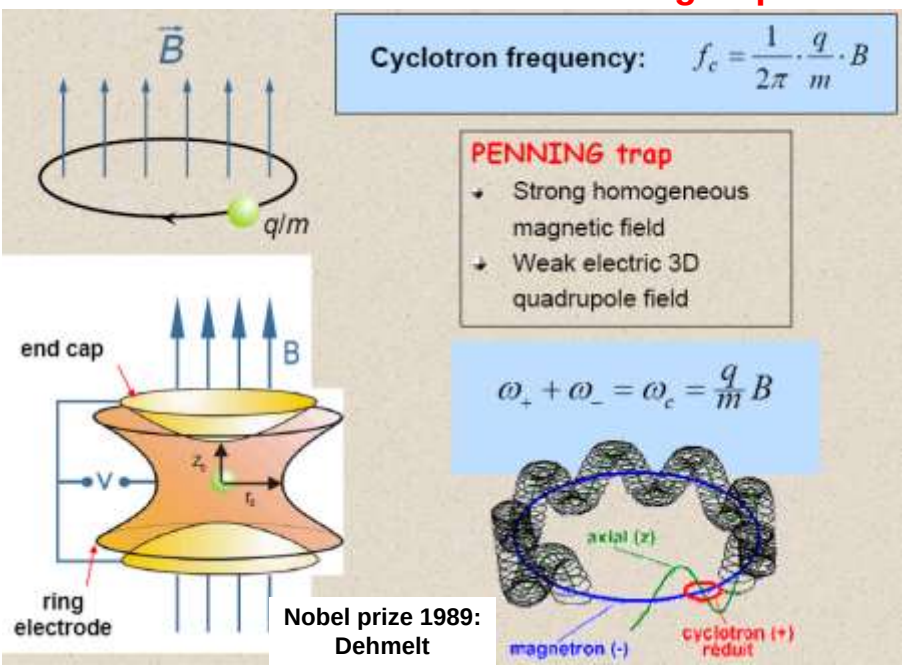

Nobel prize 1989: Dehmelt

Resonance frequency measurement via TOF method

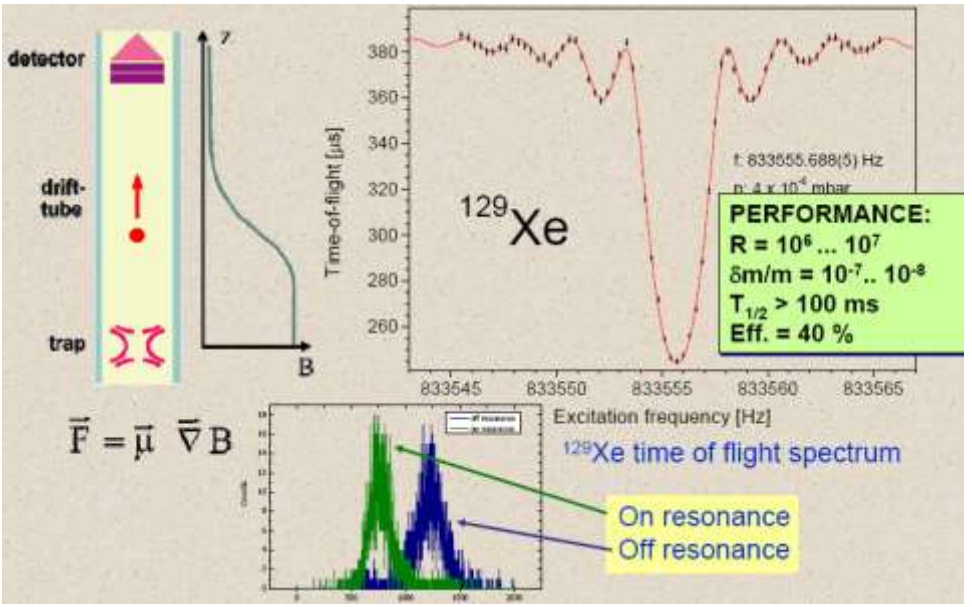

M. König et al., Int. J. Mass Spectr. Ion Proc. 142 (1995) 95.

Mass measurements with ISOLTRAP

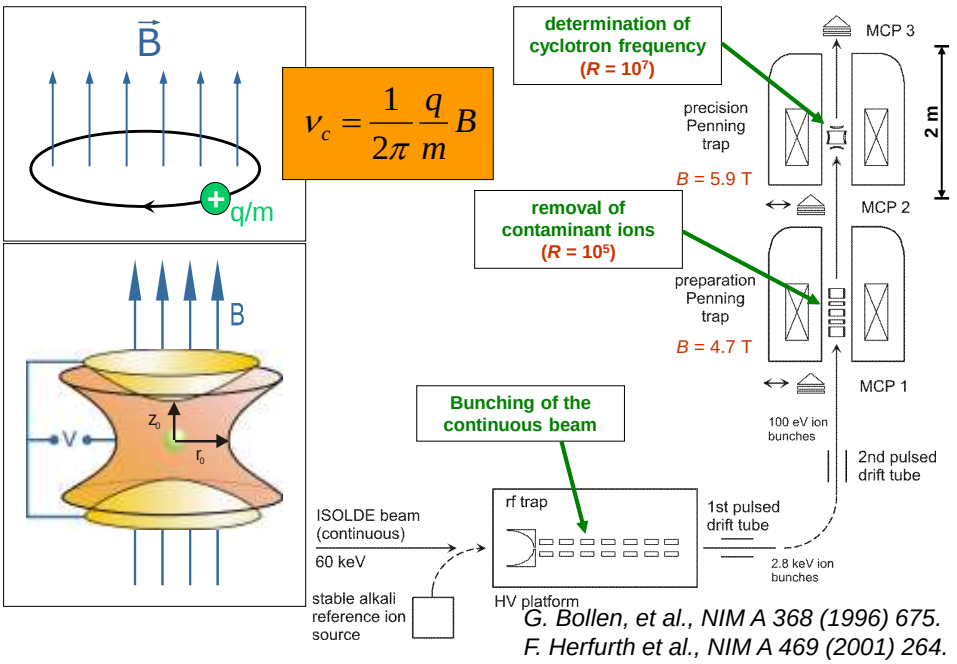

G. Bollen, et al., NIM A 368 (1996) 675.
F. Herfurth et al., NIM A 469 (2001) 264.

Solving the ^{70}Cu mass puzzle

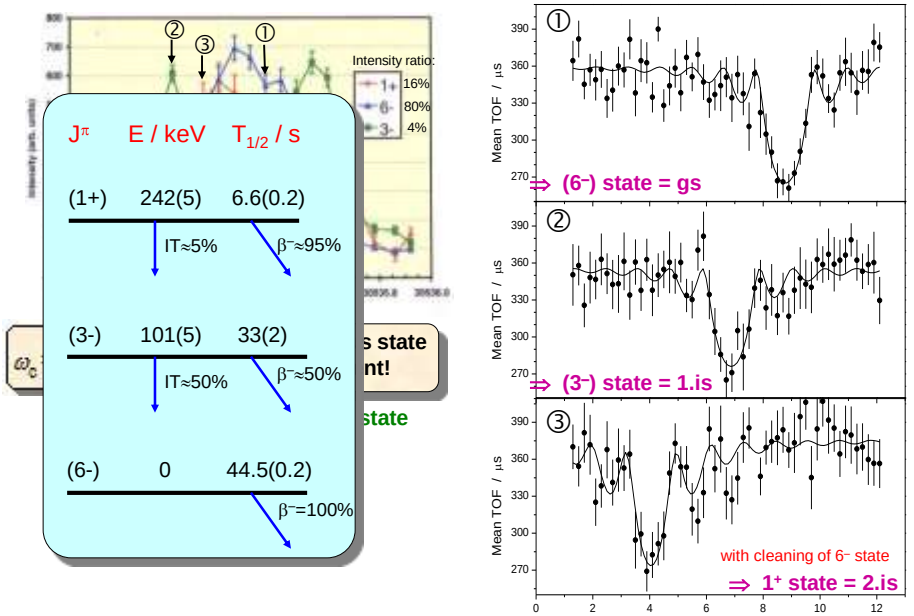

J. Van Roosbroeck et al., Phys. Rev. Lett. 92 (2004) 112501.

Linear TOF spectrometer

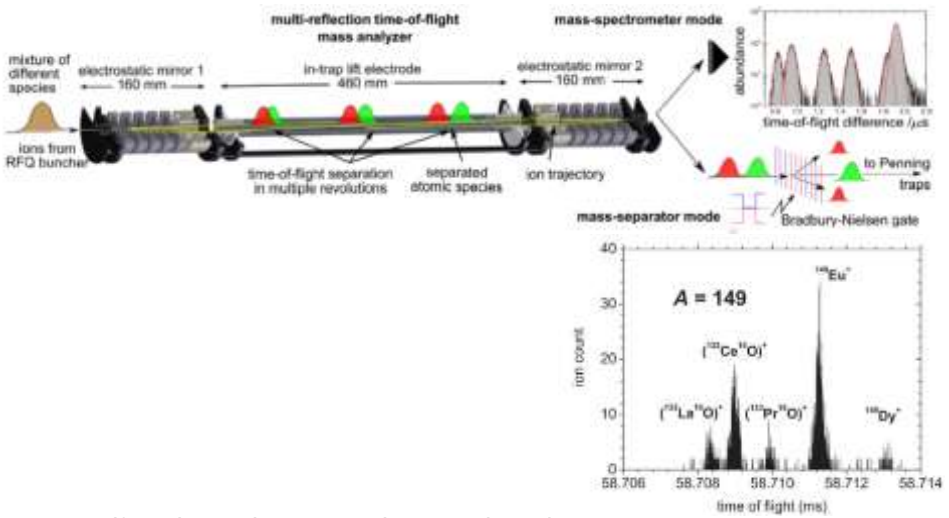

R.N. Wolf et al., Nucl. Instr. Meth. A686 (2012) 82.

R.N. Wolf et al., Int. J. Mass Spectrometry 349/350 (2013) 123.

S. Kreim et al., Nucl. Instr. Meth. B 317 (2013) 492.

Many many traps at CERN !

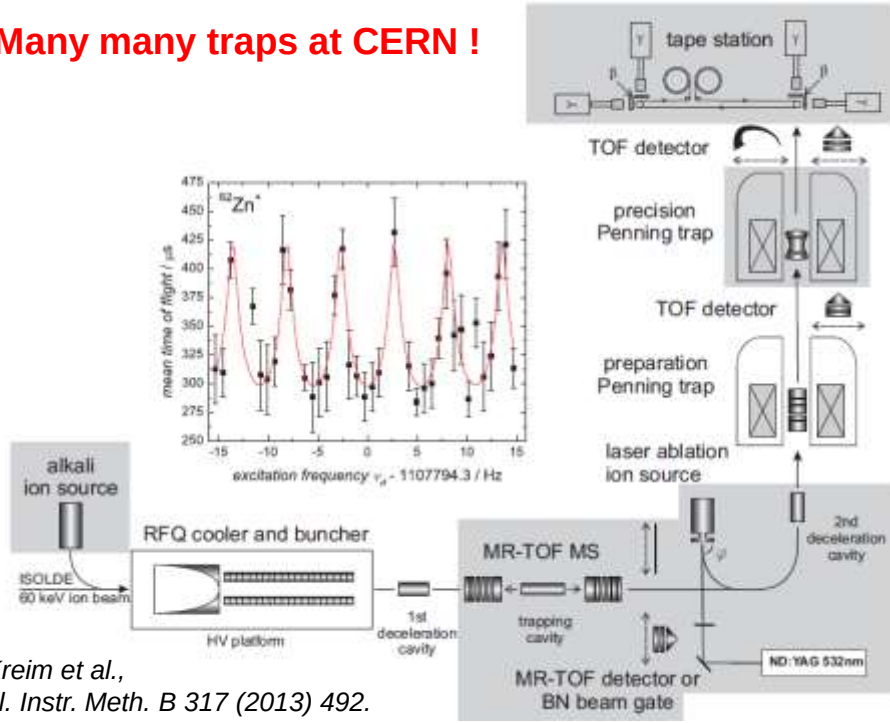

S. Kreim et al.,
Nucl. Instr. Meth. B 317 (2013) 492.

CERN accelerator structure

Antiproton decelerator

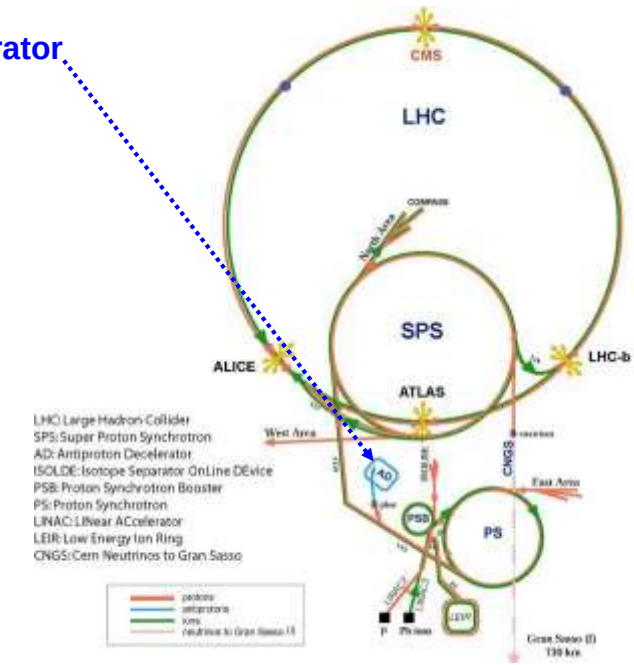

Antiproton traps at CERN

G. Gabrielse et al., Phys. Rev. Lett. 100 (2008) 113001.
M. Amoretti et al., Phys. Lett. B 583 (2004) 59.
D. Brown, R. Howard et al., "Angels and Demons" (2009).

Elements ionizable with CVL or Nd-YAG pumped dye or Ti:Sa lasers

elements ionized with ISOLDE RILIS
tested ionization scheme
possible ionization scheme (untested)
refractory elements

1 H																	2 He
3 Li	4 Be											5 B	6 C	7 N	8 O	9 F	10 Ne
11 Na	12 Mg											13 Al	14 Si	15 P	16 S	17 Cl	18 Ar
19 K	20 Ca	21 Sc	22 Ti	23 V	24 Cr	25 Mn	26 Fe	27 Co	28 Ni	29 Cu	30 Zn	31 Ga	32 Ge	33 As	34 Se	35 Br	36 Kr
37 Rb	38 Sr	39 Y	40 Zr	41 Nb	42 Mo	43 Tc	44 Ru	45 Rh	46 Pd	47 Ag	48 Cd	49 In	50 Sn	51 Sb	52 Te	53 I	54 Xe
55 Cs	56 Ba	57 La	72 Hf	73 Ta	74 W	75 Re	76 Os	77 Ir	78 Pt	79 Au	80 Hg	81 Tl	82 Pb	83 Bi	84 Po	85 At	86 Rn
87 Fr	88 Ra	89 Ac	104 Rf	105 Db	106 Sg	107 Bh	108 Hs	109 Mt	110 Ds	111 Rg	112 Cp	113	114 Fl	115	116 Lv	117	118

58 Ce	59 Pr	60 Nd	61 Pm	62 Sm	63 Eu	64 Gd	65 Tb	66 Dy	67 Ho	68 Er	69 Tm	70 Yb	71 Lu
90 Th	91 Pa	92 U	93 Np	94 Pu	95 Am	96 Cm	97 Bk	98 Cf	99 Es	100 Fm	101 Md	102 No	103 Lr

Hf beams at ISOLDE

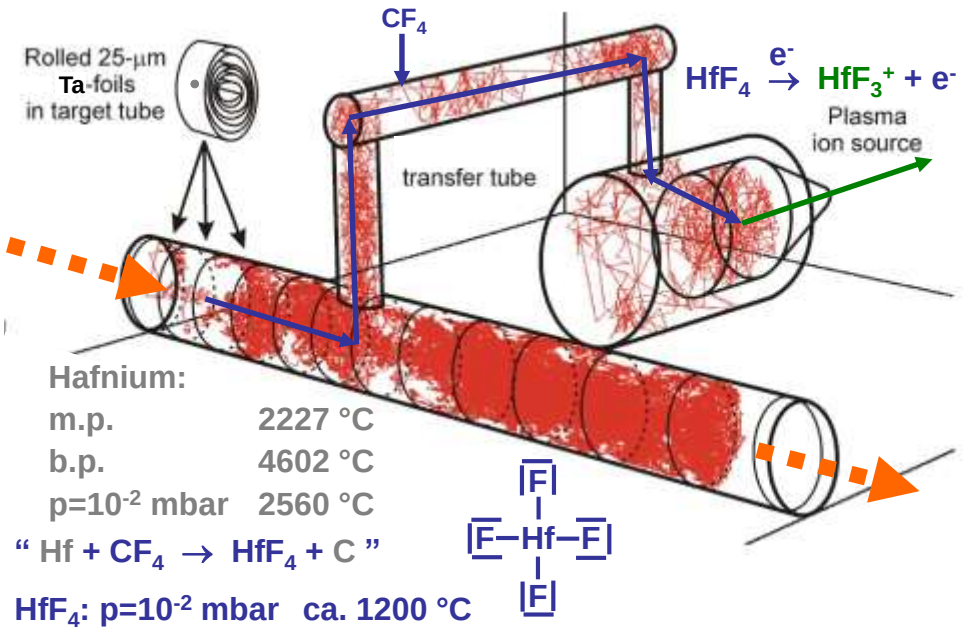

Ta/W foil target + MK5 + CF_4

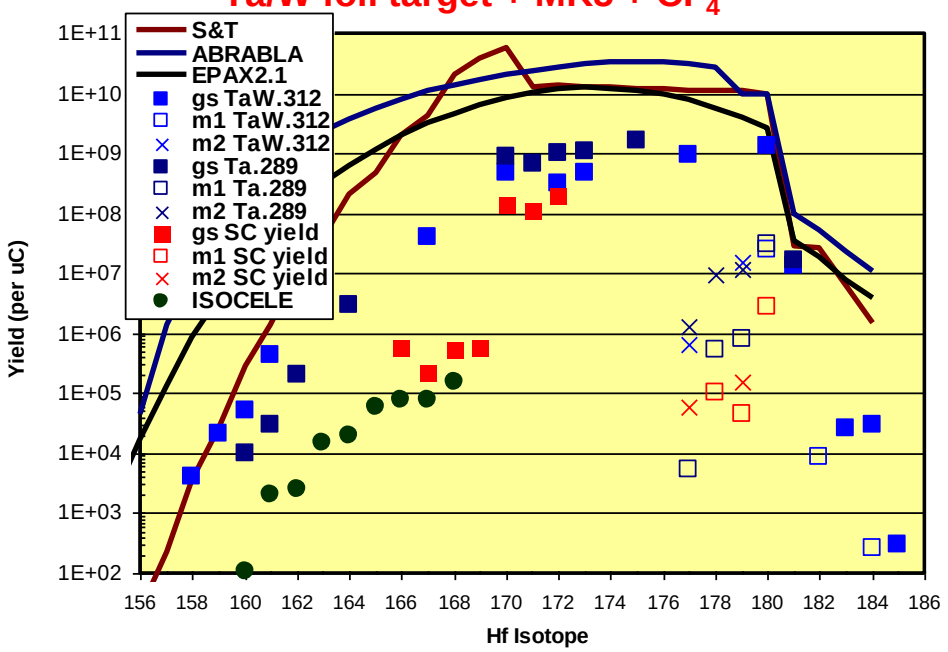

Eur. Phys. J. Spec. Topics 150 (2007) 293.

Overview of molecular ISOL beams

Separation as XF^+, XCl^+

Separation as XO_x^+

Separation as XCO^+

Separation as XF_2^+

Separation as XS^+

Separation as AlX^+

Separation as XF_3^+

Separation as HX^+

Separation as XF_4^+

Separation as NX^+

1 H																	2 He
3 Li	4 Be											5 B	6 C	7 N	8 O	9 F	10 Ne
11 Na	12 Mg											13 Al	14 Si	15 P	16 S	17 Cl	18 Ar
19 K	20 Ca	21 Sc	22 Ti	23 V	24 Cr	25 Mn	26 Fe	27 Co	28 Ni	29 Cu	30 Zn	31 Ga	32 Ge	33 As	34 Se	35 Br	36 Kr
37 Rb	38 Sr	39 Y	40 Zr	41 Nb	42 Mo	43 Tc	44 Ru	45 Rh	46 Pd	47 Ag	48 Cd	49 In	50 Sn	51 Sb	52 Te	53 I	54 Xe
55 Cs	56 Ba	57 La	72 Hf	73 Ta	74 W	75 Re	76 Os	77 Ir	78 Pt	79 Au	80 Hg	81 Tl	82 Pb	83 Bi	84 Po	85 At	86 Rn
87 Fr	88 Ra	89 Ac	104 Rf	105 Db	106 Sg	107 Bh	108 Hs	109 Mt	110	111	112	112	112	112			

58 Ce	59 Pr	60 Nd	61 Pm	62 Sm	63 Eu	64 Gd	65 Tb	66 Dy	67 Ho	68 Er	69 Tm	70 Yb	71 Lu
90 Th	91 Pa	92 U	93 Np	94 Pu	95 Am	96 Cm	97 Bk	98 Cf	99 Es	100 Fm	101 Md	102 No	103 Lr

Nucl. Instr. Meth. B266 (2008) 4229.

Nuclear chart at ISOLDE

> 600 isotopes available at ISOLDE-SC

> 1100 isotopes produced at ISOLDE till today

> 2000 isotopes in principle feasible with ISOL method

Extension needs target and ion source development!

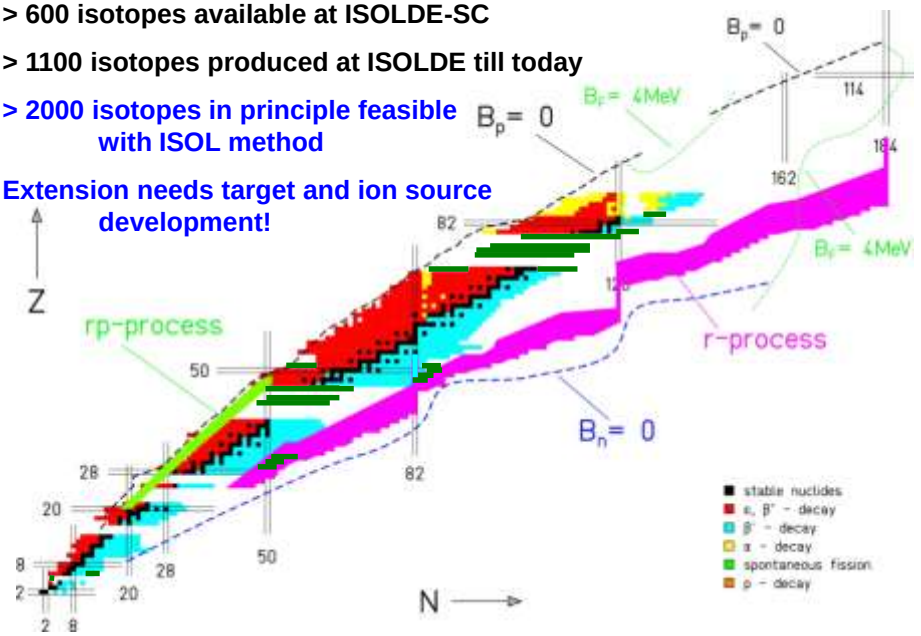

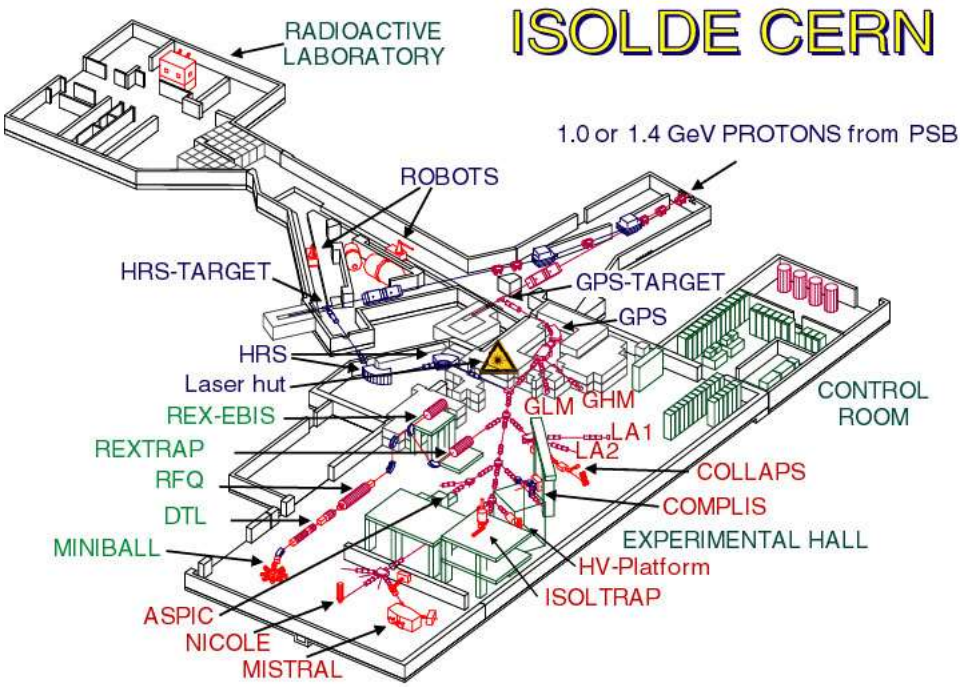

Beam transport

electrostatic beam transport is mass-independent (E=60 keV), but has space charge limit for high beam intensities (>10 μA)
⇒ high current beams need magnetic beam transport

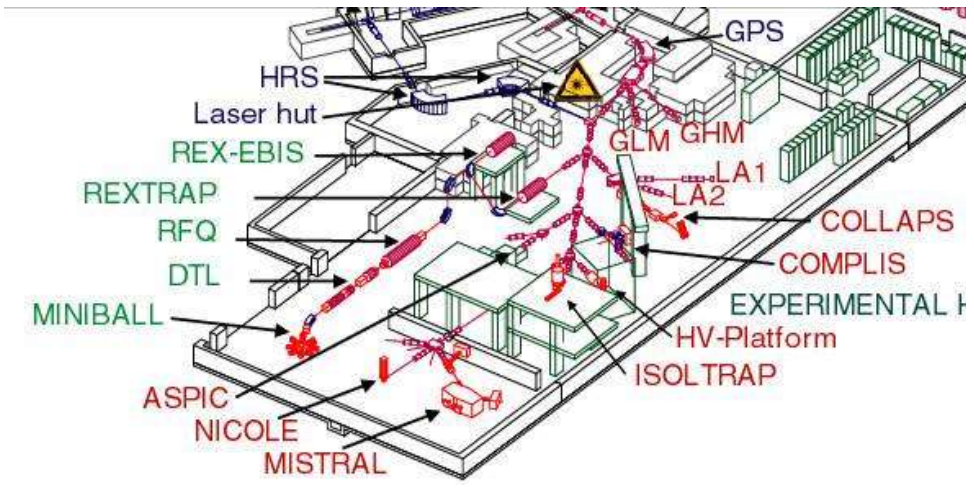

Applications

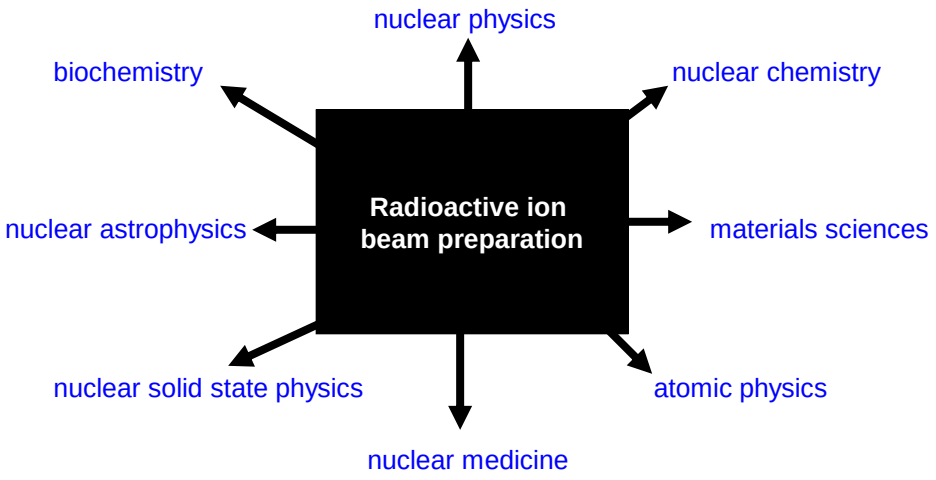

Experimental access to *r*-process nuclides

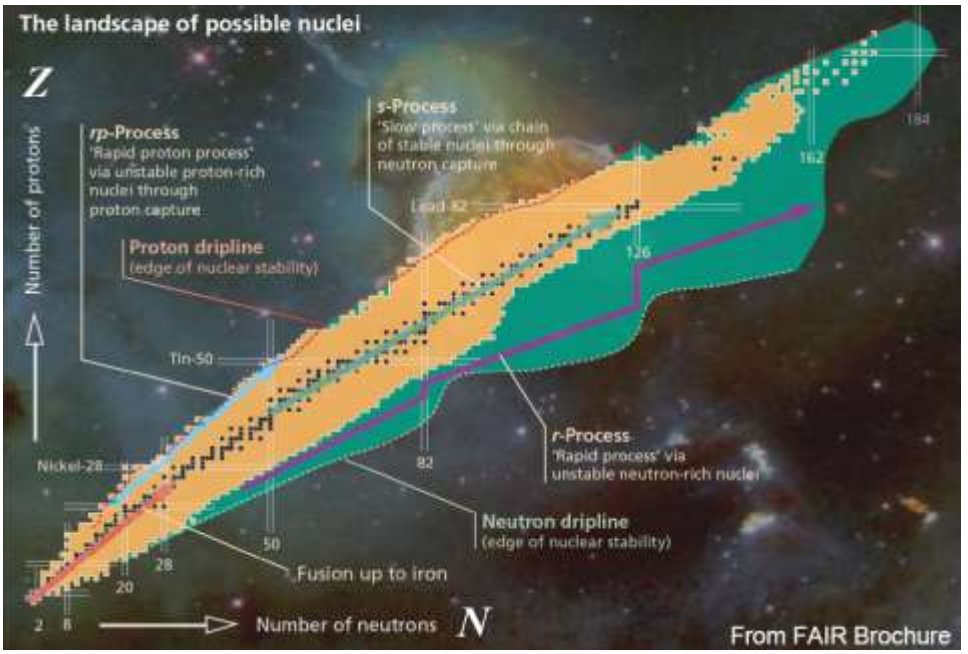

Production of ^{12}C in stars

		C 8 2E-21 s	C 9 127 ms	C 10 19.3 s	C 11 20 m	C 12	C 13	C 14 5.7 ka
		B 7 4E-24 s	B 8 770 ms	B 9 8E-19 s	B 10	B 11	B 12 20 ms	B 13 17 ms
		Be 6 5E-21 s	Be 7 53.3 d	Be 8 7E-17 s	Be 9	Be 10 1.5 Ma	Be 11 13.8 s	Be 12 21 ms
		Li 5 4E-22 s	Li 6	Li 7	Li 8 840 ms	Li 9 178 ms	Li 10 2E-21 s	Li 11 8.5 ms
	He 3	He 4	He 5 7E-22 s	He 6 807 ms	He 7 3E-21 s	He 8 119 ms	He 9 7E-21 s	He 10 3E-21 s
H 1	H 2	H 3 12.3 a						

The triple-alpha process: rate

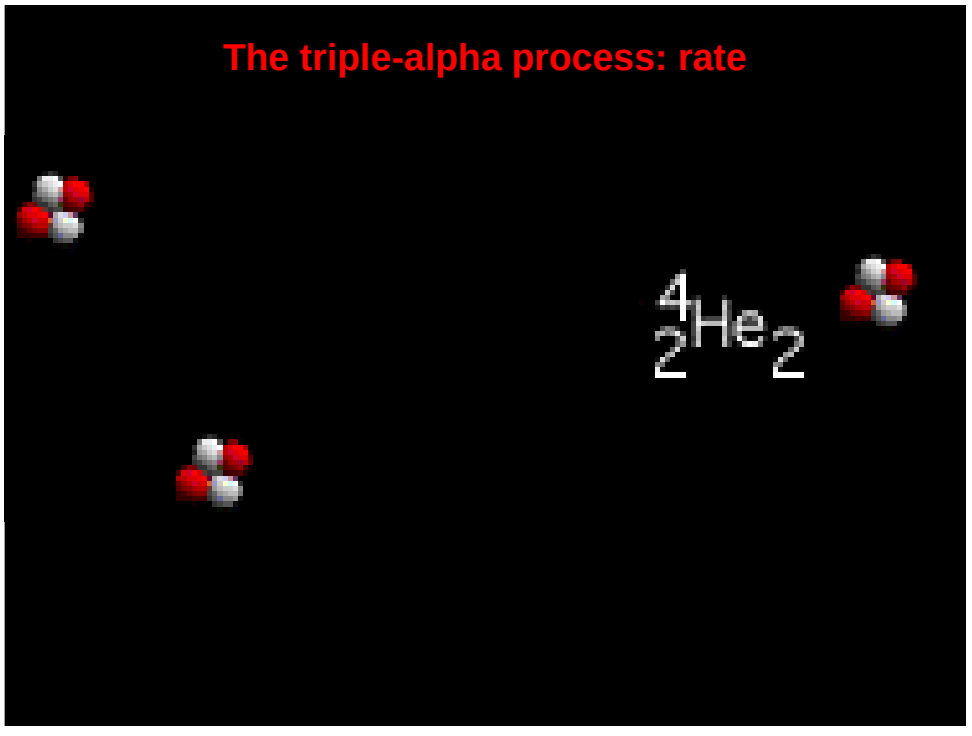

The triple-alpha process

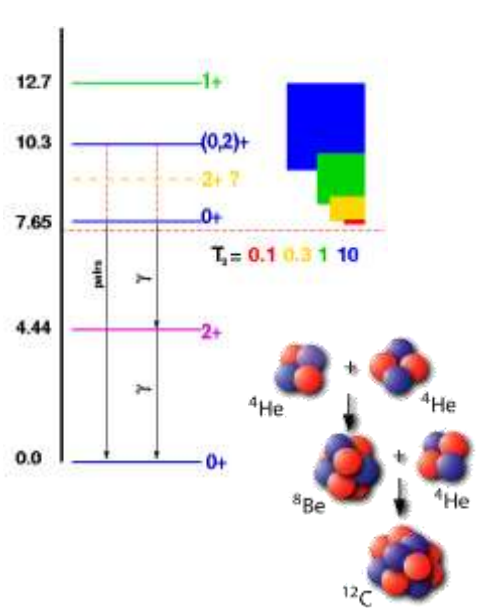

$r_{3\alpha} \propto \Gamma_{rad}\, e^{-Q/kT}$

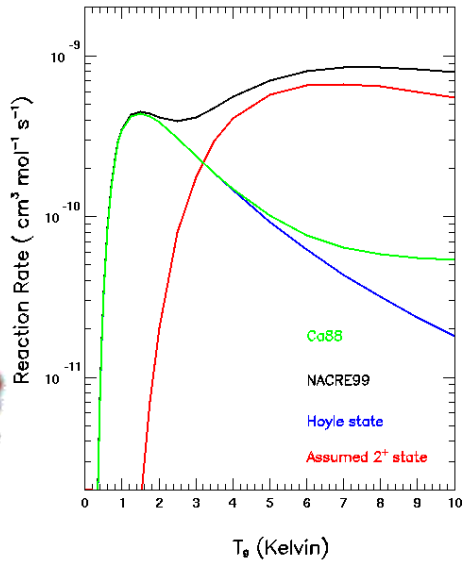

Setup for study of three-body-fusion?

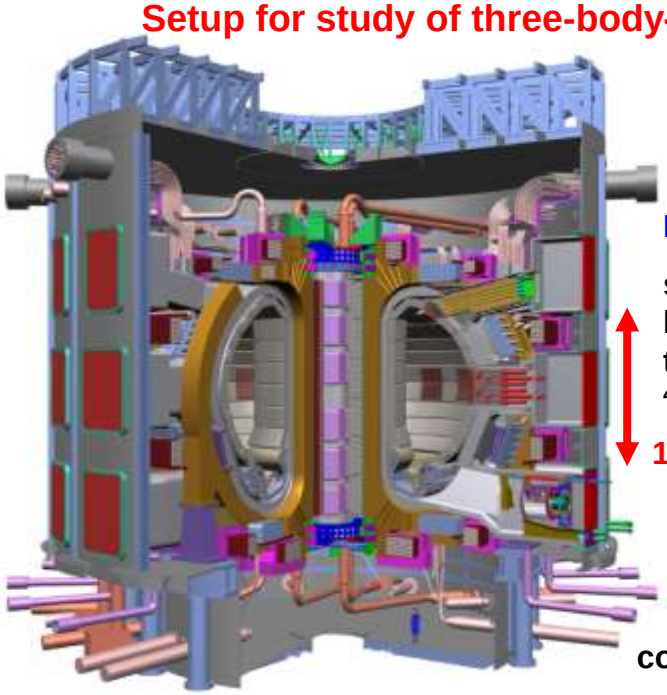

Exercise:

scale from two-body fusion d+t to three-body fusion ^{4}He+^{4}He+^{4}He!

14 m

cost ca. 10^{10} EUR

Setup for study of triple alpha reaction!

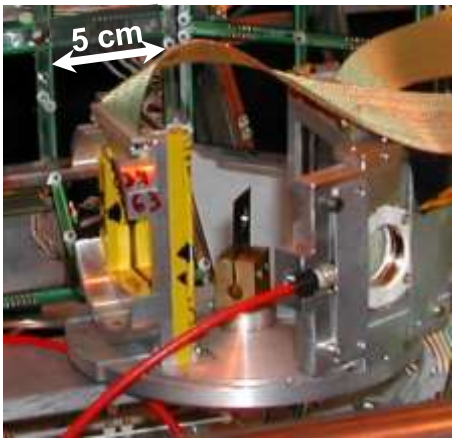

New detector design

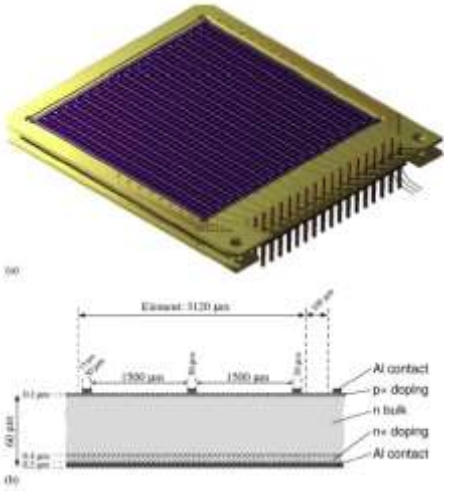

Reduced deadlayer

Inverse reaction: $^{12}B(\beta,3\alpha)$ decay

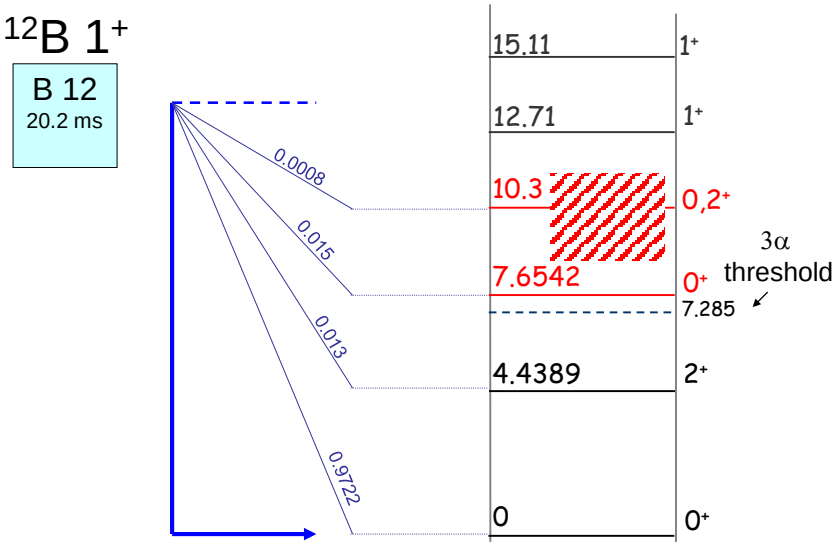

The triple-alpha process: ^{12}B and ^{12}N decays

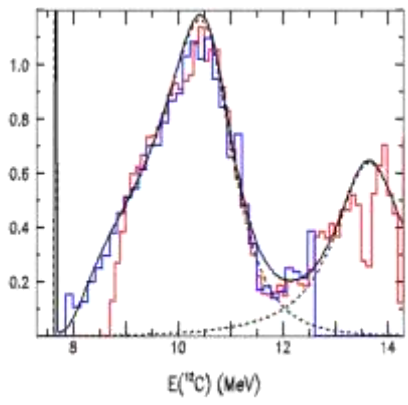

Combined R-matrix fit of ^{12}B and ^{12}N

ISOLDE - JYFL

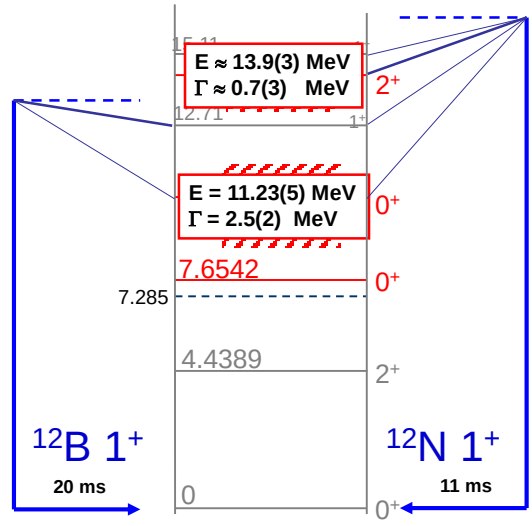

H.O.U. Fynbo et al., Nature 433 (2005) 136.

New rates for the triple-alpha process

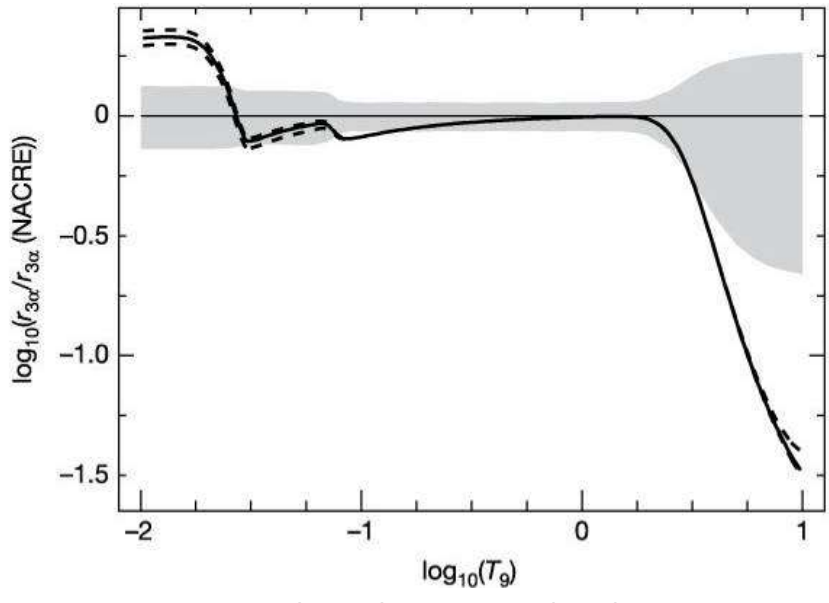

H.O.U. Fynbo et al., Nature 433 (2005) 136.

Applications

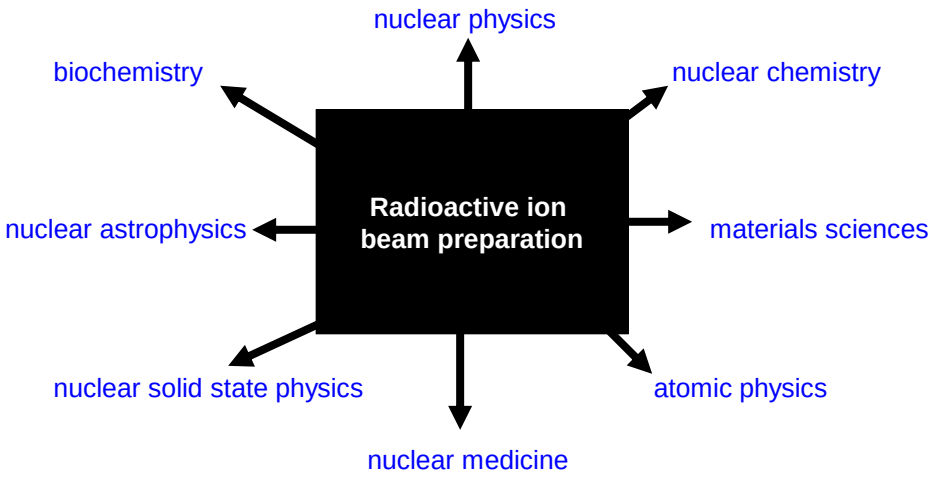

Development of pharmaceuticals

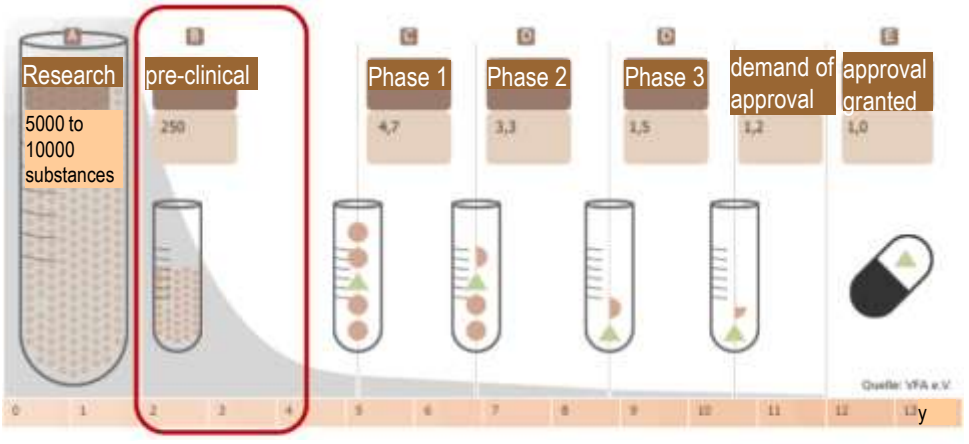

Screening **in vitro tests**
animal exp.

tests with humans

toxicity **wanted effect** **comparison**
side effects **with standard**

20-80 healthy volunteers **100-300 patients** **x00-x000 patients**

Pre-clinical studies (1)

Pre-clinical studies (2)

Pre-clinical studies (3)

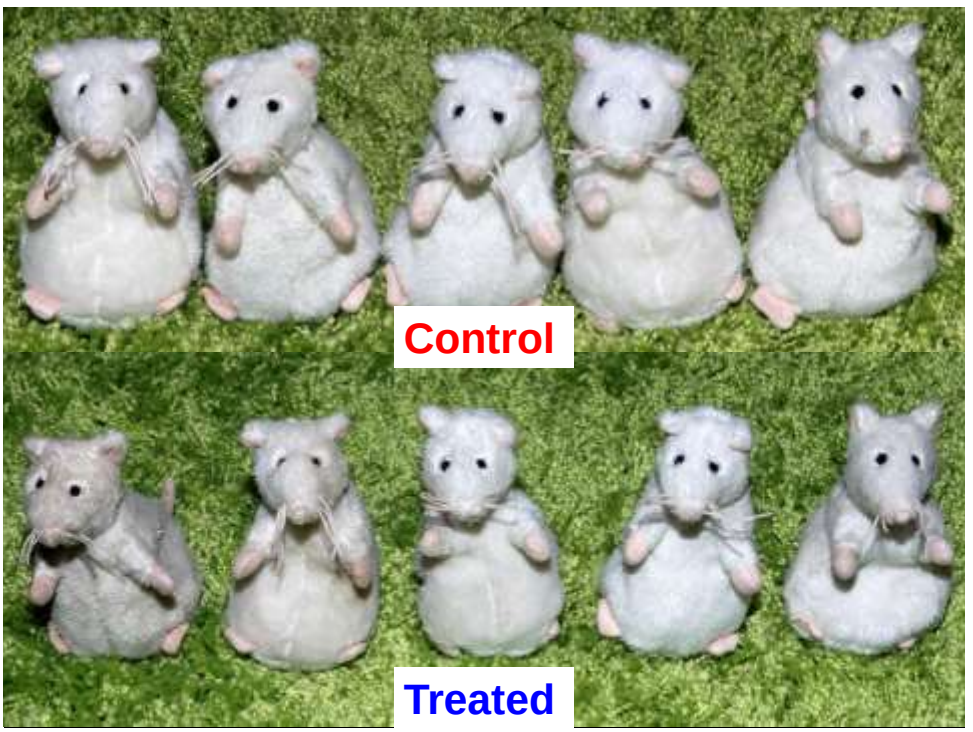

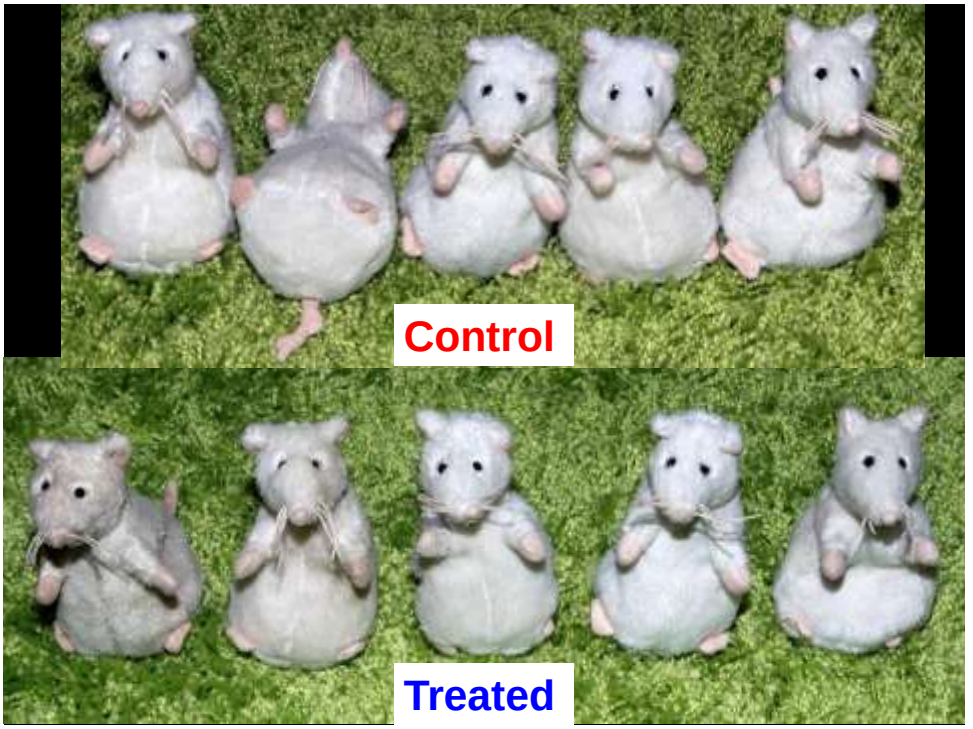
Control
Treated

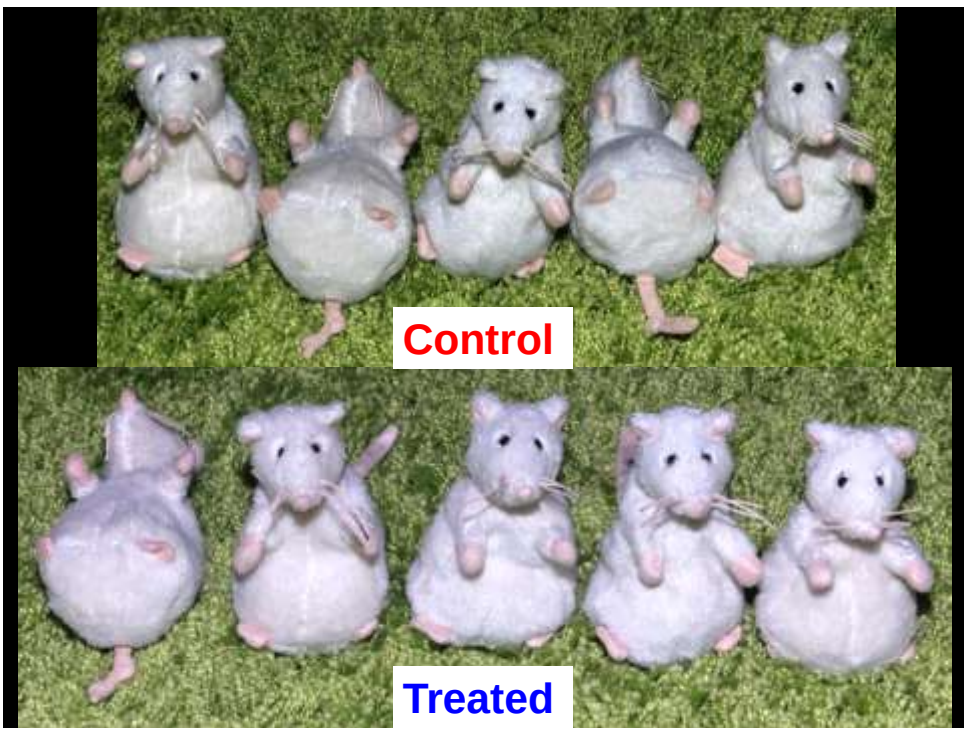
Control
Treated


Control
Treated

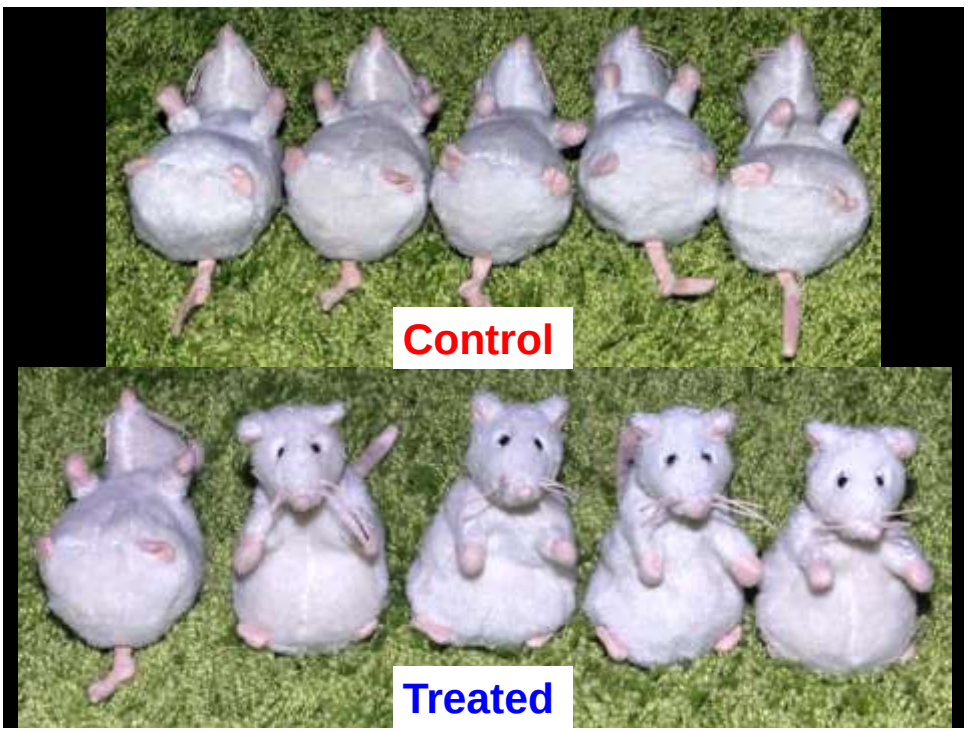
Control
Treated

Survival curve

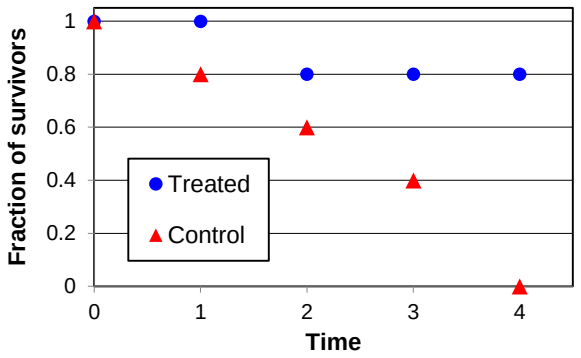

- medium survival time, median survival time, survival benefit
- shows final benefit but not detailed mechanism

- more information from bio-distribution studies
- preferentially on-line with suitable radiotracers
  and small animal SPECT or PET

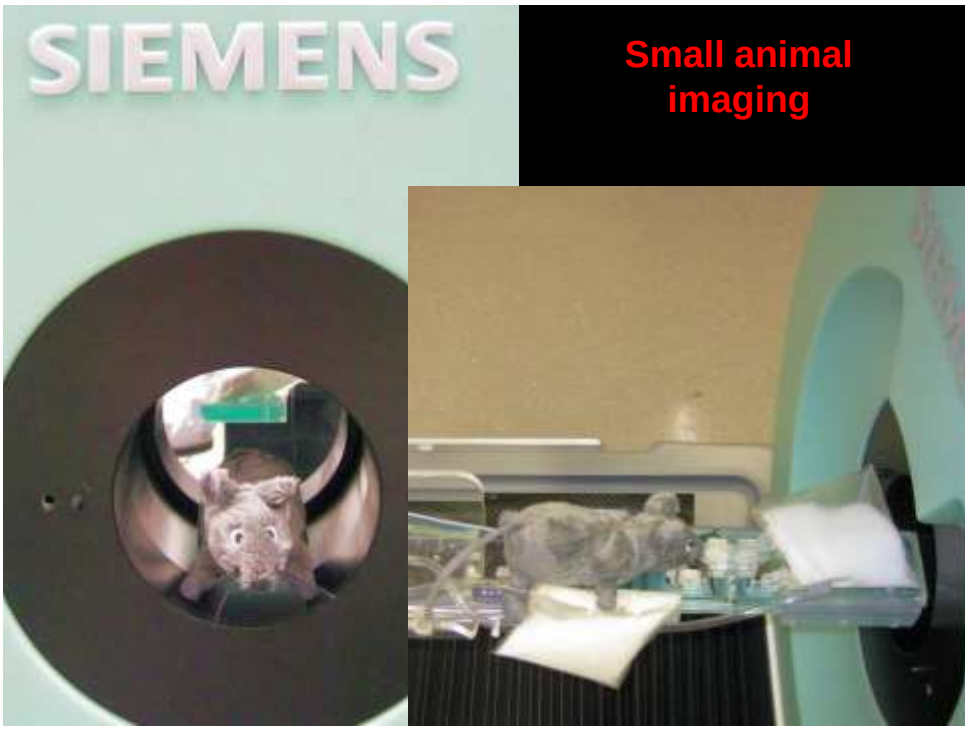

New generation of small animal SPECT

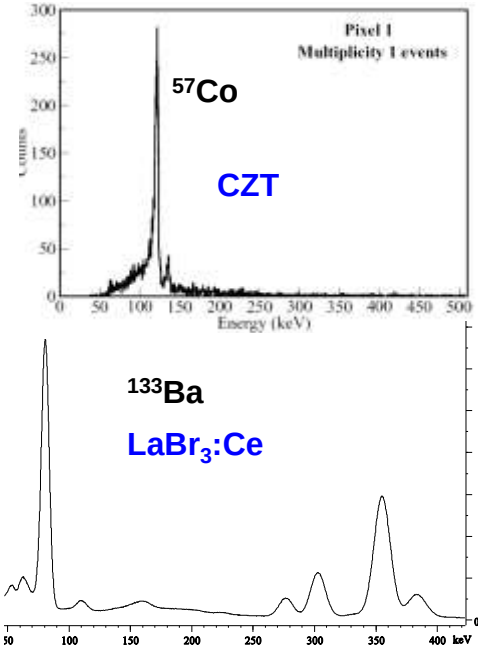

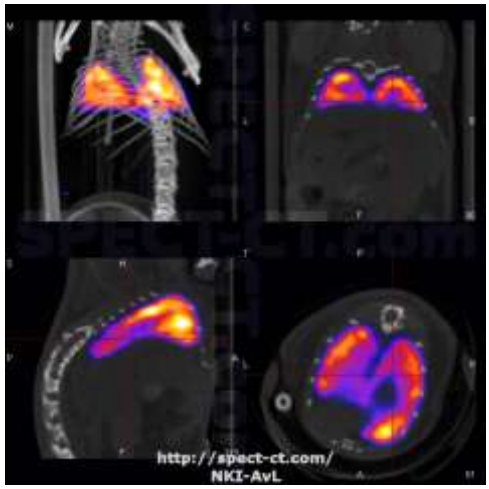

systematic biodistribution studies with different radiotracers **become possible with dedicated small animal SPECT**

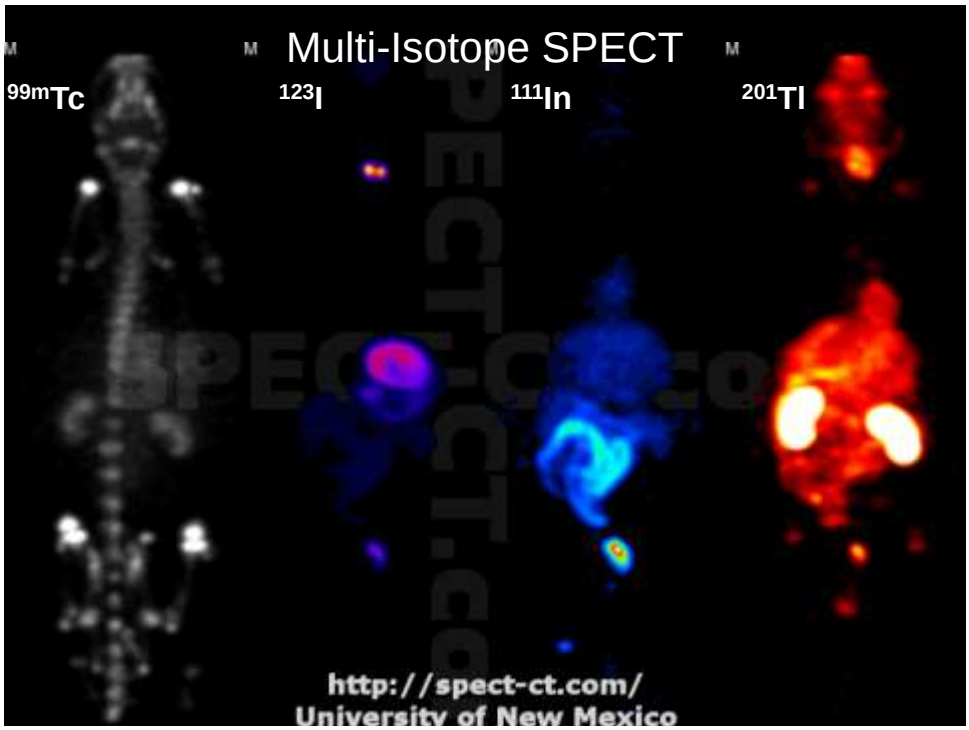

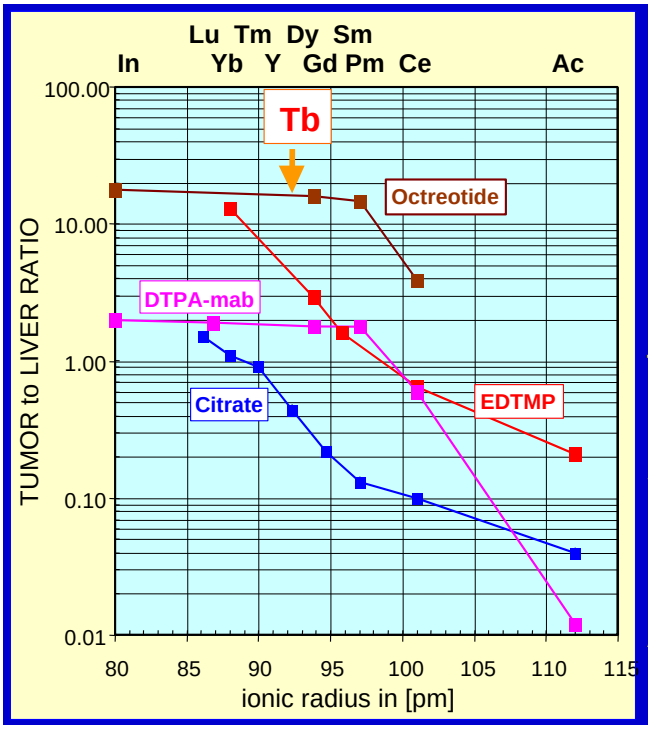

Comparison
of the
bio-distribution
of different
tumor seeking tracers
labeled with
radio-lanthanides, ^{225}Ac and ^{111}In

free chelates:
Citrate
EDTMP

specific tracers:
Octreotide
and
Mab

Linker:
Aminobenzyl-DTPA

*G.J.Beyer, Hyperfine Interactions **129** (2000) 529.*

Radionuclides for RIT and PRRT

Radio-nuclide	Half-life	E mean (keV)	Eγ (B.R.) (keV)	Range
Y-90	64 h	934 β	-	12 mm
I-131	8 days	182 β	364 (82%)	3 mm
Lu-177	7 days	134 β	208 (10%) 113 (6%)	2 mm
Tb-161	7 days	154 β 5, 17, 40 e^-	75 (10%)	2 mm 1-30 µm
Tb-149	4.1 h	3967 α	165,..	25 µm
Ge-71	11 days	8 e^-	-	1.7 µm
Er-165	10.3 h	5.3 e^-	-	0.6 µm

cross-fire

Estab-lished isotopes

Emerging isotopes

R&D isotopes: supply-limited!

localized

Modern, better targeted bioconjugates require shorter-range radiation ⇒ need for adequate (R&D) radioisotope supply.

Terbium: a unique element for nuclear medicine

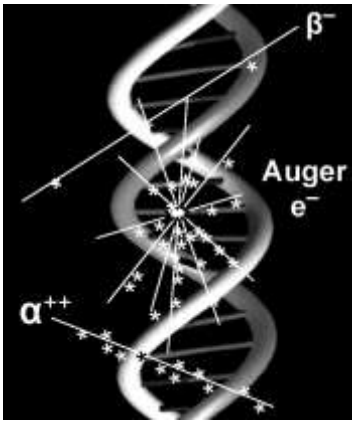

General Purpose Separator (GPS)

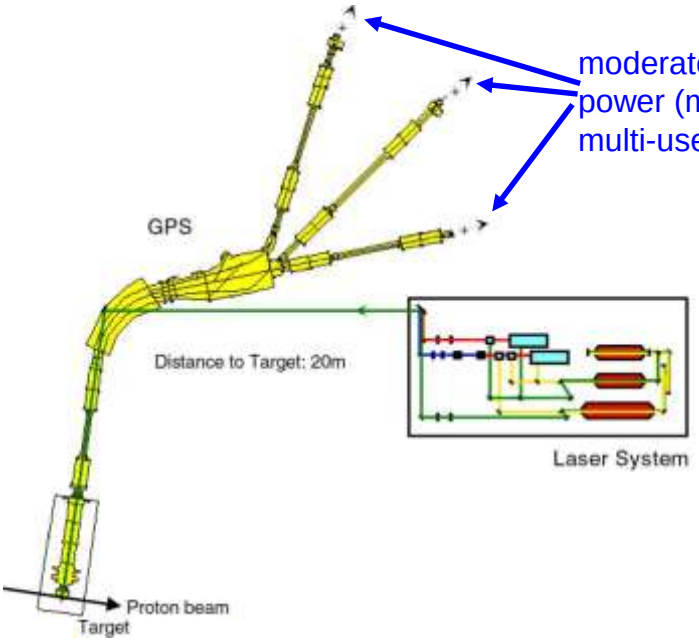

Theranostics with terbium isotopes

PET *SPECT* *SPECT*

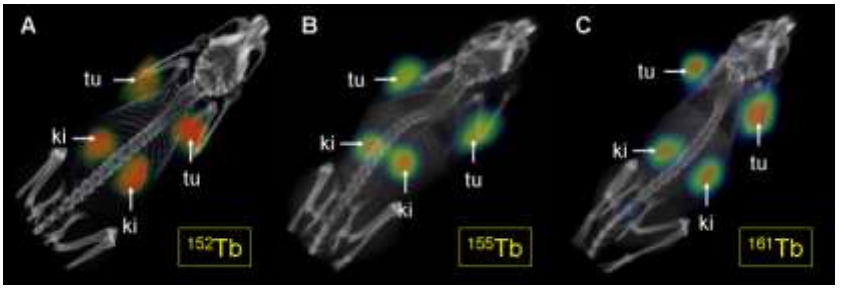

^{152}Tb-folate: 9 MBq
Scan Start: 24 h p.i.
Scan Time: 4 h

^{155}Tb-folate: 4 MBq
Scan Start: 24 h p.i.
Scan Time: 1 h

^{161}Tb-folate: 30 MBq
Scan Start: 24 h p.i.
Scan Time: 20 min

IS528 Collaboration: C. Müller et al., J. Nucl. Med. 53 (2012) 1951.

The Nuclear Medicine Alphabet

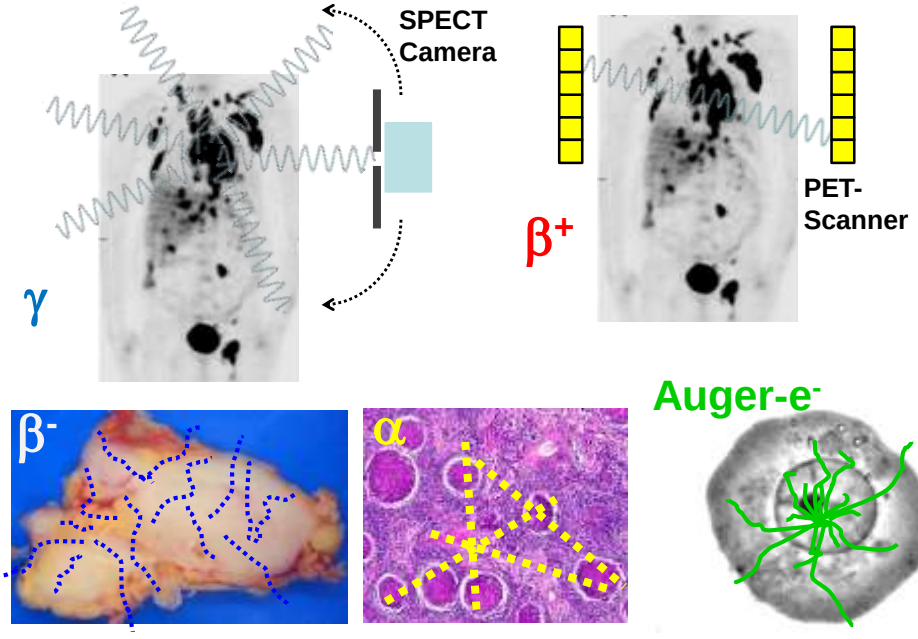

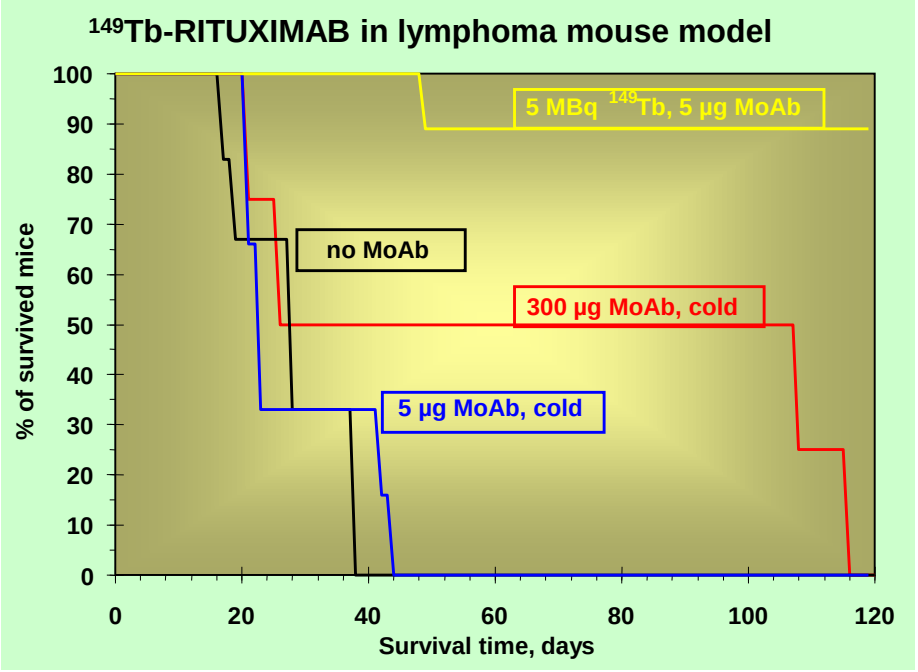

G.J. Beyer et al., Eur. J. Nucl. Med. Mol. Imaging 31 (2004) 547.

Applications

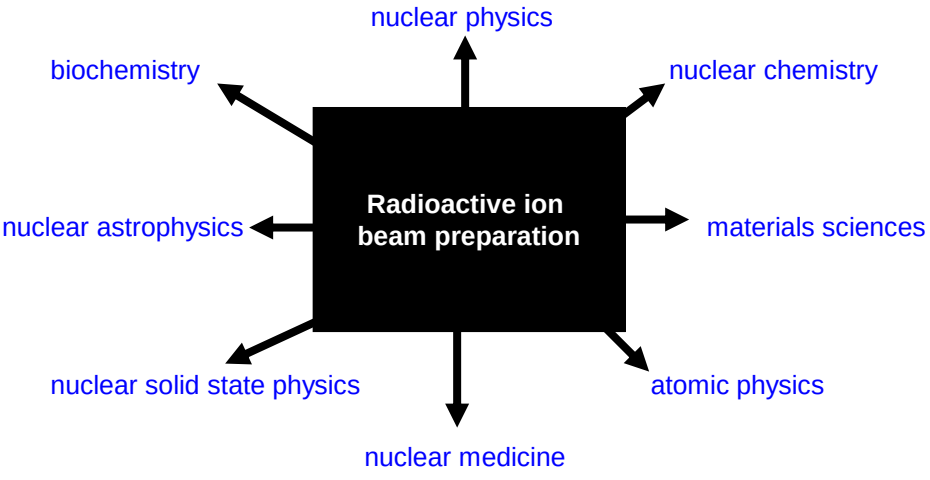

Types of commercial mass spectrometers

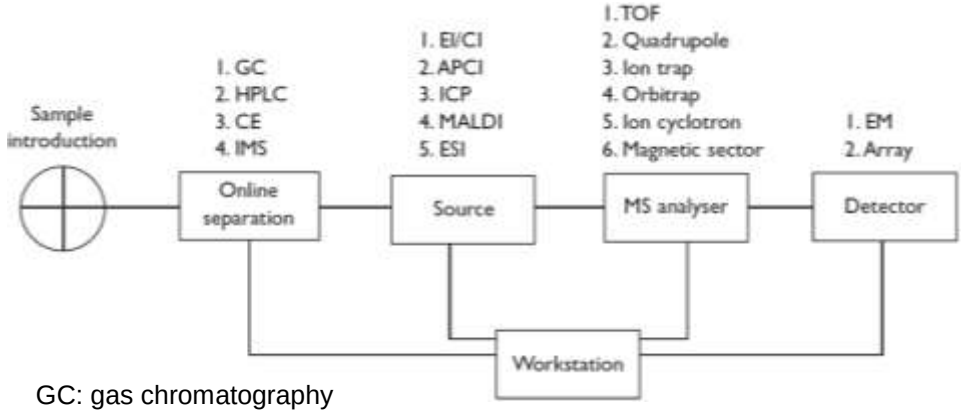

GC: gas chromatography
HPLC: high pressure liquid chromatography
CE: capillary electrophoresis
IMS: ion mobility spectroscopy
EI/CI: electron impact/chemical ionization
APCI: atmospheric pressure chem. ioniz.
ICP: inductively coupled plasma
MALDI: matrix assisted laser desorption/ioniz.
ESI: electrospray ionization

S. Naylor and P.T. Babcock, Drug Discovery World (Fall 2010) 73.

Inductively Coupled Plasma-MS

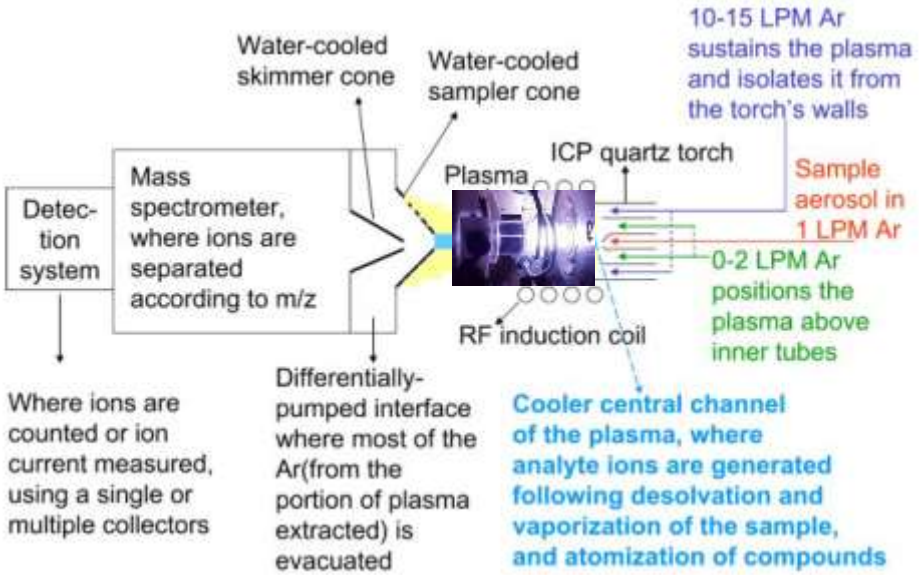

D. Beauchemin, Mass Spectrom. Rev. 29 (2010) 560.

TOF-SIMS
time-of-flight secondary ion mass spectrometer

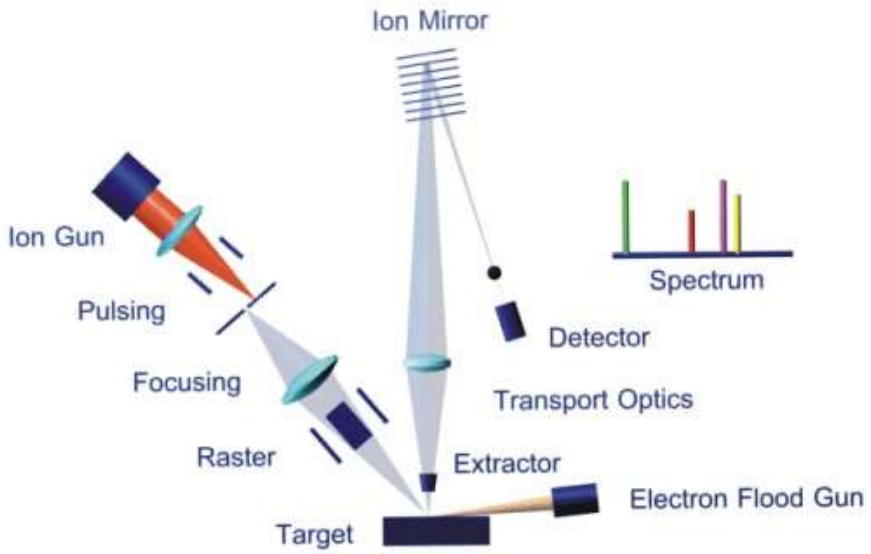

MALDI-TOF
matrix assisted laser desorption/ionization TOF

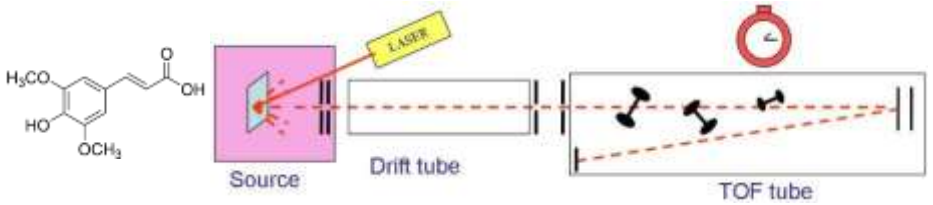

Matrix:
- low vapor pressure for operation at low pressure
- polar groups for use in aqueous solutions
- strong absorption in UV or IR for efficient evaporation by laser
- low molecular weight for easy evaporation
- acidic: provides easily protons for ionization of analyte

Mass selectivity of radio-frequency quadrupoles

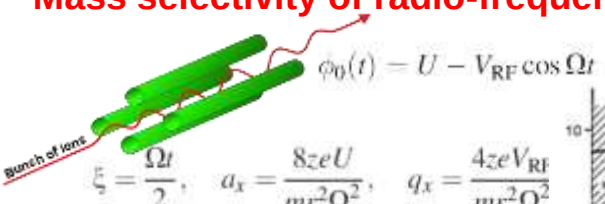

$$\phi_0(t) = U - V_{RF}\cos\Omega t$$

$$\xi = \frac{\Omega t}{2}, \quad a_x = \frac{8zeU}{mr_0^2\Omega^2}, \quad q_x = \frac{4zeV_{RF}}{mr_0^2\Omega^2}$$

$$\frac{d^2x}{d\xi^2} + (a_x - 2q_x\cos 2\xi)x = 0$$

Mathieu equation

$$a_y = -a_x, \quad q_y = -q_x$$

$m_1 < m_2 < m_3$

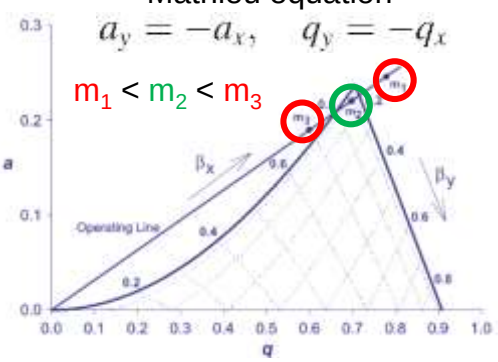

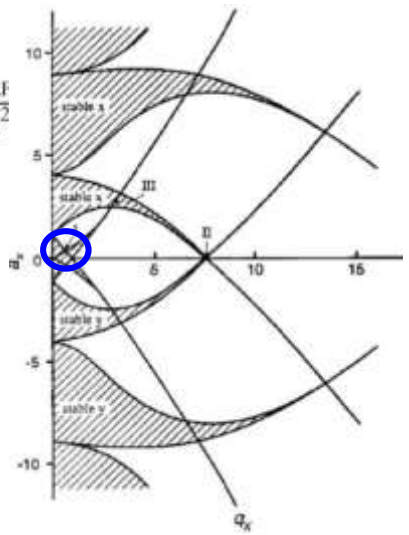

D.J. Douglas,
Mass Spectrom. Rev. 28 (2009) 937.

Ultrahigh-mass mass spectrometry

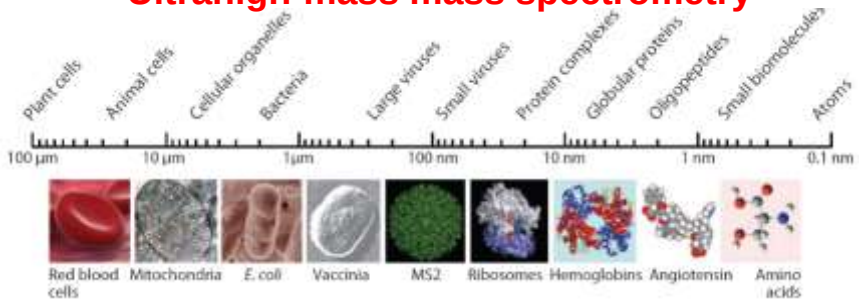

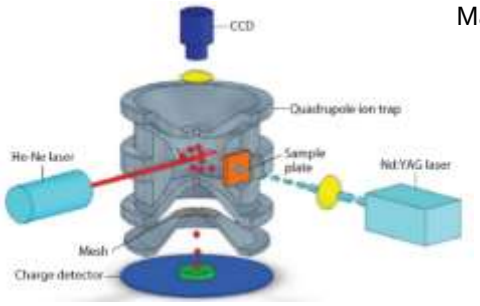

Mass distribution of human erythrocytes

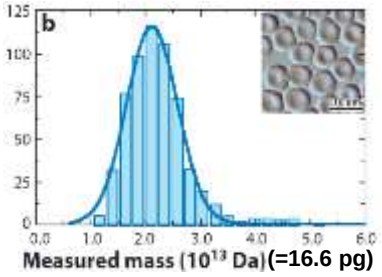

(=16.6 pg)

H.-C. Chang, Annu. Rev. Anal. Chem. 2 (2009) 169.

Forensic applications

- trace detection of drugs, poisons, explosives, etc.
- composition analysis of paint, tissue, etc.
- pesticide control
- measurement of isotopic composition
- etc.

Doping control

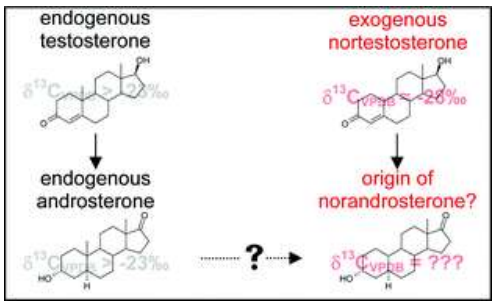

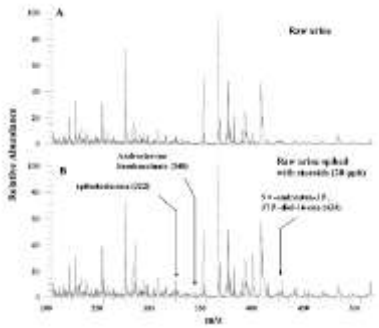

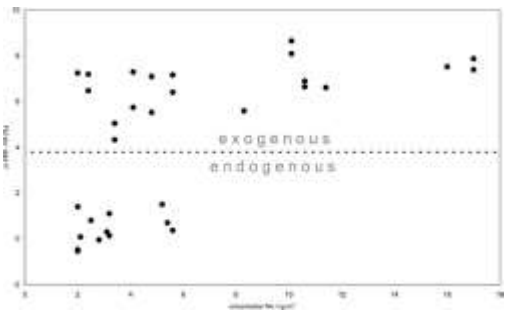

M. Hebestreit et al., Analyst 131 (2006) 1021.

Radiocarbon dating

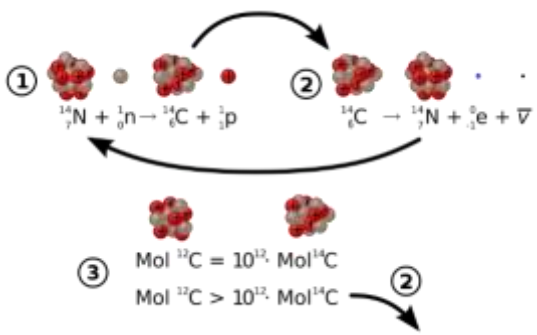

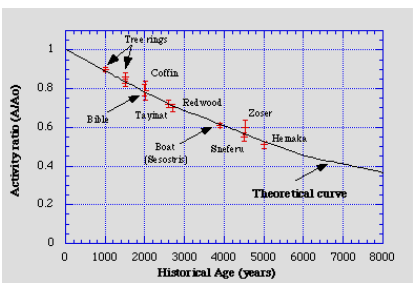

- **Cosmic radiation > spallation neutrons > $^{14}N(n,p)^{14}C$ reactions**
- **Living organisms: equilibrium with atmospheric $^{14}C/^{12}C$ ratio**
- **After death: $^{14}C/^{12}C$ decreases due to ^{14}C decay ($T_{1/2}$=5370 y)**

Problem: measure $^{14}C^{+}$ at ppt level without interference from
$^{14}N^{+}$, $^{12}CH_2^{+}$, $^{13}CH^{+}$, $^{28}Si^{++}$, $^{12}C^{16}O^{++}$, $^{42}Ca^{+++}$, $^{56}Fe^{++++}$,…

Multistep-Separation in Accelerator Mass Spectrometry

1. **Negative ion formation** — **$^{14}N^-$ anions do not exist**
2. **Acceleration and stripping** — **breakup of molecules**
3. **Z-selective ion detector** — $\frac{dE}{dx} \sim \frac{Z^2}{E}$

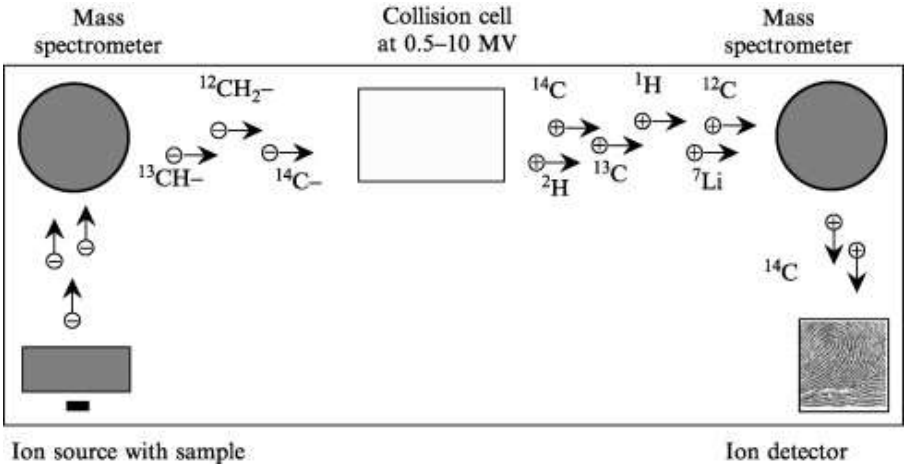

The shroud of Turin AD 1260-1390

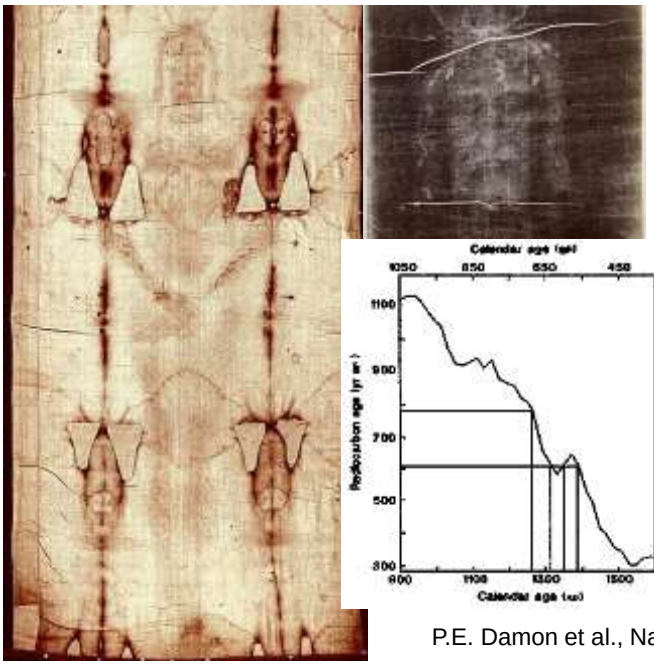

AMS measurements at Arizona, Oxford and Zurich.

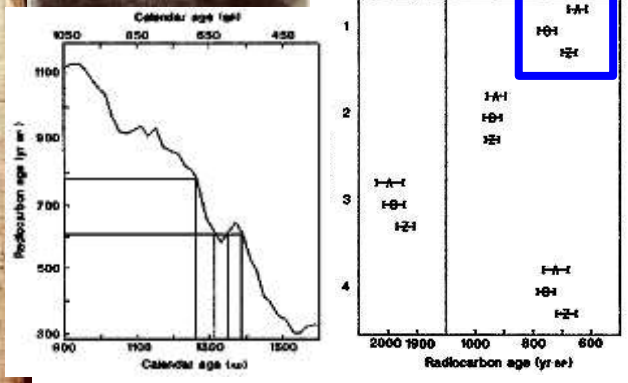

P.E. Damon et al., Nature 337 (1989) 611.

Winter smog

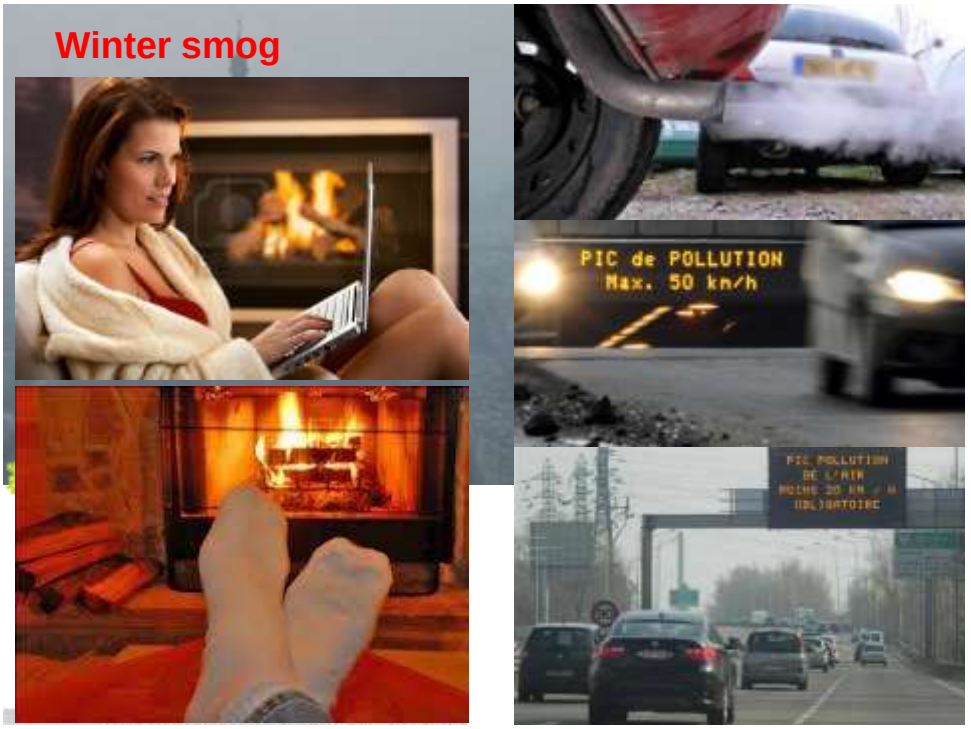

Aerosol composition in Swiss alpine valleys

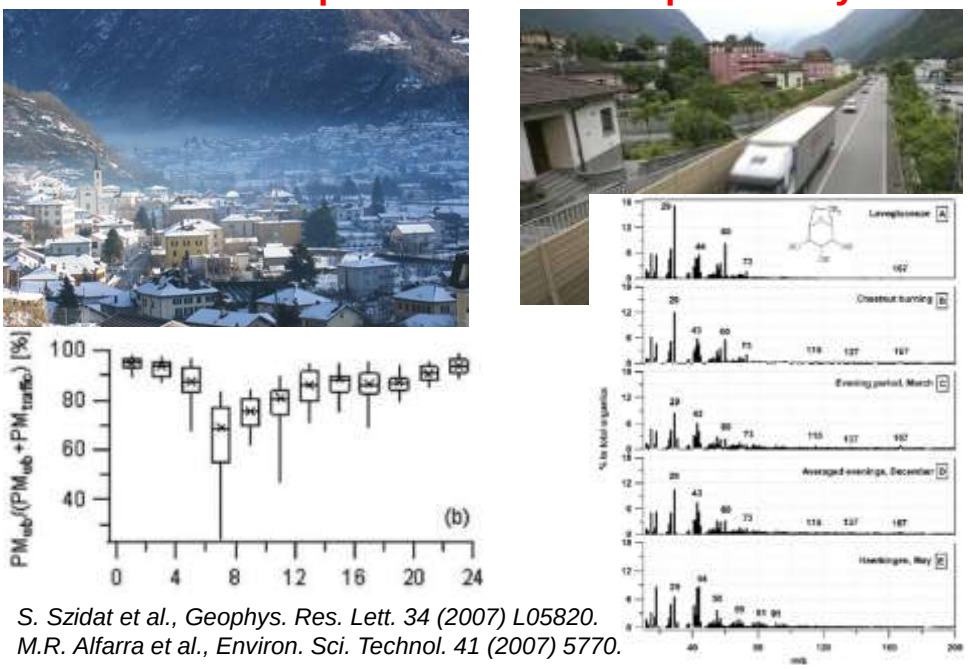

S. Szidat et al., Geophys. Res. Lett. 34 (2007) L05820.
M.R. Alfarra et al., Environ. Sci. Technol. 41 (2007) 5770.

Asian haze: biomass burning contributes !

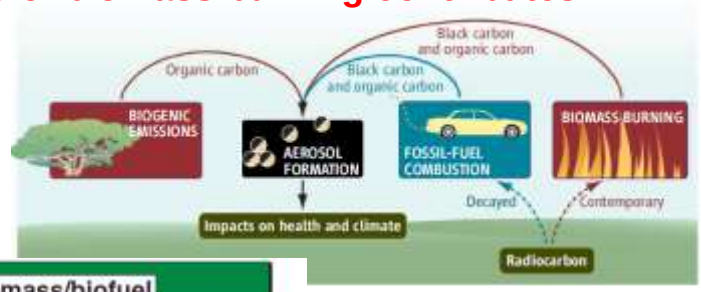

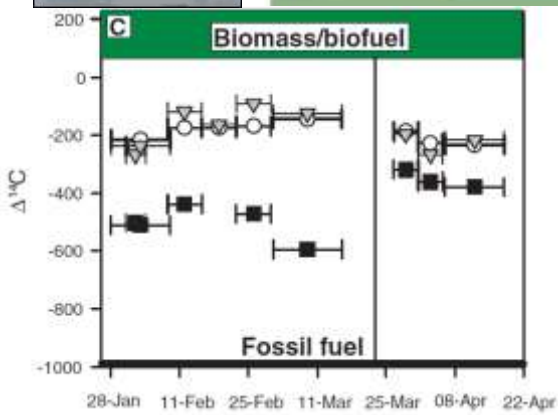

S. Szidat,
Science 323 (2009) 470.
Ö. Gustafsson et al.,
Science 323 (2009) 495.

6 MV tandem: the “working horse” for AMS

ETH Zürich, Laboratory for Ion Beam Physics

0.6 MV TANDY: the “working pony” for AMS

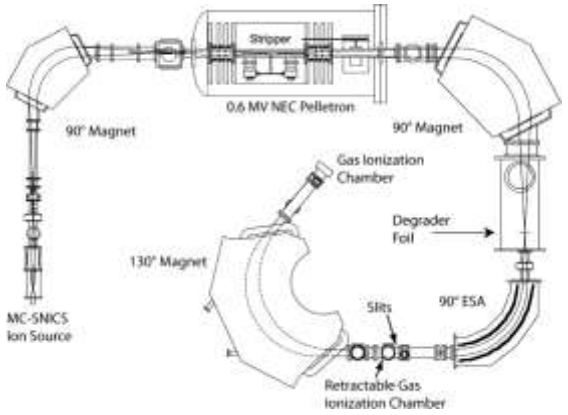

Routine measurements of: ^{10}Be, ^{41}Ca, ^{129}I, ^{236}U, Pu, etc.
longer-lived than ^{14}C: geology, cosmochronology,…

ETH Zürich, Laboratory for Ion Beam Physics

MICADAS (Mini-radioCArbon-DAting-System): 0.2 MV AMS

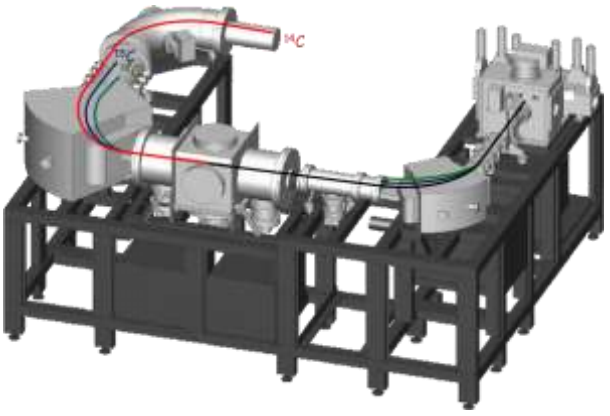

2.3 x 3 m^2 “tabletop”

Routine measurements of: ^{14}C

ETH Zürich, Laboratory for Ion Beam Physics

MUCADAS (MICRO-radioCArbon-DAting-System): 45 kV AMS

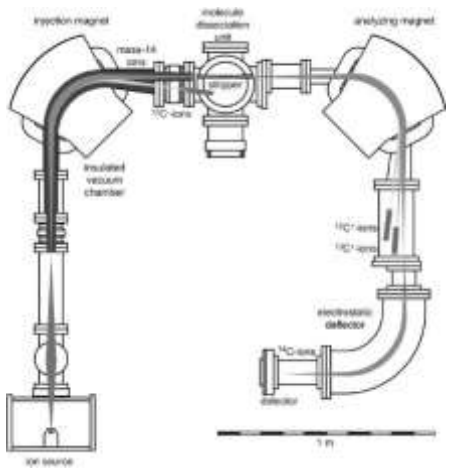

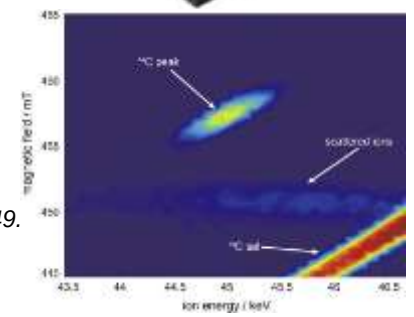

H.A. Synal et al., Nucl. Instr. Meth. B294 (2013) 349.

ETH Zürich, Laboratory for Ion Beam Physics

Retardation spectrometer

- **electrostatic energy measurement**
- **charged particles move against electrostatic potential; transmission measured as function of repulsive potential**
- **analyzes only the energy component perpendicular to the analyzer**
- **total energy measurement requires perfectly parallel beam**

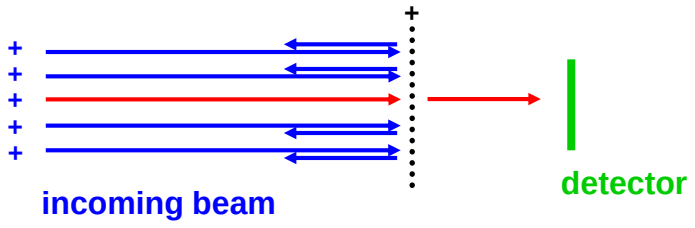

Examples of MAC-E retardation spectrometer

1. **WITCH at ISOLDE: weak interaction studies via recoil detection after EC/β^+ decay**

2. **aSPECT at ILL: precision spectroscopy of angular correlation between neutron spin and decay protons**

3. **KATRIN in Karlsruhe: precision measurement of beta endpoint in tritium decay for neutrino mass determination**

ß-decay and neutrino mass

model independent neutrino mass from ß-decay kinematics

$$\frac{d\Gamma_i}{dE} = C\,p\,(E+m_e)\,(E_0-E)\sqrt{(E_0-E)^2-m_i^2}\,F(E)\,\theta(E_0-E-m_i)$$

$$C = G_F^2 \frac{m_e^5}{2\pi^3}\cos^2\theta_C\,|M|^2$$

experimental observable is m_ν^2

E_0 = 18.6 keV
$T_{1/2}$ = 12.3 y

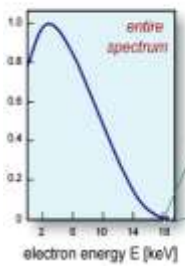

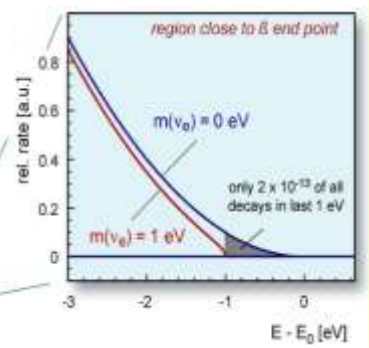

ß-source requirements :

- high ß-decay rate (short $t_{1/2}$)
- low ß-endpoint energy E_0
- superallowed ß-transition
- few inelastic scatters of ß's

ß-detection requirements :

- high resolution (ΔE< few eV)
- large solid angle ($\Delta\Omega \sim 2\pi$)
- low background

Electrostatic filter with Magnetic Adiabatic Collimation

MAC-E-Technique

adiabatic guiding of ß-particles along the magnetic field lines

inhomogen. B-Feld: stray field of 2 super-conducting magnets

B_{max} = 3 - 6 T

B_{min} < 1 mT

very large solid angle !

$\Delta\Omega \sim 2\pi$

$\vec{F} = (\vec{\mu} \cdot \vec{\nabla})\vec{B} + q\vec{E}$

$\mu = E_{\perp} / B = const$

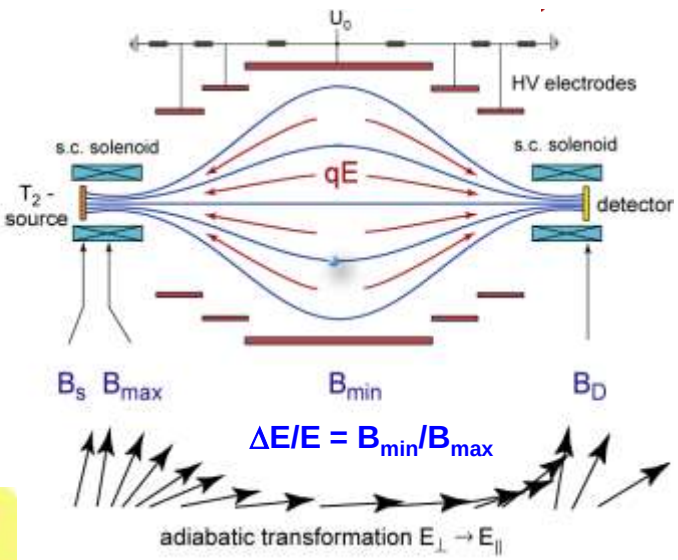

A. Picard et al., Nucl. Instr. Meth. B63 (1992) 345.

KATRIN experiment

Karlsruhe **Tri**tium **N**eutrino Experiment

at Forschungszentrum Karlsruhe

unique facility for closed T_2 cycle: Tritium Laboratory Karlsruhe

40 g ^{3}H per day

~ 75 m linear setup with 40 s.c. solenoids

< 1E-11 mbar

< 1E-20 mbar ^{3}H

main spectrometer – design

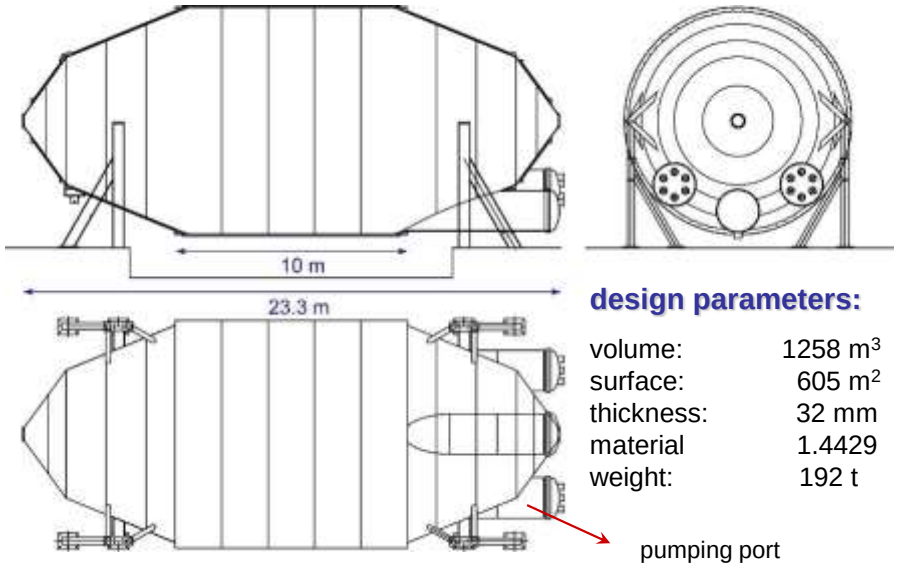

design parameters:

volume:	1258 m^3
surface:	605 m^2
thickness:	32 mm
material	1.4429
weight:	192 t

pumping port
for getters

Identification ≠ Separation

- **Identification:**
  The beam composition is determined but not changed.
  e.g. time-of-flight measurement, ΔE measurement,...

- **Separation:**
  Beam contaminations are removed.
  e.g. mass separation, chemical separation,...

- **Unique isotope selection requires the combination of at least two different identification/separation methods.**

- **A higher-fold combination gives improved suppression factors.**

Prism

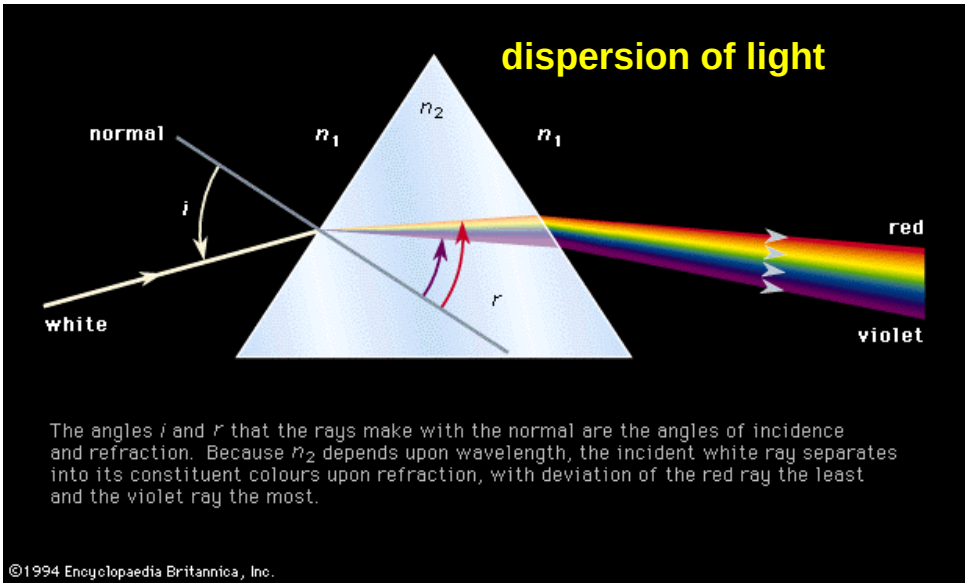

Dispersive ion optical elements

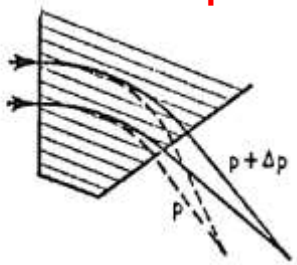

FIG. 5.15 A system with momentum dependent deflection of the central ray, showing lateral displacement due to momentum spread.

- **magnets are momentum dispersive**
- **electrostatic deflectors are energy dispersive**
- **Wien filters are velocity dispersive**

Focusing by tilted entrance/exit of magnetic field

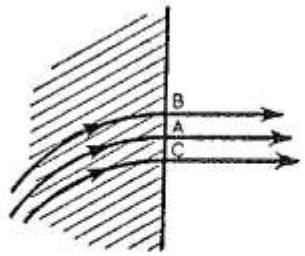

FIG. 5.3 Particles leaving a magnetic field normal to the edge.

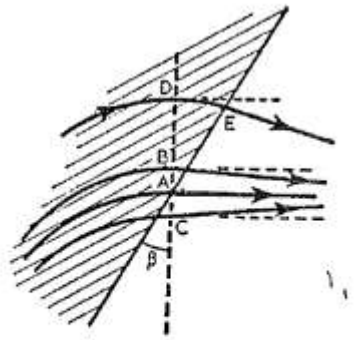

FIG. 5.4 Particles leaving a magnetic field at an angle to the edge. Dotted lines are for normal exit (cf. Fig. 5.3).

horizontal focusing effect

Focusing by tilted entrance/exit of magnetic field

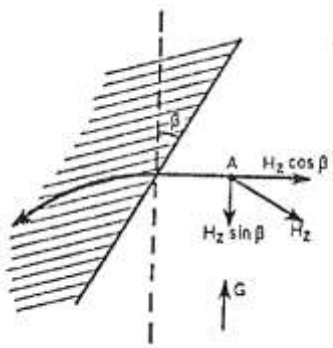

FIG. 5.5 Plan view of a positively charged particle entering a magnetic field directed into the paper. The trajectory makes an angle β with the normal. For view in the direction of arrow G see Fig. 5.6.

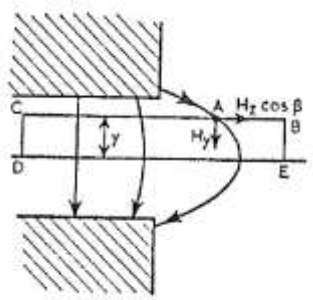

FIG. 5.6 View of Fig. 5.5 in the direction of arrow G. DE is the median plane on which $H_z = 0$.

vertical defocusing effect

Quadrupoles

Electrostatic:

$V = U (x^2 - y^2)/a^2$

$\mathcal{E} = -\text{grad } V$

$\mathcal{E}_x = -dV/dx = -2U/a^2\, x$

$\mathcal{E}_y = -dV/dy = 2U/a^2\, y$

$F_x = -2\, Uqe/a^2\, x$

$F_y = 2\, Uqe/a^2\, y$

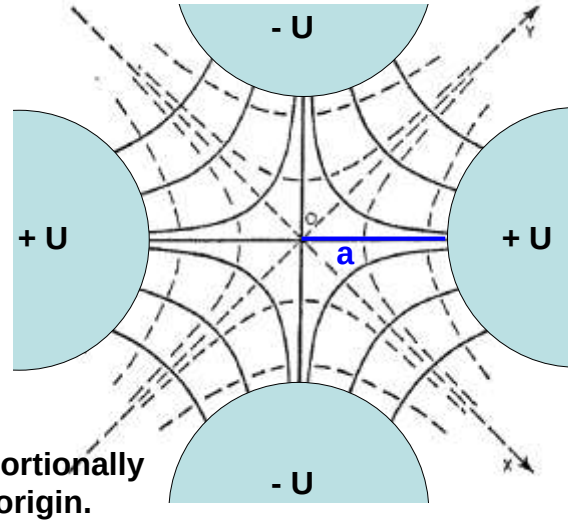

1. Force increases proportionally to distance from origin.

2. Focusing in x and defocusing in y (or vice versa).

⇒ requires quadrupole doublet or triplet to focus in x and y

Multipole correction elements

Correction of higher-order effects (aberrations) by hexapole, octupole, etc. fields. Often limited by beam diagnostics!

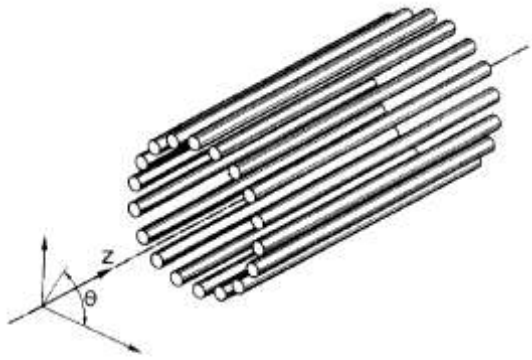

Fig. 1. Squirrel-cage-like electrode arrangement of an electrostatic $2(n+1)$ pole consisting of 18 wires, i.e. a squirrel-cage with $n = 8$. In this multipole the potential of each wire is controlled by a separate power supply.

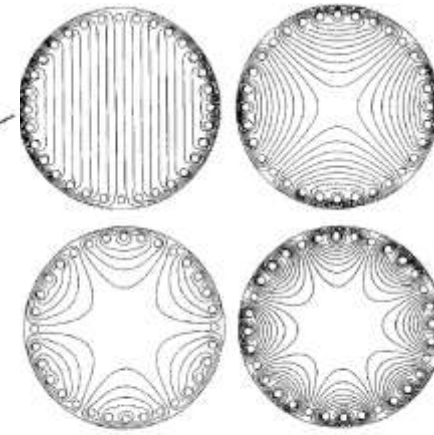

Fig. 3. Calculated potential distributions in a 32-wire squirrel-cage multipole for the cases of dipole ($V_1 \neq 0$), quadrupole ($V_2 \neq 0$), hexapole ($V_3 \neq 0$), octupole ($V_4 \neq 0$) excitations [see eq. (1)] with vanishing $\psi_1, \psi_2, \psi_3, \psi_4, \ldots$.

M. Antl and H. Wollnik, Nucl. Instr. Meth. A274 (1989) 45.

Ion-optical calculations

1. Matrix calculation:
TRANSPORT, COSY-INFINITY, GIOS, GICO, LISE++,…

2. MC simulations/ray tracing:
SIMION, ZGOUBY, RAYTRACE, LISE++, MOCADI,…

Focal plane of LOHENGRIN

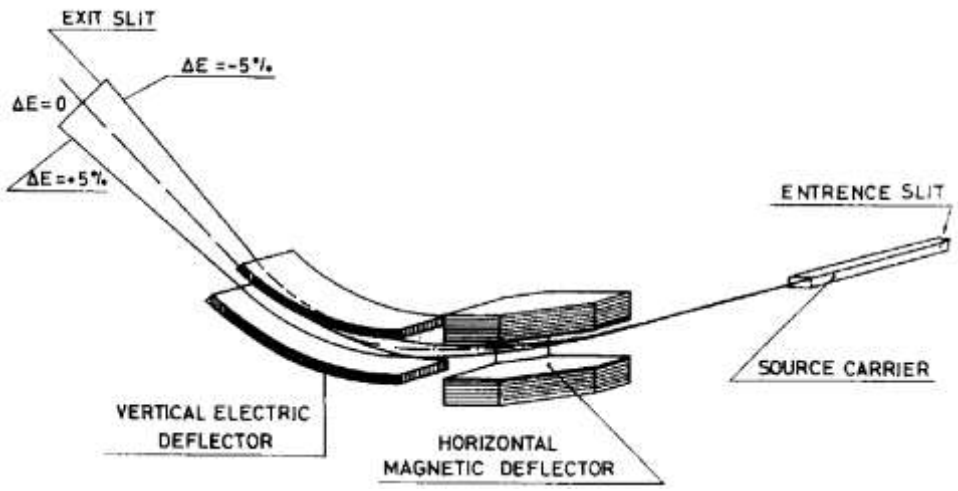

P. Armbruster et al., Nucl. Instr. Meth. 139 (1976) 213.

LOHENGRIN focal plane

Energy dispersion: $\Delta x = D_E \ \Delta E/E = 7.2$ cm/% = 7.2 m

Mass dispersion: $\Delta y = D_m \ \Delta m/m = 3.24$ cm/% = 3.24 m

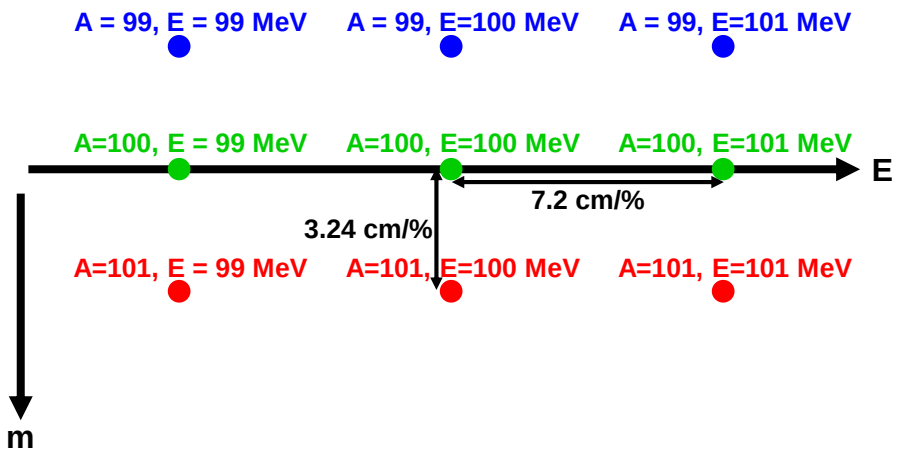

Measured kinetic energy distribution

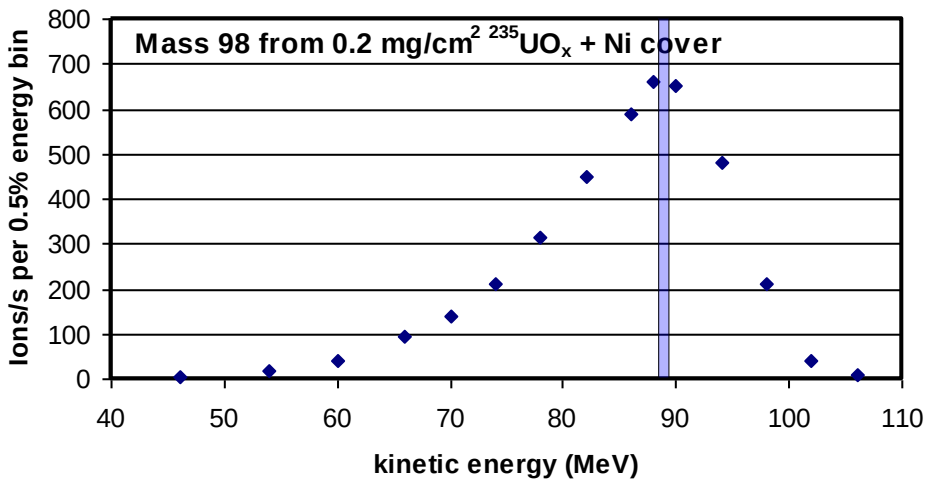

kinetic energy acceptance: $\Delta E/E = 1\%$

Reverse Energy Dispersion magnet

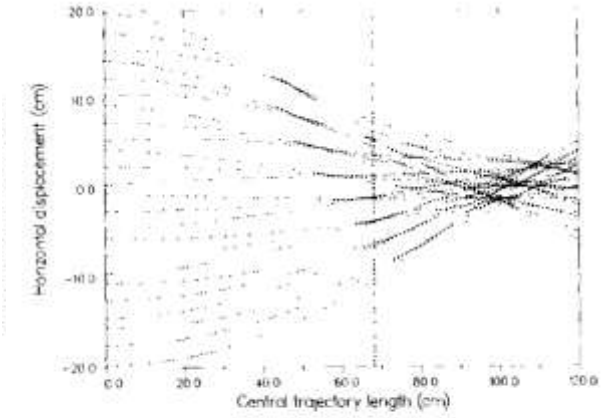

Fig. 5. Horizontal displacement with respect to the central trajectory of a beam arising from a 5×70 mm^2 target vs the central trajectory length. The vertical dashed and dotted lines show respectively the extent of the pole pieces and the focal position.

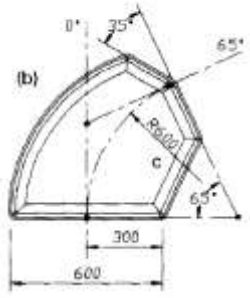

G. Fioni et al., Nucl. Instr. Meth. A332 (2003) 175.

LOHENGRIN Setup

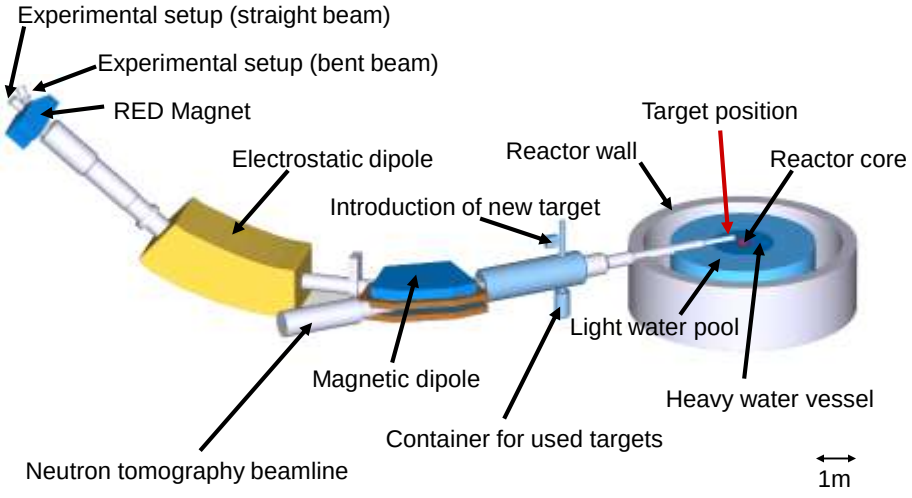

Measured kinetic energy distribution

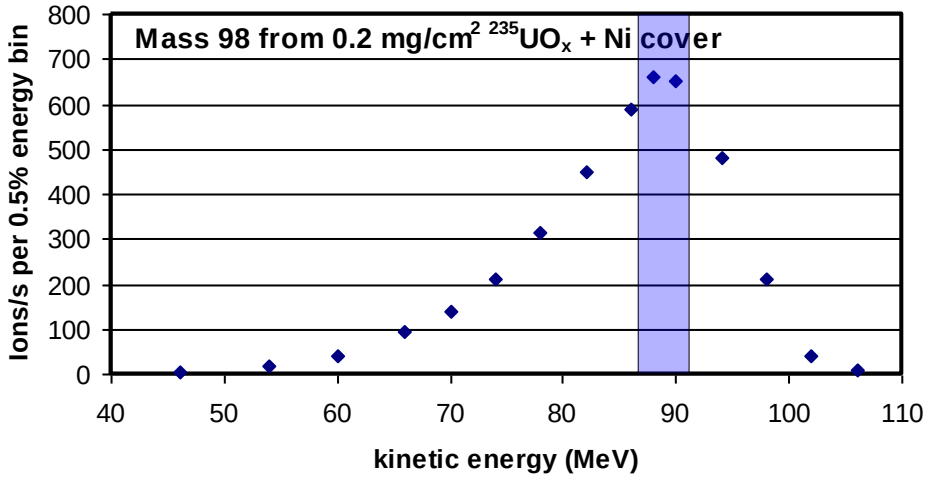

kinetic energy acceptance: $\Delta E/E = 5\%$

$\Rightarrow$ 10-60% transmission (low for thick spectroscopy targets)

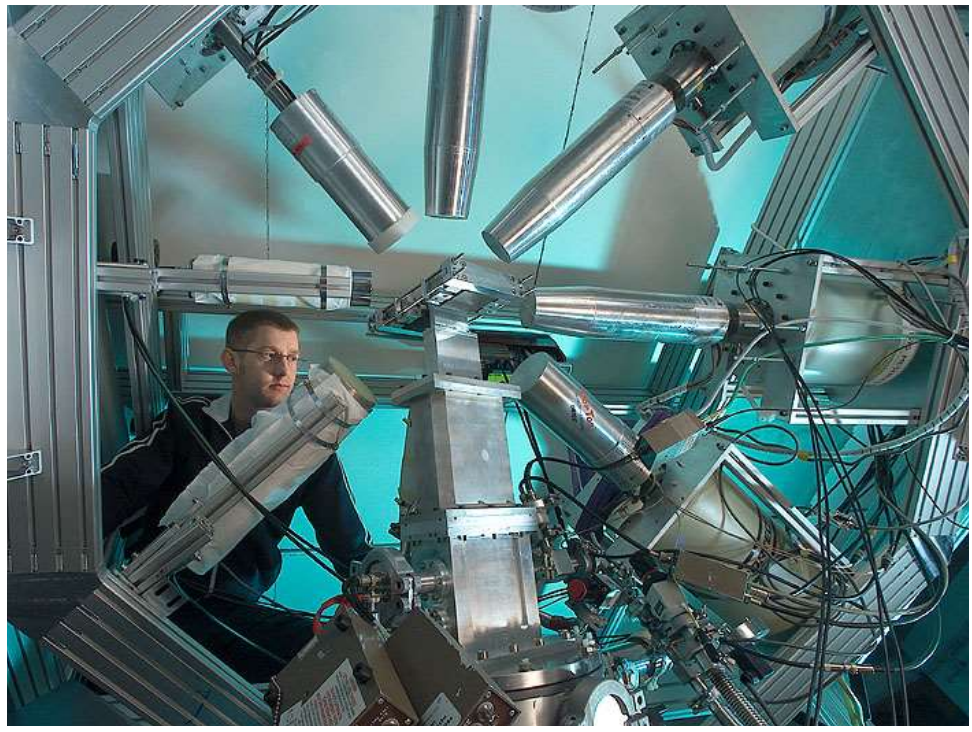

Gamma decay of 7.6 μs ^{98}Y isomer

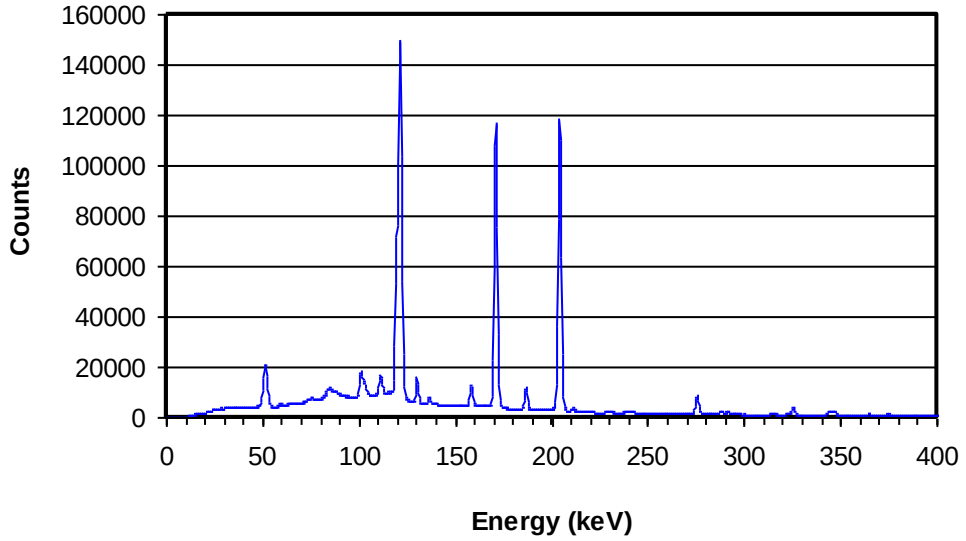

17^{-} isomer at 6.6 MeV in ^{98}Zr

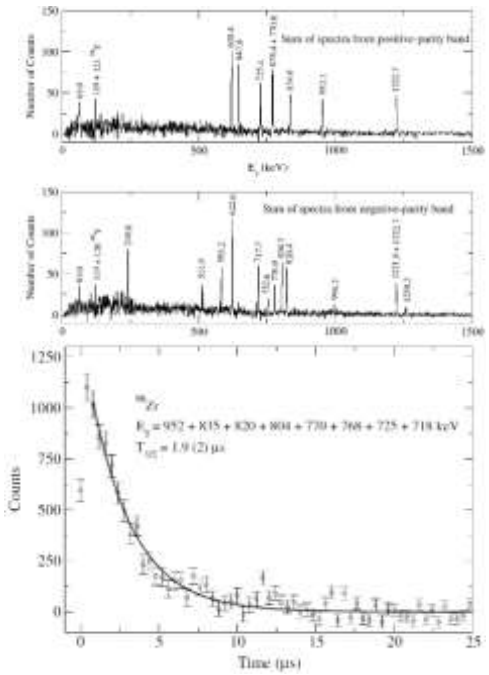

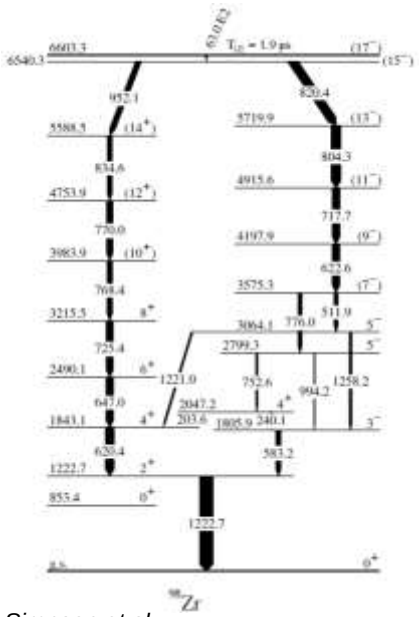

G. Simpson et al.,
Phys. Rev. C 74 (2006) 064308.

The LOHENGRIN fission fragment separator

mass-separated fission fragments,

up to 10^5 per second, $T_{1/2} \geq$ microsec.

$\Delta A/A$ = 3E-4 – 3E-3

$\Delta E/E$ = 1E-3 – 1E-2

flux $5.5 \cdot 10^{14}$ n./cm^2/s

few mg fission target

several 10^{12} fissions/s

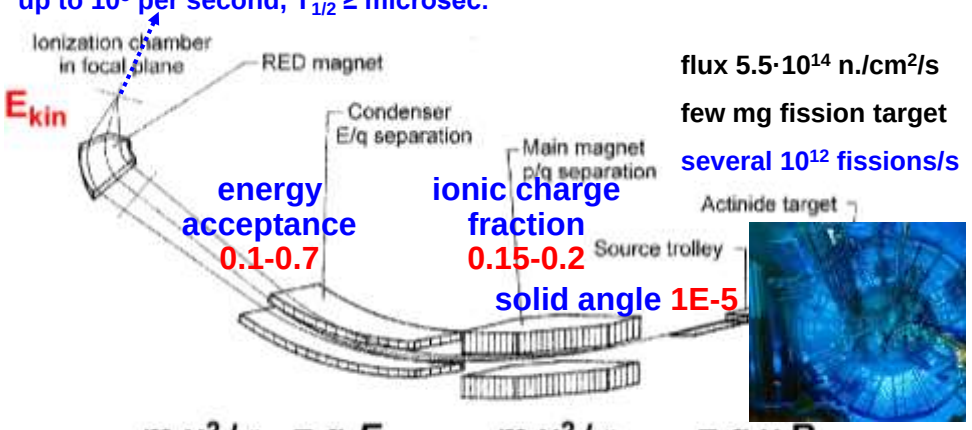

$m\,v^2 / r_{el} = q\,E$ $\qquad$ $m\,v^2 / r_{magn} = q\,v\,B$

$E_{kin} / q = E / 2\,r_{el}$ $\qquad$ $m\,v / q = B\,r_{magn}$

Ionic charge separation

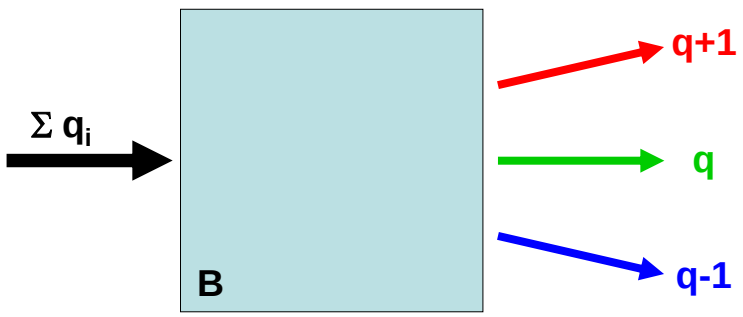

Ionic charge state distribution

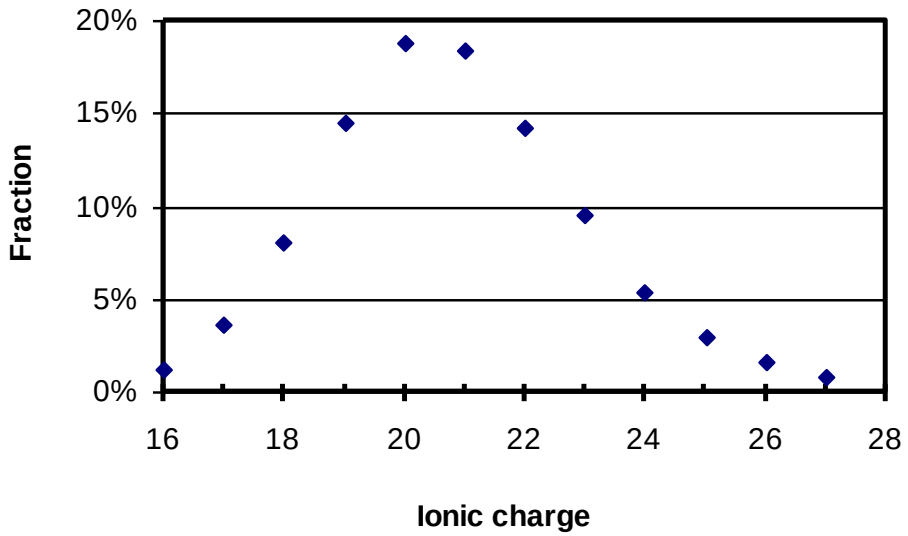

Ionic charge separation

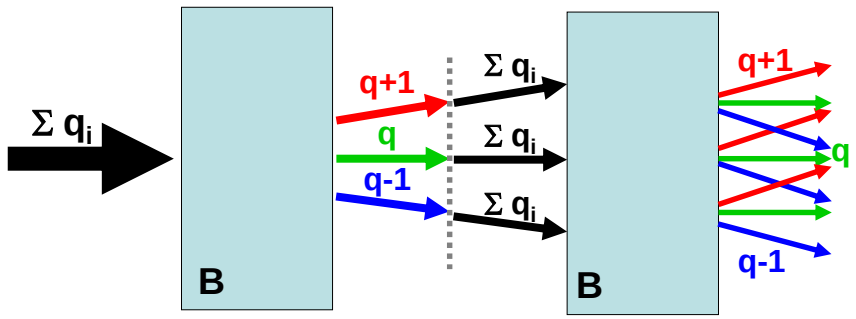

Ionic charge separation

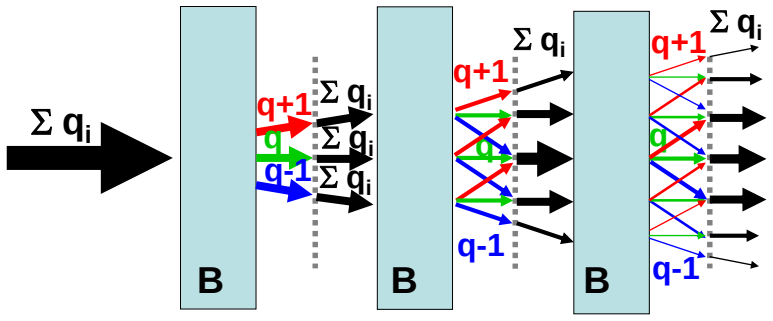

Separation with gas-filled magnet

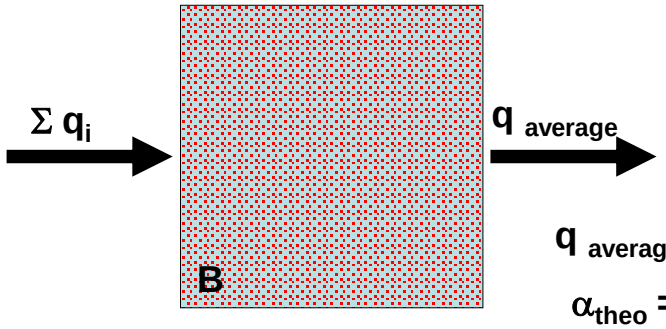

He or N_2 at few mbar

$q_{average} = v/v_{Bohr}\, Z^{\alpha}$

$\alpha_{theo} = 1/3$ (Bohr)

$\alpha_{exp} = 0.33 - 0.7$

Isotope selection with gas-filled separators

- Gas collisions give average $q = fkt(Z,v) \propto Z^{1/3}\, v/v_{Bohr}$
- p/q selection by magnetic deflection
- $B\rho \propto A/Z^{1/3}$ (*A. Ghiorso et al., Nucl. Instr. Meth. A269 (1988) 192*)

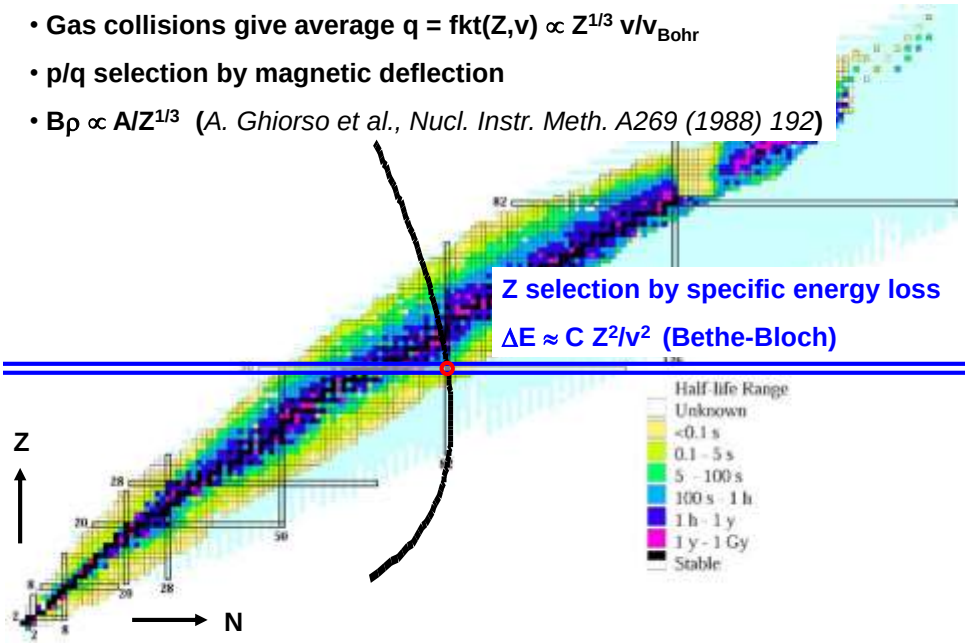

Multistep-Separation in Accelerator Mass Spectrometry

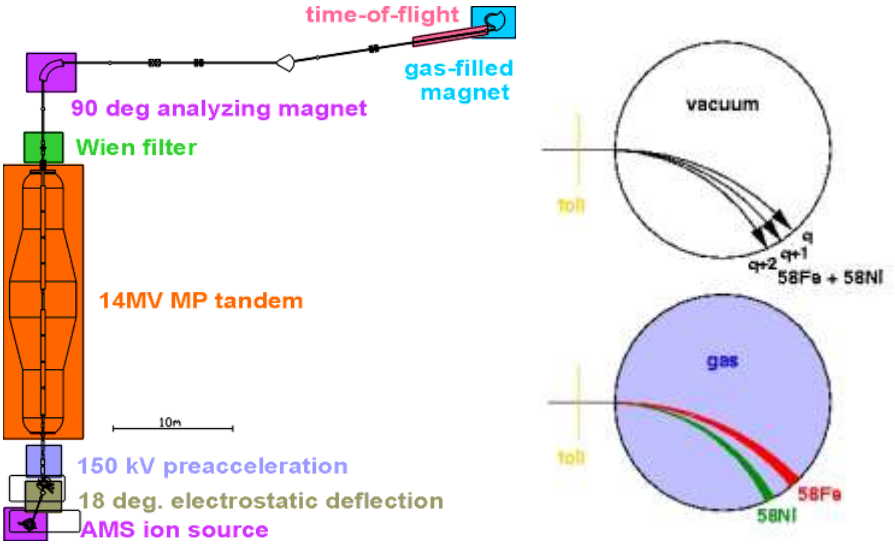

10^{-15} sensitivity!

From ISOL beams to RIBs with higher energies

ISOL beams

- **have well-defined energy ($\Delta E/E \approx$ 1eV / 60 keV)**
- **have usually small emittance (e.g. 10 π mm mrad), i.e. limited opening angle**
- **have often well-defined ionic charge q=1**
- **Z selection is performed before the mass separator**

Recoils or fragments of nuclear reactions:

- **have large energy spread**
- **large angular spread**
- **different ionic charge states**
- **depending on nuclear reaction different Z**

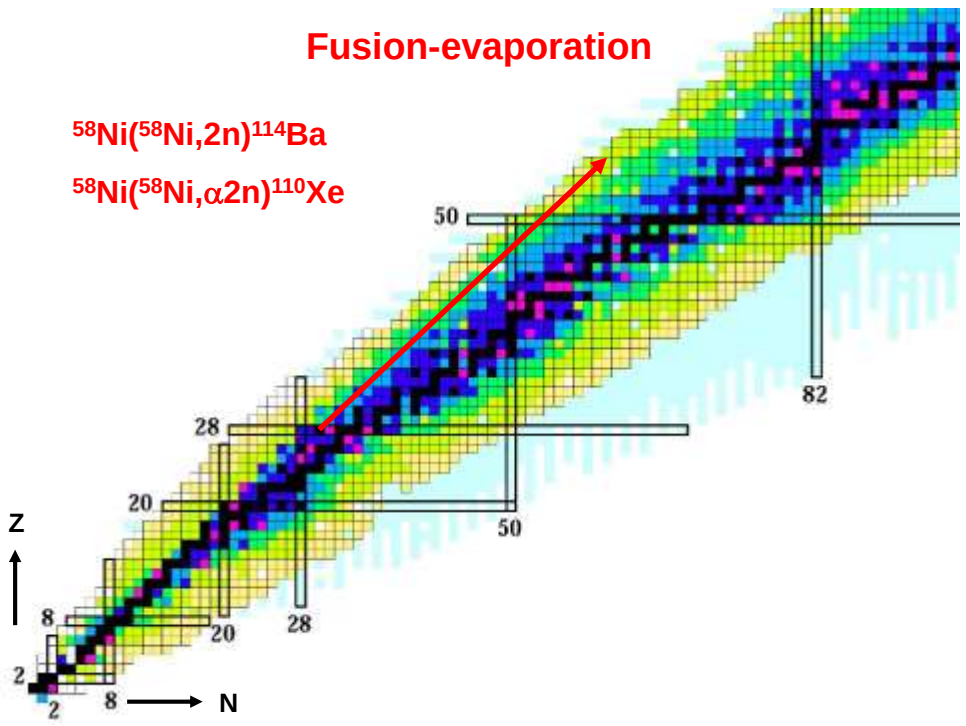

Requirements for in-flight separators

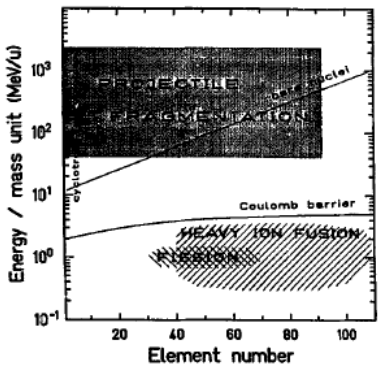

Fig. 2. Domains of kinetic energies of the reaction products from various nuclear reactions.

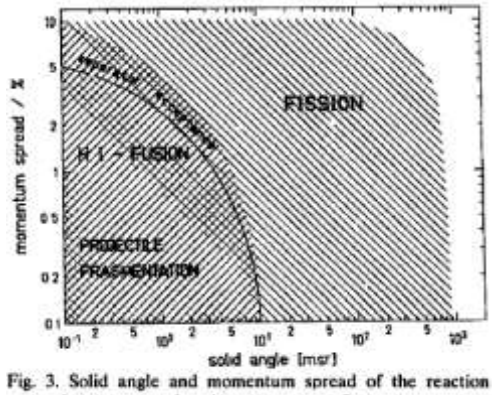

Fig. 3. Solid angle and momentum spread of the reaction products compared to the acceptances of spectrometers.

G. Münzenberg, Nucl. Instr. Meth. B70 (1992) 265.

Recoil separators

- **separate the products of a nuclear reaction (recoils) from the projectile beam**
- **early dumping of unwanted beam**
- **optionally also A/q separation of reaction products**
- **usually kinetic energies up to 10 MeV/nucleon**
- **mass dispersion achieved by combination of magnetic dipoles, electric dipoles or Wien filter**
- **usually additional quadrupoles for focusing**

SHIP at GSI Darmstadt

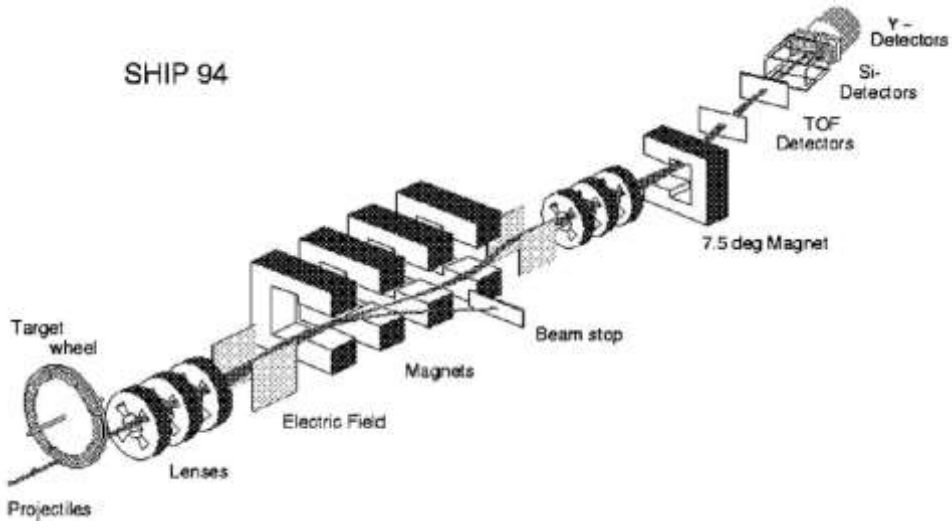

G. Münzenberg et al., Nucl. Instr. Meth. 161 (1979) 65.

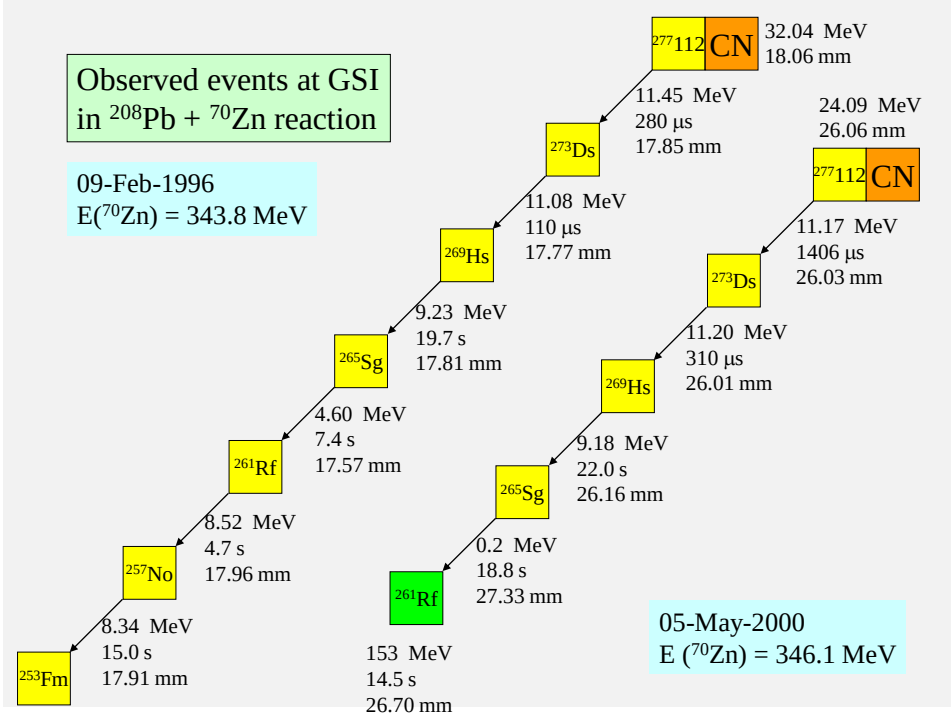

VASSILISSA

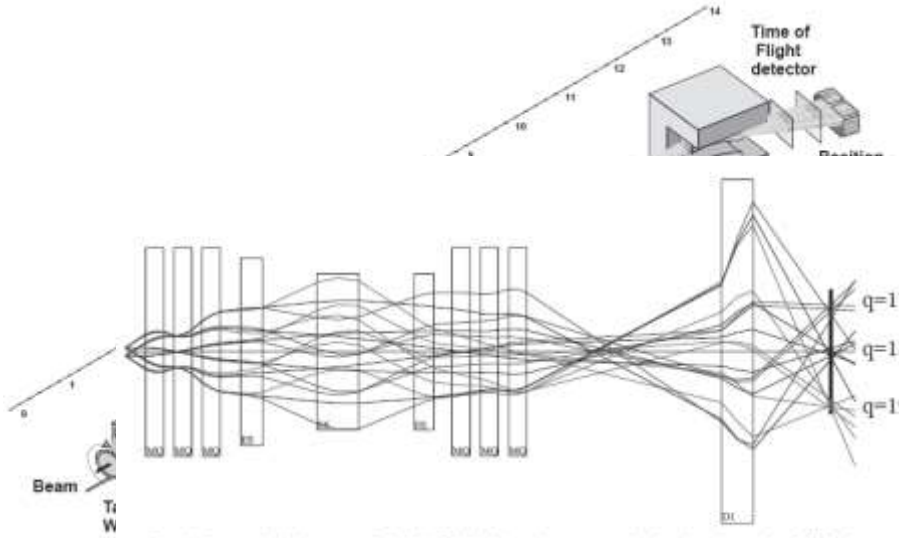

Fig. 5. Ion-optical elements of the VASSILISSA and computer-simulated trajectories of ^{208}Po ions.

A.G. Popeko et al., Nucl. Instr. Meth. A510 (2003) 371.

DGFRS: Dubna Gas-Filled Recoil Separator

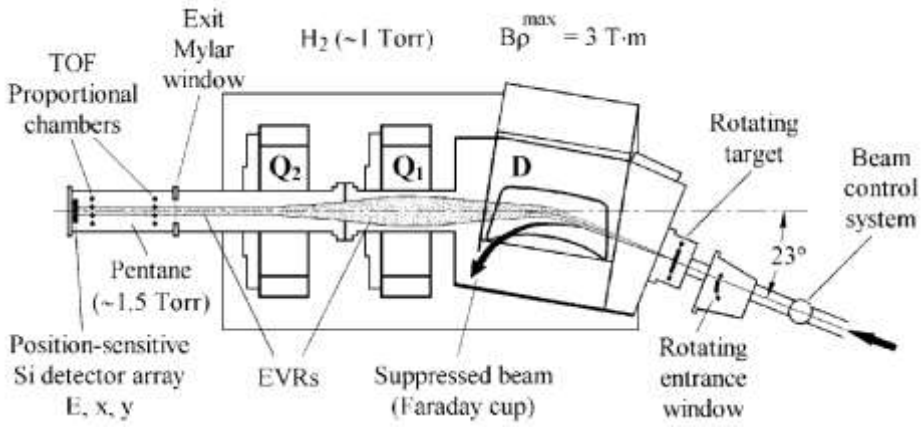

K. Subotic et al., Nucl. Instr. Meth. A481 (2002) 71.

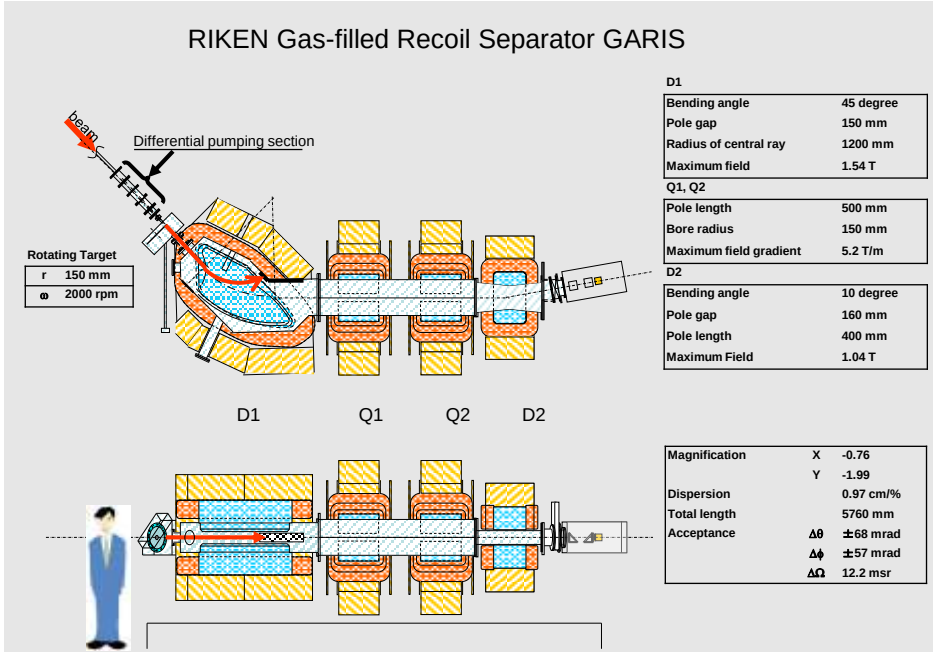
RIKEN Gas-filled Recoil Separator GARIS
beam
Differential pumping section
Rotating Target
r 150 mm
ω 2000 rpm
D1
Bending angle 45 degree
Pole gap 150 mm
Radius of central ray 1200 mm
Maximum field 1.54 T
Q1, Q2
Pole length 500 mm
Bore radius 150 mm
Maximum field gradient 5.2 T/m
D2
Bending angle 10 degree
Pole gap 160 mm
Pole length 400 mm
Maximum Field 1.04 T
D1
Q1
Q2
D2
Magnification X -0.76
Y -1.99
Dispersion 0.97 cm/%
Total length 5760 mm
Acceptance Δθ ±68 mrad
Δϕ ±57 mrad
ΔΩ 12.2 msr

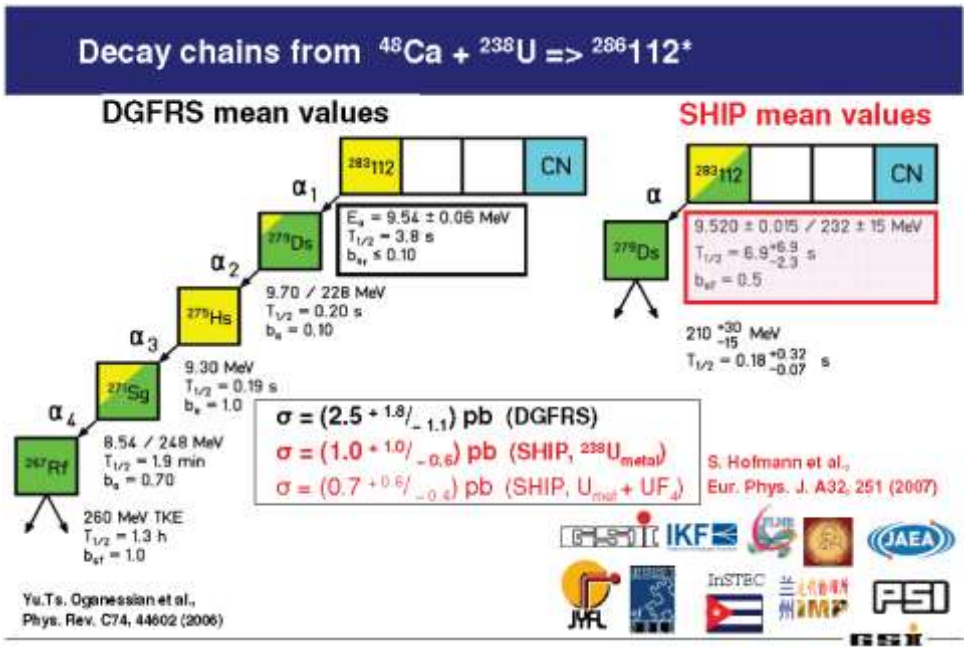
Decay chains from 48Ca + 238U => 286112*
DGFRS mean values
SHIP mean values
283112
CN
α1
279Ds
Ea = 9.54 ± 0.06 MeV
T1/2 = 3.8 s
bsf ≤ 0.10
α2
275Hs
9.70 / 228 MeV
T1/2 = 0.20 s
bs = 0.10
α3
271Sg
9.30 MeV
T1/2 = 0.19 s
bs = 1.0
α4
267Rf
8.54 / 248 MeV
T1/2 = 1.9 min
bs = 0.70
260 MeV TKE
T1/2 = 1.3 h
bsf = 1.0
σ = (2.5 +1.8/-1.1) pb (DGFRS)
σ = (1.0 +1.0/-0.6) pb (SHIP, 238Umetal)
σ = (0.7 +0.6/-0.4) pb (SHIP, Umetal + UF4)
α
9.520 ± 0.015 / 232 ± 15 MeV
T1/2 = 6.9 +6.9/-2.3 s
bsf = 0.5
210 +30/-15 MeV
T1/2 = 0.18 +0.32/-0.07 s
S. Hofmann et al.,
Eur. Phys. J. A32, 251 (2007)
Yu.Ts. Oganessian et al.,
Phys. Rev. C74, 44602 (2006)
IKF
JAEA
InSTEC
PSI
GSI

VAMOS at GANIL

Very wide acceptance ⇒ trajectory reconstruction for aberration correction

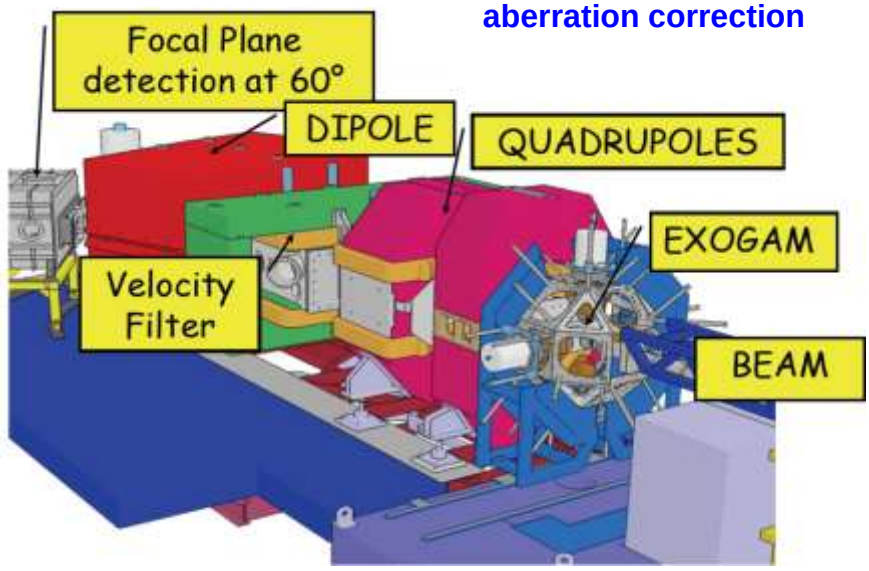

H. Savajols for the VAMOS Collaboration, Nucl. Instr. Meth. B204 (2003) 146.

GANIL/SPIRAL1/SPIRAL2 facility

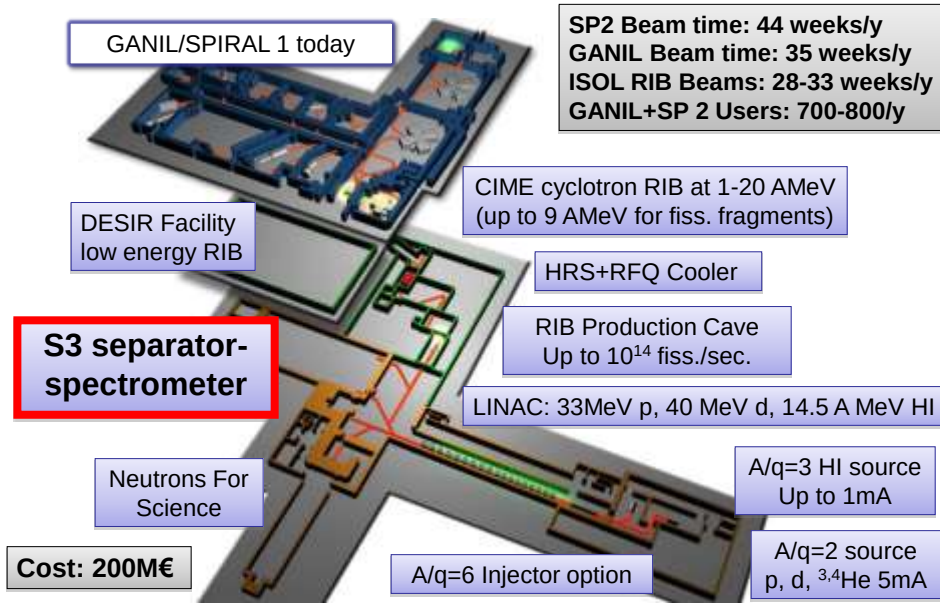

S3 at SPIRAL2, GANIL, Caen

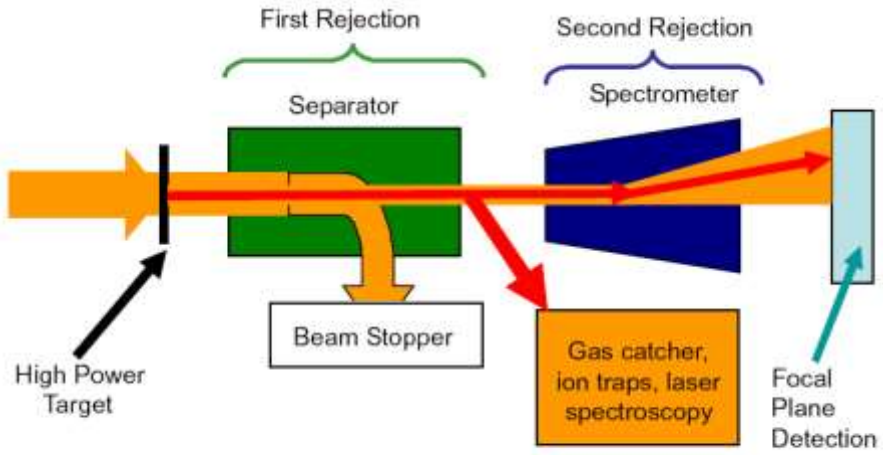

Fig. 1. Schematic idea for S^3 showing the two stage separator.

S3 at SPIRAL2, GANIL, Caen

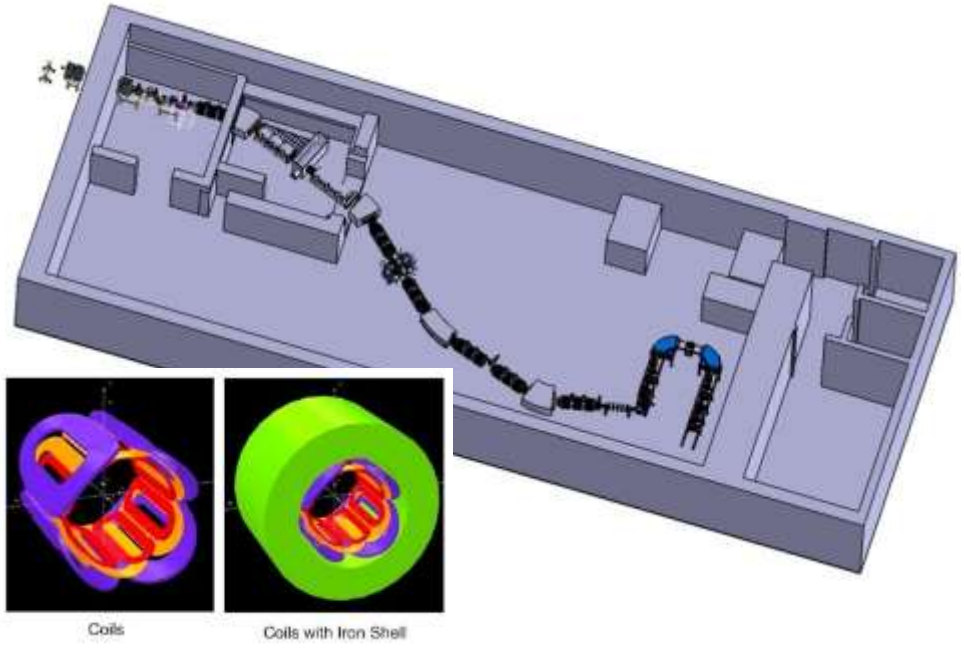

DRAGON

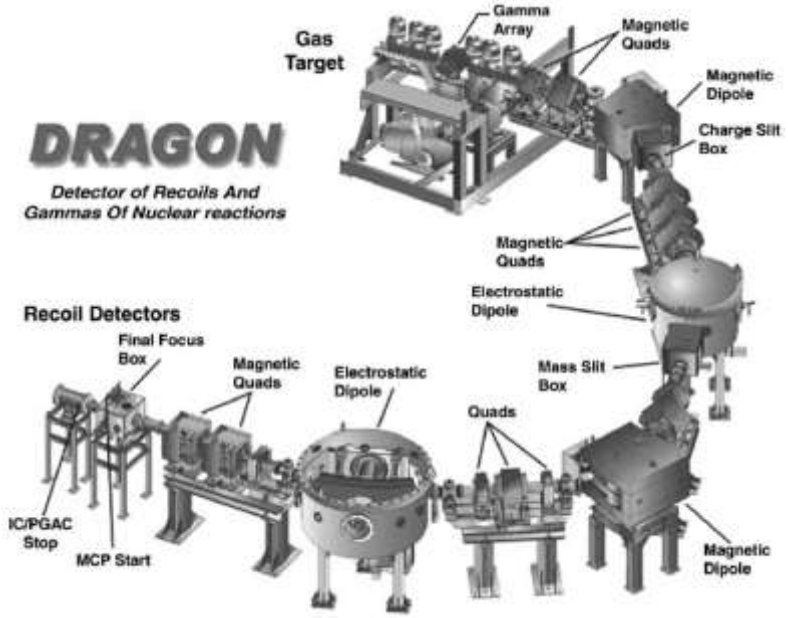

D. Hutcheon, Nucl. Instr. Meth. A498 (2003) 190.

Spallation + Fragmentation + Fission

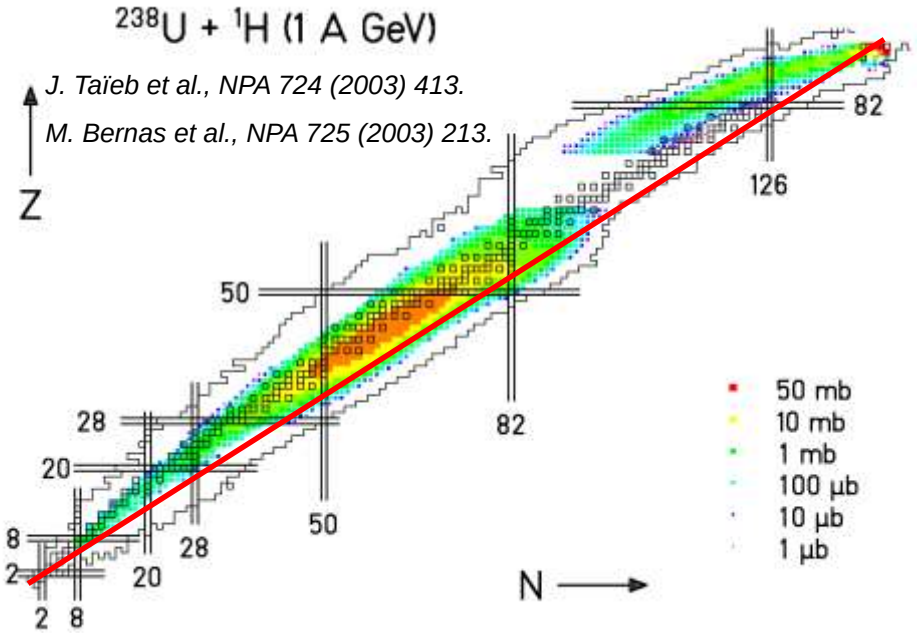

Normal kinematics: n, p or light ions on heavy target

- "conventional" accelerator providing "easily" high beam intensity
- dedicated target required
- reaction products emitted into 4π

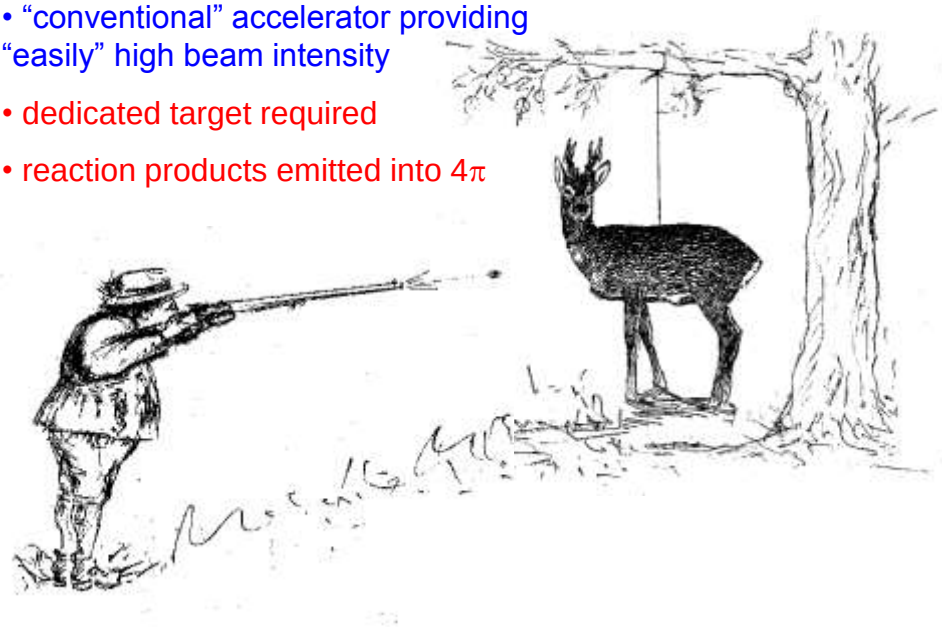

Inverse kinematics: heavy ions on light target

- complex and expensive accelerator
- reaction products forward focused

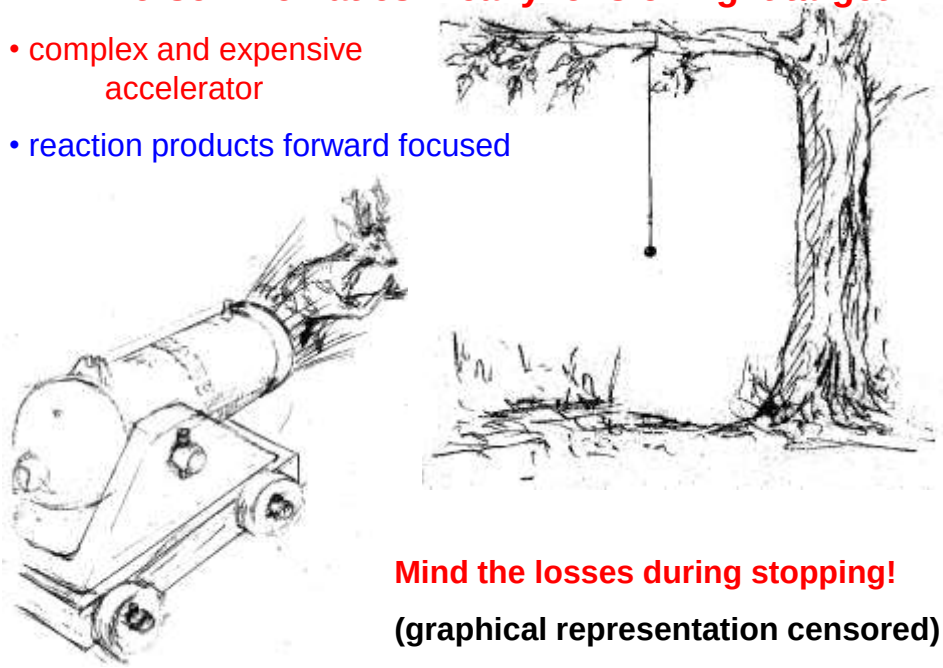

Mind the losses during stopping!

(graphical representation censored)

Spallation + Fragmentation + Fission

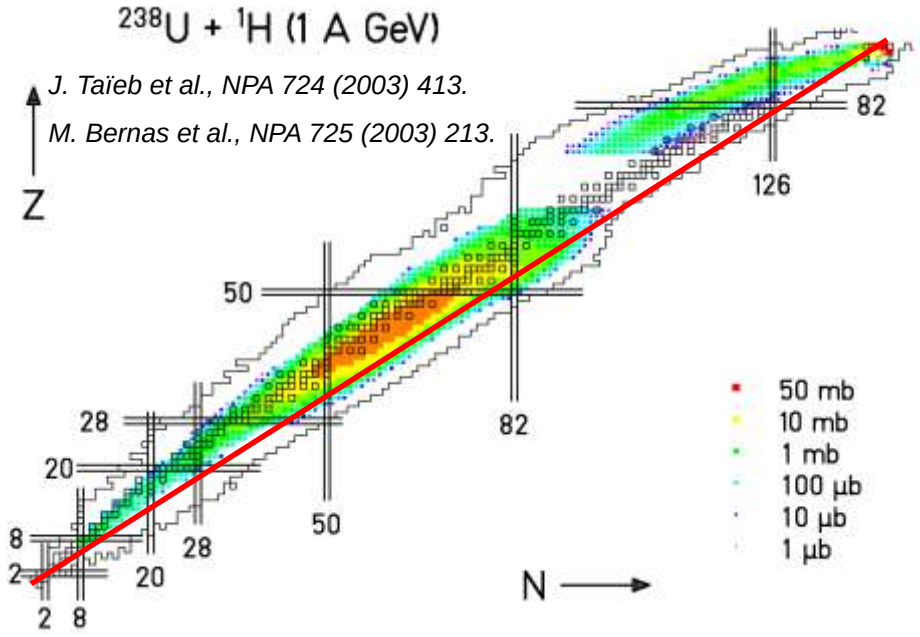

Momentum-loss achromat (Wedge separation)

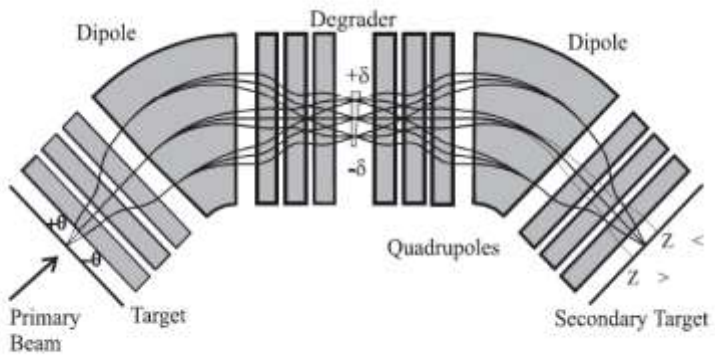

Fig. 4. Schematic representation of the ion-optics used in a momentum-loss achromat to separate projectile fragments.

D.J. Morrissey and B.M. Sherill, Lecture Notes in Physics 651 (2004) 113.

LISE

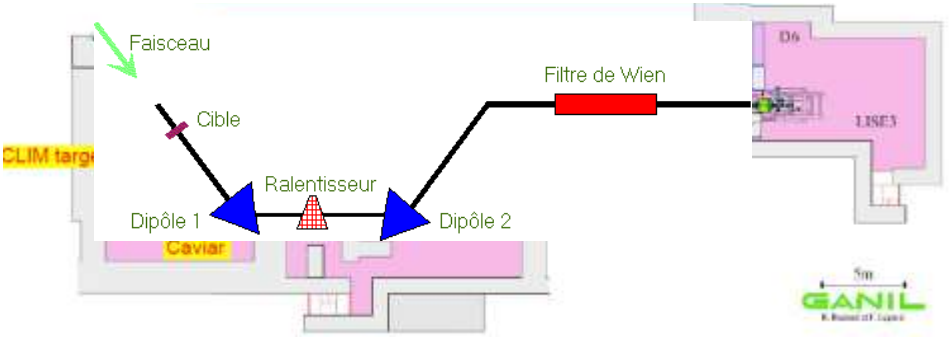

R. Anne et al., Nucl. Instr. Meth. A257 (1987) 215.
R. Anne et al., Nucl. Instr. Meth. B70 (1992) 276.

Dispersive ion optical elements

- **magnets are momentum dispersive**
- **electrostatic deflectors are energy dispersive**
- **Wien filters are velocity dispersive**
- **achromatic wedges are dispersive in mZ^2/E or $(Z/v)^2$**
- **RF kicker are flight time selective**

Effect of wedge selection

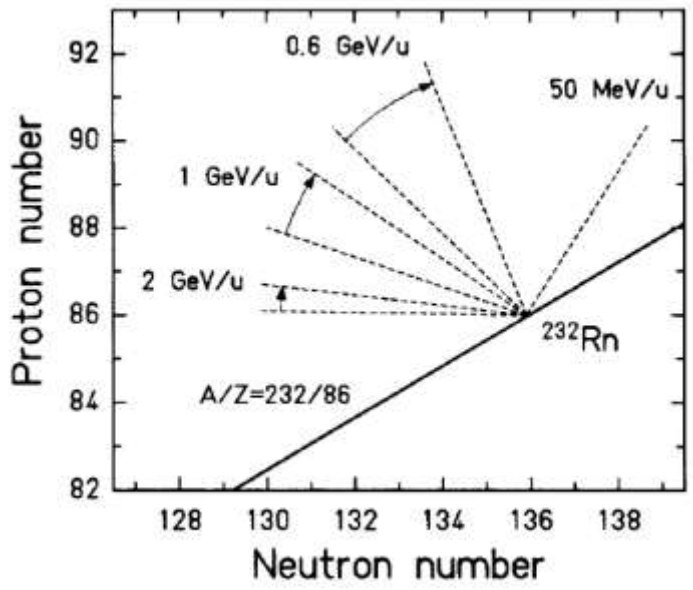

K.H. Schmidt et al., Nucl. Instr. Meth. A260 (1987) 287.

Effect of wedge selection

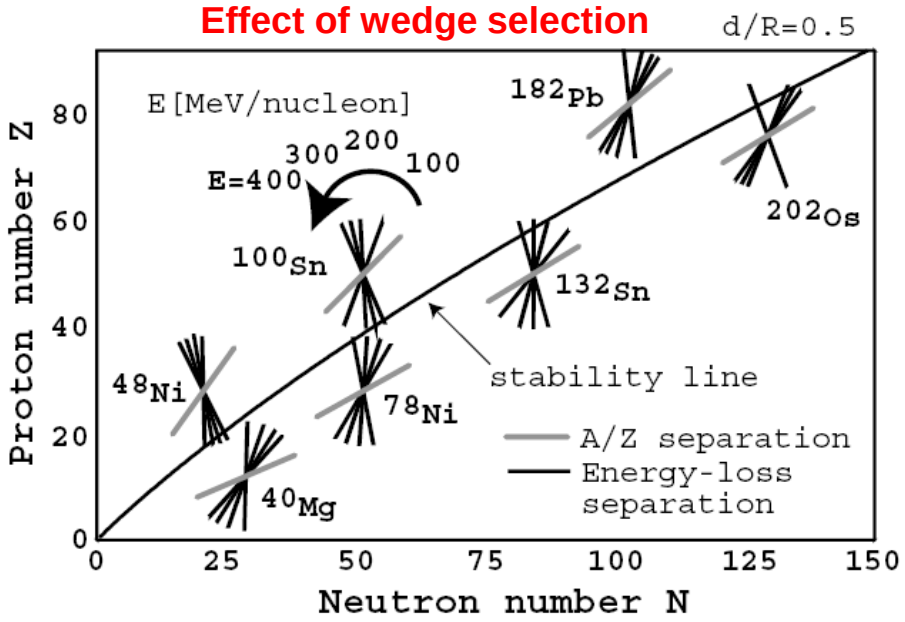

T. Kubo, Nucl. Instr. Meth. B204 (2003) 97.

In-flight production of rare isotopes

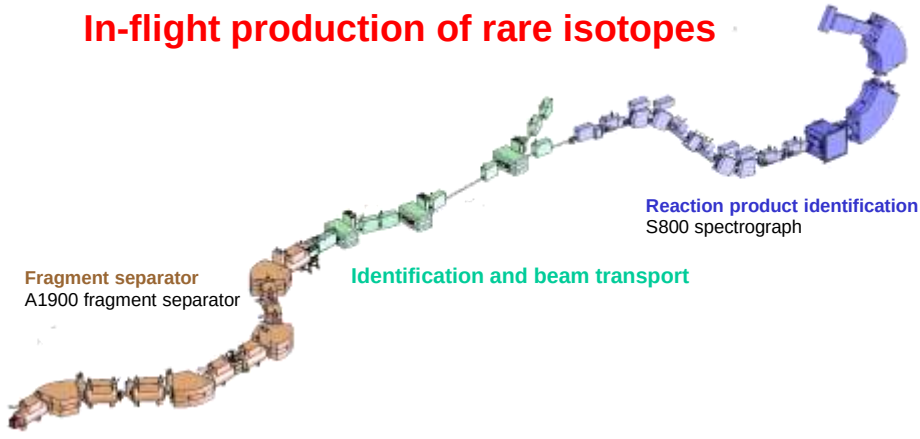

Driver accelerator (v = 0.25-0.6 c)

- **Fragment separator (A1900 NSCL, FRS GSI, BigRIPS RIKEN, ALPHA spectrometer/LISE GANIL)**
- **Identification and beam transport**
  - Stopped beam experiments, reaccelerated beam experiments
  - Fast beam experiments
    - Secondary reaction
    - Reaction product identification (S800 spectrograph, CATE/Aladin, Silicon telescopes/TOF wall, SPEG)

In-flight production of rare isotopes

Example: ^{78}Ni from ^{86}Kr at NSCL

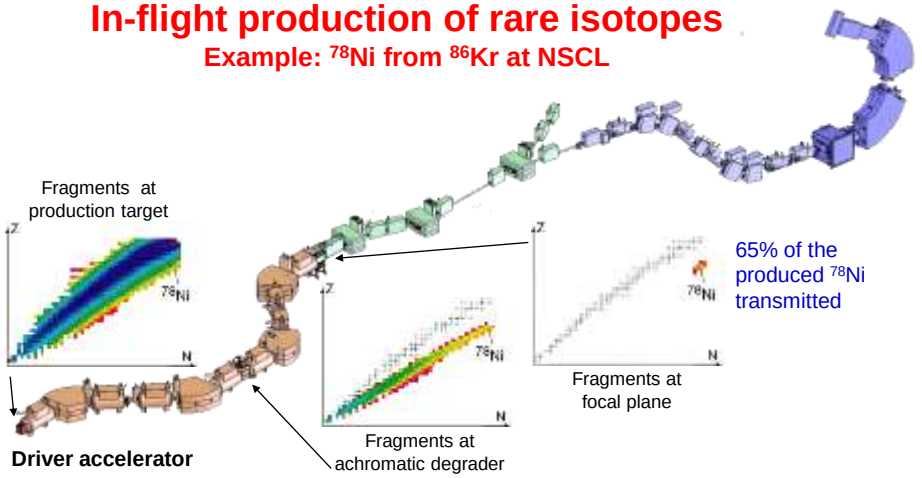

- **Fragment separator (A1900 NSCL, FRS GSI, BigRIPS RIKEN, ALPHA/LISE GANIL)**
- **Identification and beam transport**
  - Stopped beam experiments
  - Fast beam experiments
    - Secondary reaction
    - Reaction product identification (S800 spectrograph, CATE/Aladin, Silicon telescopes/TOF wall, SPEG)

Isotope selection at (high E) in-flight separators

- Ionization to q = Z (high energies!)
- A/Z selection by magnetic deflection
- $B\rho \propto A/Z\ v\ \gamma$
- v can be measured by time of flight or selected by Wien filter

Z selection by specific energy loss

$\Delta E \approx C\ Z^2/v^2$ (Bethe-Bloch)

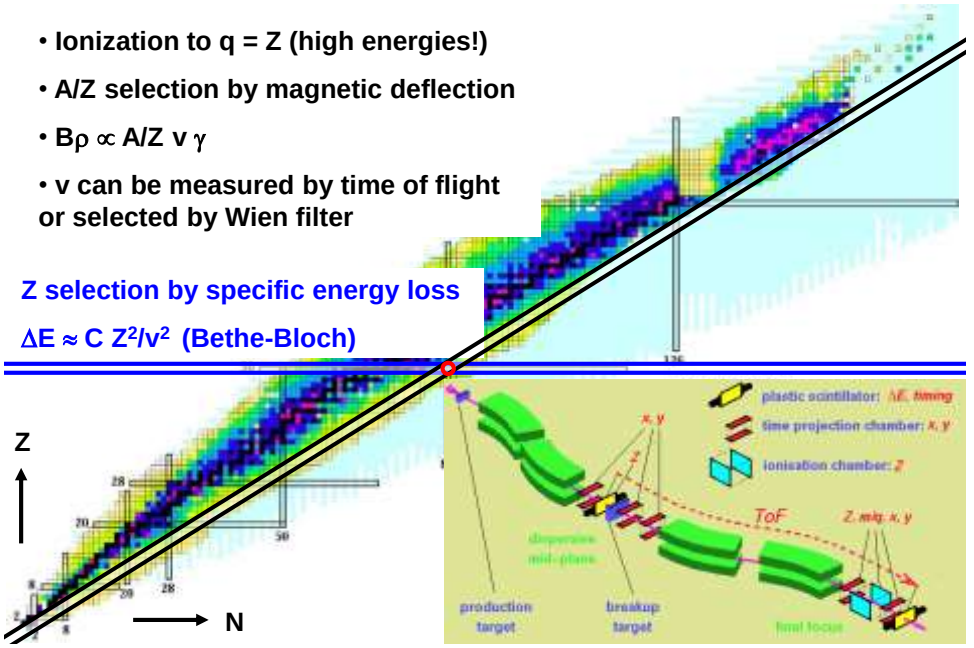

Perfect isotope identification at high energy

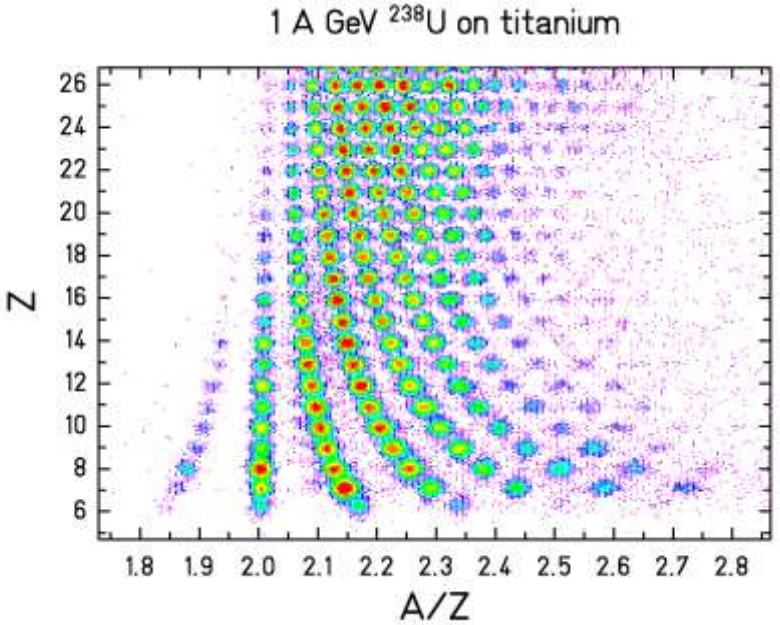

M.V. Ricciardi et al.,Nucl. Phys. A733 (2004) 299.

Optimum energy for FRS-like momentum achromat

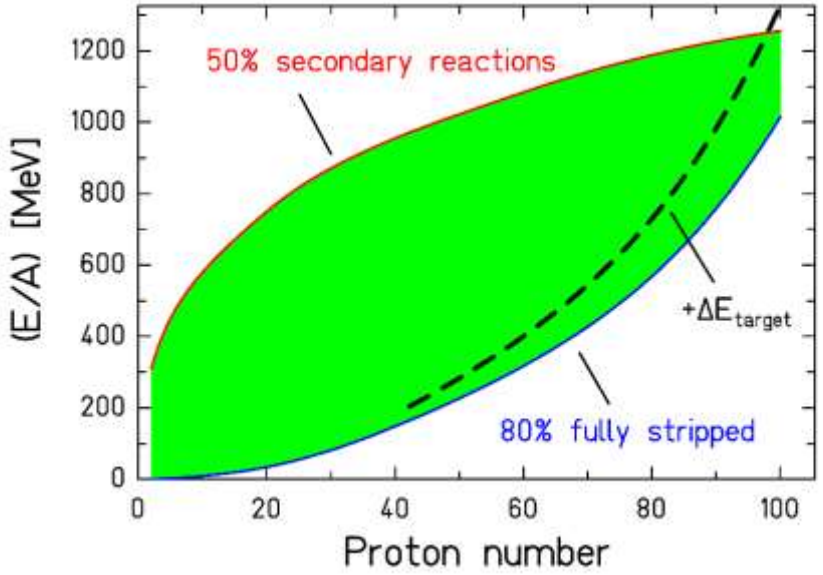

K.H. Schmidt, Euroschool Leuven 2000.

BigRIPS at RIKEN, Japan

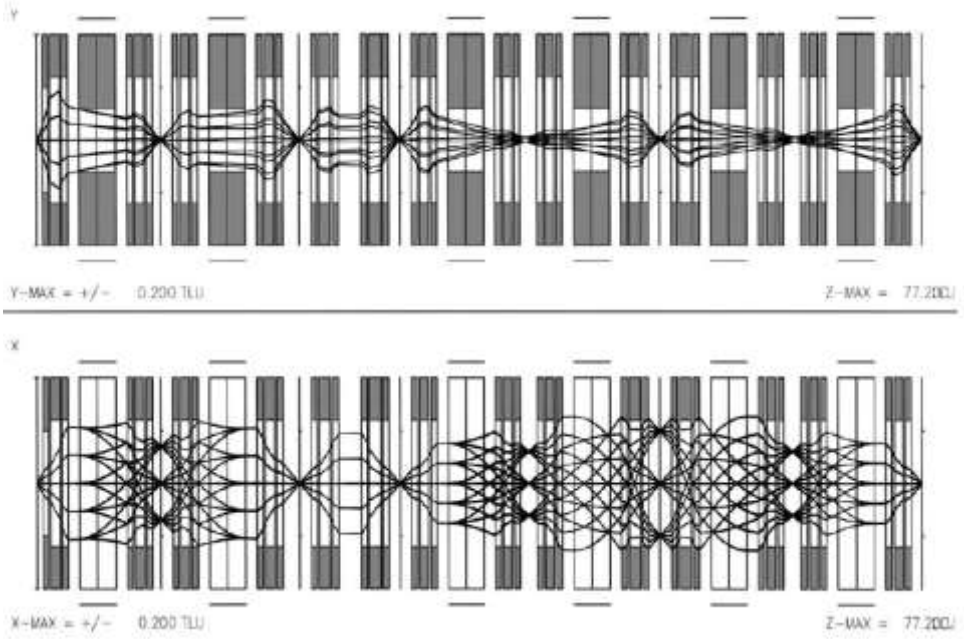

BigRIPS at RIKEN, Japan

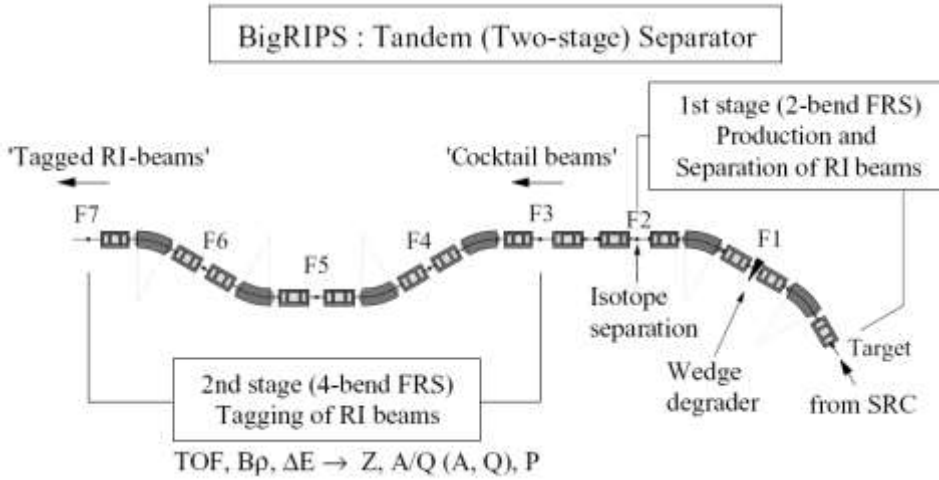

T. Kubo, Nucl. Instr. Meth. B204 (2003) 97.

Super-FRS at FAIR, Darmstadt

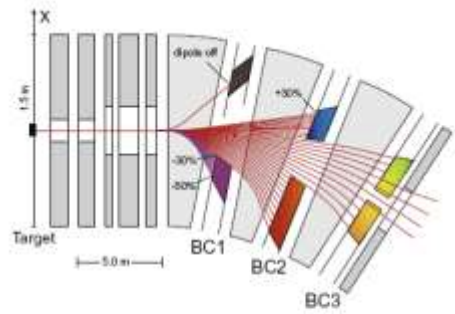

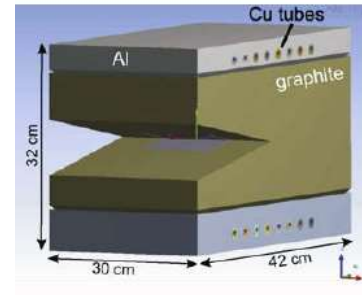

Fig. 4. Beam catcher locations in the first dipole stage of the pre-separator. Depending on the fragment setting the primary beam will be dumped at the position given by the relative difference in magnetic rigidity. Plotted are trajectories of primary beams with different $\delta_{B\rho}$ values in steps of 1%.

Fig. 5. Layout of the front part of the beam catcher. The V-shaped graphite block will absorb the beam energy of up to 50 kW and is actively cooled.

M. Winkler et al., Nucl. Instr. Meth. B266 (2008) 4183.

Q3D Spectrometer

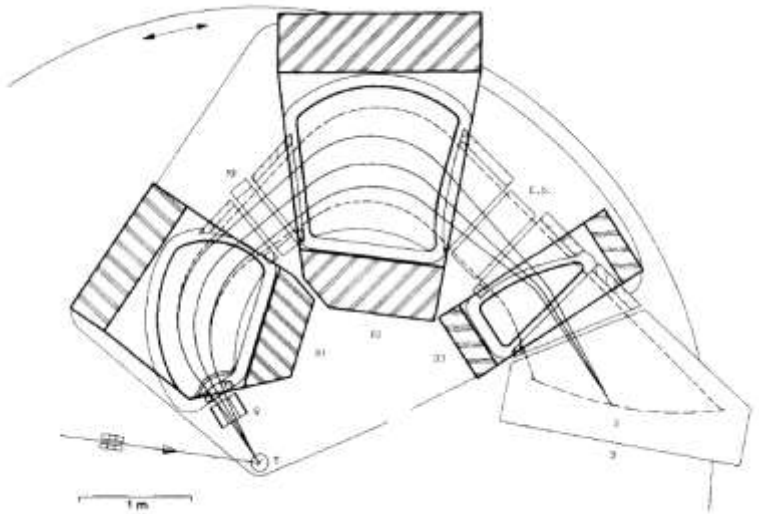

Fig. 1. Ion optical layout of the QDDD spectrograph. T – target chamber; ME – multipole element; D1, D2, D3 – dipole magnets; E.D. – electrostatic deflector; F – focal surface; D – detector chamber.

M. Löffler et al., Nucl. Instr. Meth. 111 (1973) 1.

Example spectrum ^{180}Hf(d,p)

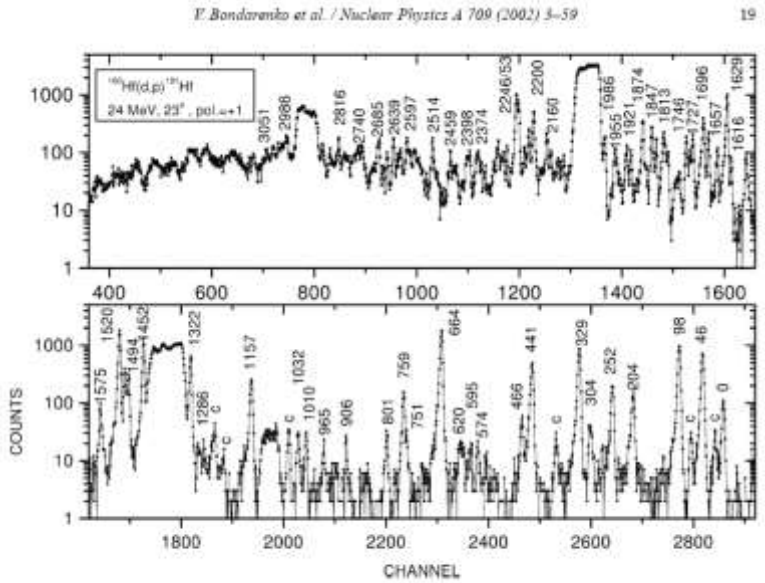

Fig. 3. An example of proton spectra from the reaction ^{180}Hf($\vec{d}$, p)^{181}Hf. The peaks are labelled by the excitation energy in keV. The proton groups labeled with 'c' belong to contaminant isotopes.

The SPEG spectrometer at GANIL

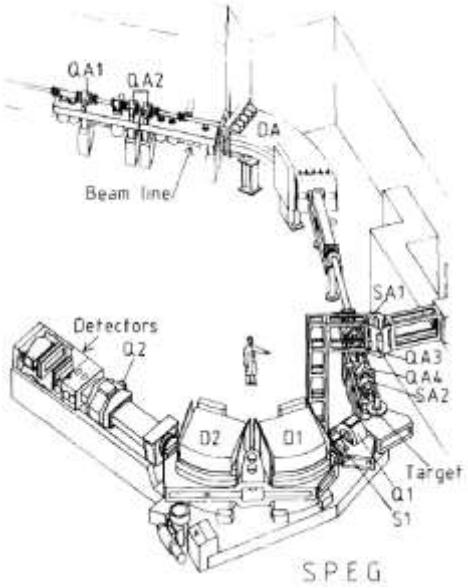

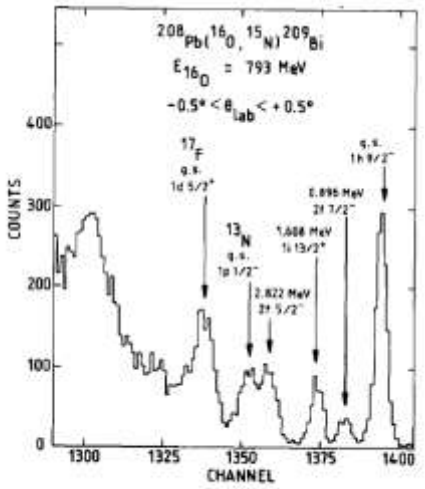

Fig. 20. Zero degree spectrum measured for the $^{208}Pb(^{16}O, ^{15}N)^{209}Bi$ reaction.

L. Bianchi et al., Nucl. Instr. Meth. A276 (1989) 509.

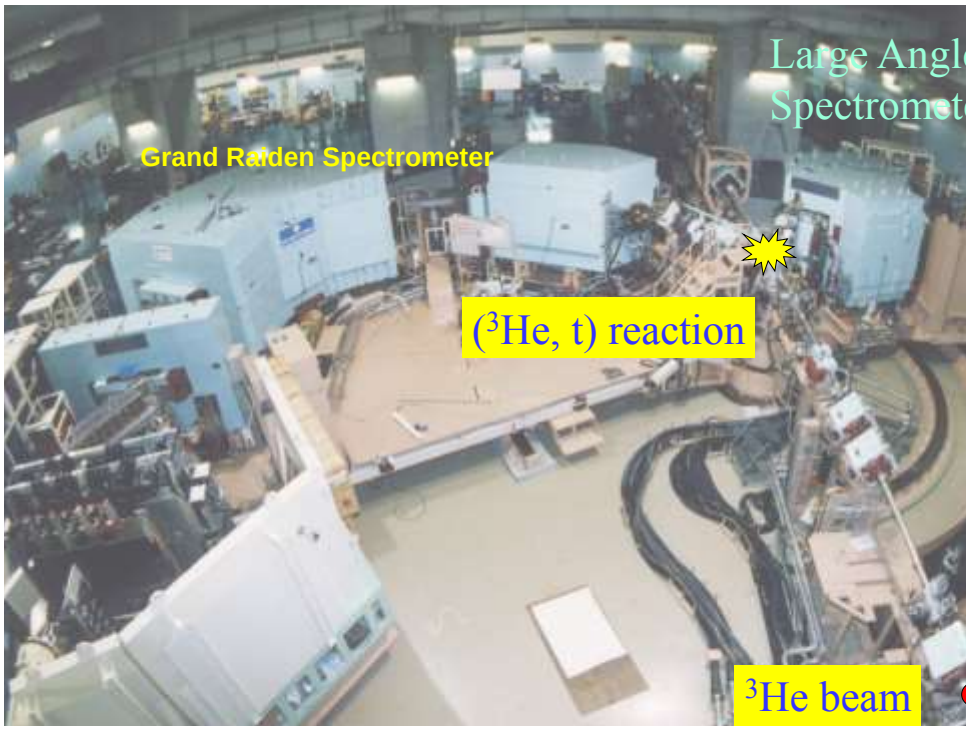

Beam line WS-course at RCNP

T. Wakasa et al., NIM A482 (2002) 79.

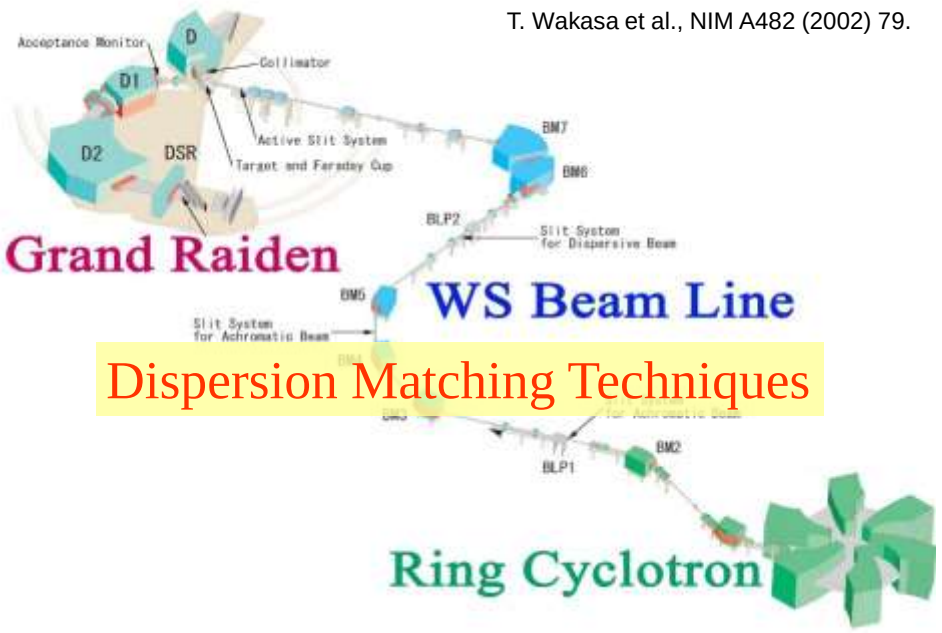

^{9}Be(^{3}He,t)^{9}B spectrum (at various scales)

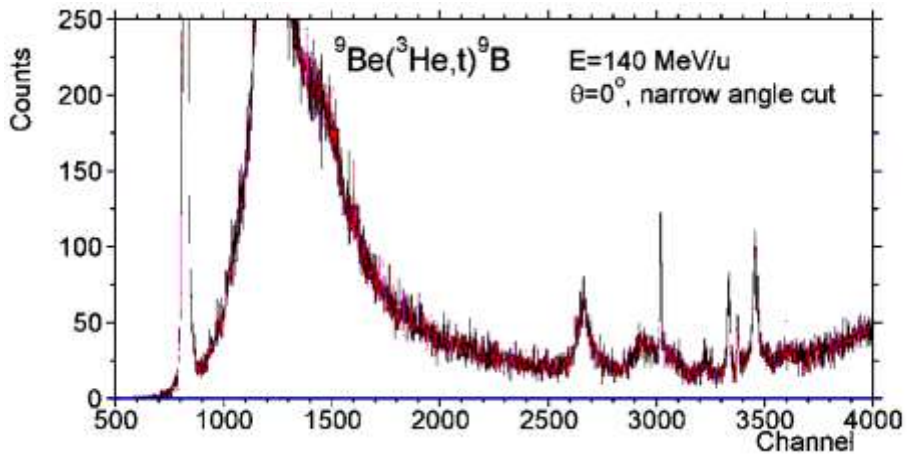

C. Scholl et al. Phys. Rev. C84 (2011) 014308.

$^{9}Be(^{3}He,t)^{9}B$ spectrum (II)

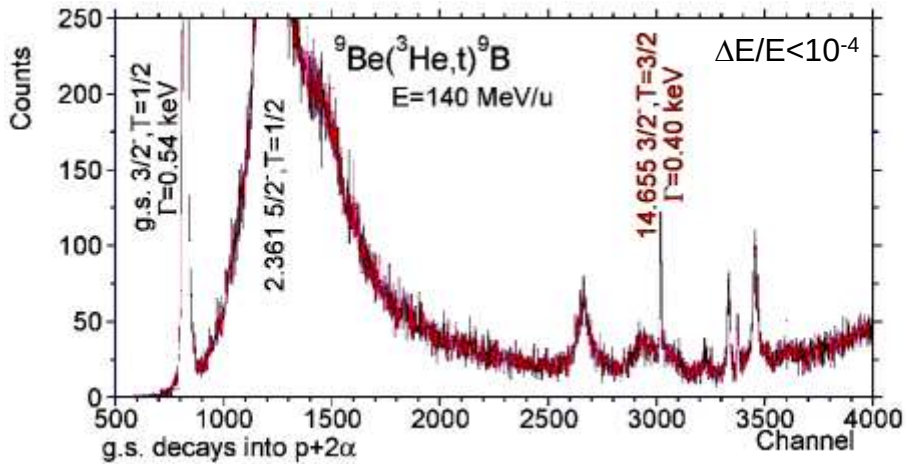

Isospin selection rule prohibits
proton decay of **T=3/2** state!

C. Scholl et al. Phys. Rev. C84 (2011) 014308.

References

- **Inorganic Mass Spectrometry: Principles and Applications, Sabine Becker, Wiley, 2007.**
- **Optics of Charged Particles, Hermann Wollnik, Academic Press 1987.**
- **Mass spectroscopy, H.E. Duckworth et al., Cambridge Univ. Press, 1986.**
- **The transport of charged particle beams, A.P. Banford, E. & F.N. Spon, 1966.**
- **Proceedings of the EMIS (Electromagnetic Isotope Separation) Conferences:**
  Nucl. Instr. Meth. B317, B266, B204, B126, B70, …